Journal
of
The Franklin Institute
Devoted to Science and the Mechanic Arts

Vol. 235 MAY, 1943 No. 5

THE FLUID TORQUE CONVERTER AND COUPLING

BY

RUPEN EKSERGIAN, Ph.D.

The majority of torque converters are modifications of the Föttinger transmission, but such transmissions in addition incorporate the fluid fly wheel clutch. Recent developments are the Voith Sinclair and Lysholm-Smith hydraulic transmissions and the Vulcan Sinclair Fluid couplings and the Trilok or Hydroflex Gear.

Fundamentally, any type of torque converter must include stationary guide vanes or channels as the reaction member for augmenting the primary or engine torque. In fluid couplings, no reaction member exists, so that there is no torque augmentation, the coupling acting merely as a fluid clutch.

The torque converter consists essentially of a centrifugal pump connected to the engine shaft and a hydraulic turbine, the rotating vanes being connected with the secondary shaft and the fixed vanes as part of the casing. The fluid medium, however, recirculates in a closed path, and the pump and turbine rotors are arranged in a compact casing with a short recirculating circuit, so that the losses are reduced to a minimum. The recirculating flow is set up by a differential pressure head due to the torque and power input at the primary or pump rotor.

In the circulation of the fluid through the converter, the total change in angular momentum about the shaft axis in a

---

(Note—The Franklin Institute is not responsible for the statements and opinions advanced by contributors in the JOURNAL.)

complete circulation is nil under steady motion. Therefore, the resultant torque reaction impressed on the flow is also nil. The impressed torque on the circulating flow consists of the primary or pump impeller torque Φ_P, the reacting torque of the stationary guides of the housing Φ_R and the torque reaction of the secondary or turbine runner vanes Φ_S. If A.M. = the total angular momentum of the circulating flow, then in steady motion,

$$\Phi_P + \Phi_R - \Phi_S = \frac{d(\text{A.M.})}{dt} = 0;$$

$$\therefore \quad \Phi_S = \Phi_P + \Phi_R, \tag{1}$$

so that the delivered torque is equal to the primary torque augmented by the torque reaction of the housing.

In the fluid coupling no reaction member exists, the circulation taking place directly between primary and secondary rotating members, so that $\Phi_S = \Phi_P$. In other words, we have a mutual reaction between the primary and secondary rotors as in an ordinary coupling or clutch.

In a torque converter, if ω_P = engine or pump rotor speeds, and ω_S = secondary rotor speed, then the power output is $\Phi_S\omega_S$ and the input is $\Phi_P\omega_P$, so that the overall efficiency is

$$\epsilon = \frac{\Phi_S\omega_S}{\Phi_P\omega_P} = \frac{(\Phi_P + \Phi_R)\omega_S}{\Phi_P\omega_P}, \tag{2}$$

which suggests measuring the torque reaction of primary motor for Φ_P and the torque reaction on the converter housing for Φ_R and noting primary and secondary speeds.

In a fluid coupling, since the mutual reaction Φ between primary and secondary rotors is equal and opposite, the efficiency varies directly as the slip S. If ω_P = primary shaft speed, then $(1 - S)\,\omega_P$ = secondary speed, so that

$$\epsilon = \frac{(1 - S)\Phi\omega_P}{\Phi\omega_P} = 1 - S, \tag{3}$$

i.e., the efficiency varying linearly with the slip.

Since applications of the torque converter are usually to variable speed operation on the secondary or turbine side and at constant speed on the primary or pump impeller side, it is necessary to estimate the variation of circulating flow and the torque for both pump and turbine rotors at different secondary speeds.

In the following analysis we are primarily concerned with the angular momentum and energy relations at the terminal sections of the fluid across the pump impeller between sections one and two, then across the turbine terminal sections between sections two and three and finally across the terminal sections of the guide blades between sections three and one. Sections, radii and angles, of the guide blades will be designated by the subscript "g" with an additional number for the particular section. Likewise, the subscript "P" stands for the pump impeller and the subscript "S" for the turbine rotor.

The circulating flow Q measured across any section in Cu. Ft. per second is obviously the flow rate through either turbine or pump impeller. Let ρ = density of fluid, lbs./cu. ft.

1. ANALYSIS OF TORQUE AND ENERGY TRANSFER ACROSS PUMP IMPELLER AND TURBINE ROTOR.

a. Considering the interaction of the Fluid Flow with the pump impeller, let, ω_P = angular velocity of pump rotor (rads./sec.), F_{P2} and F_{g1} = the exit annular areas for the pump rotor and guide wheel (sq. ft.), r_{P2} and r_{g1} = the mean radii to center of section for the exit annular areas for the pump rotor and guide wheel (ft.), β_{P2} and α_{g1} = the blade exit angles for pump impeller and guide vanes. Then referring to Plate 1, Fig. 1,

The peripheral tangential velocity at pump rotor *exit* is the rotor blade velocity $\omega_P r_{P2}$ plus the tangential component of the *relative* fluid velocity $Q/F_{P2} \cot \beta_{P2}$ since the normal (or radial) component velocity of the fluid relative to the rotor is Q/F_{P2}.

The angular momentum of the recirculating fluid across the exit section of the rotor per unit time is

$$\frac{\rho Q}{g}\left[\omega_P r_{P2} + \frac{Q}{F_{P2}} \cot \beta_{P2}\right] r_{P2}.$$

The angular momentum of the fluid per unit time entering the impeller is likewise the angular momentum of the fluid per unit time across the exit section of the stationary guide

PLATE 1

FIG. 1

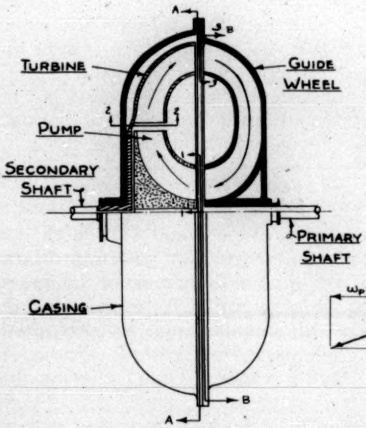
A
B
TURBINE
GUIDE WHEEL
2
2
3
PUMP
1
SECONDARY SHAFT
1
PRIMARY SHAFT
CASING
B
A

HYDRODYNAMIC TORQUE CONVERTOR

SECTION AT TOP
SHOWS ARRANGEMENT
OF PUMP
TURBINE & GUIDE WHEEL

SECTION A-A
SHOWING ONLY
PUMP, OR PRIMARY, ROTOR

CUT OUT BELOW
SHOWS EXIT FLOW
FROM PUMP

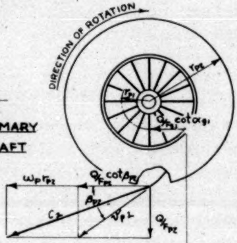
DIRECTION OF ROTATION
r_{p2}
r_{p1}
$Q_{f_{p1}} \cot\alpha_{g1}$
$\omega_p r_{p2}$
$Q_{f_{p2}} \cot\beta_{p2}$
β_{p2}
C_2
v_{p2}
$Q_{f_{p2}}$

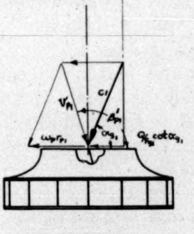
C_1
v_{p1}
β'_{p1}
α_{g1}
$\omega_p r_{p1}$
$Q_{f_{p1}} \cot\alpha_{g1}$

END VIEW
CUT OUT TO SHOW
ENTRANCE FLOW TO PUMP

vanes, i.e.,

$$\frac{\rho Q}{g}\left[\frac{Q}{F_{g1}}\cot\alpha_{g1}\right]r_{g1}.$$

Therefore, the torque exerted on the fluid by the impeller, or the torque reaction of the fluid on the pump impeller, is

$$\Phi_P = \frac{\rho Q}{g}\left[\omega_P r^2{}_{P2} + \left(\frac{\cot\beta_{P2}}{F_{P2}}r_{P2} - \frac{\cot\alpha_{g2}}{F_{g1}}r_{g1}\right)Q\right]; \qquad (4)$$

$$\therefore \quad \Phi_P = A\omega_P Q + BQ^2, \qquad (4')$$

where

$$A = \frac{\rho}{g}r^2{}_{P2}, \qquad B = \frac{\rho}{g}\left[\frac{\cot\beta_{P2}}{F_{P2}}r_{P2} - \frac{\cot\alpha_{g1}}{F_{g1}}r_{g1}\right].$$

The time rate of the energy transfer between the fluid and pump impeller is

$$P_P = \Phi_P\omega_P = [A\omega_P Q + BQ^2]\omega_P \qquad (5)$$

and this corresponds to the input to the converter or the brake power loading on the engine.

At constant flow rate, the torque on the pump impeller increases directly with the speed, while the load on the engine varies as a parabolic function of the speed. At constant speed ω_P both the brake torque and power loading on the engine varies as a parabolic function of the flow rate.

b. Considering the turbine rotor, Plate 1, let ω_S = angular velocity of turbine rotor (rad./sec.), F_{S2} and F_{S3} = the entrance and exit annular area (sq. ft.), r_{S2} and r_{S3} = the mean radii to center of section for the above areas (ft.), β_{S2} and β_{S3} = the blade exit angles of the turbine rotor.

The driving torque on the turbine rotor equals the difference between the entrance and exit angular momentum of the fluid per unit time. In the case where the turbine wheel is directly adjacent to the pump rotor, with stationary guide vanes placed beyond the turbine rotor and before the pump impeller, *the entrance fluid angular momentum per unit time to the turbine* is then *the exit fluid angular momentum per unit time from the pump impeller*, namely (See Plate 1) Fig. 2,

$$\frac{\rho Q}{g}\left[\omega_P r_{P2} + \frac{Q}{F_{P2}}\cot\beta_{P2}\right]r_{P2}.$$

The exit angular momentum of the fluid per unit time from the turbine rotor is

$$\frac{\rho Q}{g}\left[\omega_S r_{S3} + \frac{Q}{F_{S3}} \cot \beta_{S3}\right] r_{S3}.$$

The driving torque exerted by the fluid on the turbine rotor, or the torque reaction of the turbine on the fluid, is, therefore,

$$\Phi_S = \frac{\rho Q}{g}\left[\omega_P r^2{}_{P2} + \left(\frac{r_{P2} \cot \beta_{P2}}{F_{P2}} - \frac{r_{S3} \cot \beta_{S3}}{F_{S3}}\right) Q - r^2{}_{S3}\omega_S\right]; \quad (6)$$

$$\therefore \quad \Phi_S = AQ\omega_P + B'Q^2 - CQ\omega_S, \quad (6')$$

where

$$A = \frac{\rho}{g} r^2{}_{P2}, \quad B' = \frac{\rho}{g}\left[\frac{r_{P2} \cot \beta_{P2}}{F_{P2}} - \frac{r_{S3} \cot \beta_{S3}}{F_{S3}}\right], \quad C = \frac{\rho}{g} r^2{}_{S3}.$$

The power transfer between the fluid and turbine rotor is

$$P_S = \Phi_S \omega_S = [AQ\omega_P + B'Q^2 - CQ\omega_S]\omega_S. \quad (7)$$

When Q is constant and with constant impeller velocity, $\omega_P =$ const., then

$$\Phi_S = M - N\omega_S, \quad (8) \qquad P_S = \Phi_S\omega_S = (M - N\omega_S)\omega_S \quad (9)$$

For this condition, the output torque decreases as a linear function of the turbine speed, and the power output varies as a parabolic function of the speed.

For the speed at maximum output, ω_{SR},

$$\frac{dP_S}{d\omega_S} = M - 2N\omega_S = 0; \qquad \therefore \quad \omega_{SR} = \frac{M}{2N},$$

where

$$M = AQ\omega_P + B'Q^2, \qquad N = C'Q.$$

The maximum output occurs at $\omega_{SR} = M/2N$. The *starting* torque is just twice the torque developed at this latter speed.

However, at any given turbine speed ω_S, both the torque and power output varies as a parabolic function of the flow rate Q, so that the starting torque may be further augmented by an increase in flow rate with decreasing turbine speeds. See Plates 2 and 4.

V. 19

2. COMPATIBILITY RELATIONS AND ENERGY LOSSES.

The overall efficiency, $\epsilon = P_S/P_P$, depends on an energy balance for the hydraulic losses P_L in the circulating flow, where $P_L = P_P - P_S$. Further the total pressure drop, due to these losses and the pressure rise and pressure drop through the impeller and turbine corresponding to the mechanical input and output to the converter, must be nil for the complete circulation. The characteristics of these losses must be known, since equations (4) to (9) are insufficient to describe either the loading on the engine or the output on the turbine shaft as a function of the speeds. It is not always possible to absorb the full engine output at all turbine shaft speeds. The circulating flow itself varies with both impeller and turbine speeds, so that the torque amplification may be increased at low speeds on the turbine side, over that indicated by the linear relation in equation (8).

Let $H = p/\rho + c^2/2g$ = the total head for any section, between any two sets of blade systems, i.e., in the annular space between blade groups, where p is the pressure and c the *absolute* mean velocity of the flow. Since the exit velocity and entrance velocity between blade systems are the same, it is immaterial whether we consider the drops along the circuit in terms of pressures or total heads in summing up for the complete circuit.

Due to the energy transfer between the fluid and moving blade systems, there must be either a rise or drop in total head since

$$\rho Q \Delta H = \Phi\omega, \qquad \therefore \quad \Delta H = \frac{\Phi\omega}{\rho Q}. \tag{10}$$

Let H_L = the loss in head due to friction and shock loss and turbulence.

The entire system is assumed under pressure, the minimum pressure being at the section before the impeller; moreover, gravity heads are neglected.

The total *rise* in head across the pump impeller is

$$H_2 - H_1 = \Delta H_P - H_{L(1-2)}, \tag{11}$$

where

$$\Delta H_P = \frac{1}{\rho Q} \cdot \Phi_P \omega_P = \frac{1}{\rho}\left[A\omega_P + BQ\right]\omega_P.$$

PLATE 1

FIG. 2

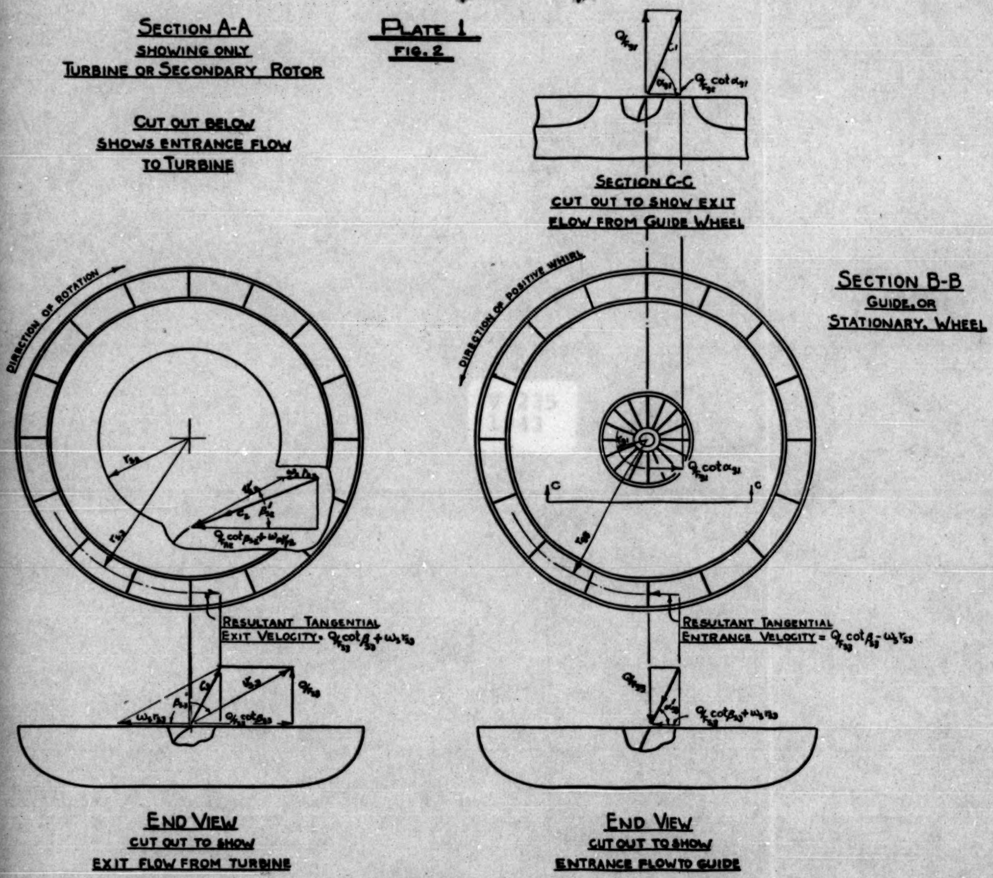
SECTION A-A
SHOWING ONLY
TURBINE OR SECONDARY ROTOR
CUT OUT BELOW
SHOWS ENTRANCE FLOW
TO TURBINE
DIRECTION OF ROTATION
r_{s2}
r_{s3}
$\omega_s r_{s2}$
w_{s2}
c_2
β'_{s2}
$Q/kr_{s2} \cot\beta_{s2} + \omega_s r_{s2}$
RESULTANT TANGENTIAL
EXIT VELOCITY $= Q/kr_{s3} \cot\beta_{s3} + \omega_s r_{s3}$
c_3
w_{s3}
β_{s3}
Q/kr_{s3}
$\omega_s r_{s3}$
$Q/kr_{s3} \cot\beta_{s3}$
END VIEW
CUT OUT TO SHOW
EXIT FLOW FROM TURBINE
Q/kr_{g1}
c_1
α_{g1}
$Q/kr_{g1} \cot\alpha_{g1}$
SECTION C-C
CUT OUT TO SHOW EXIT
FLOW FROM GUIDE WHEEL
SECTION B-B
GUIDE, OR
STATIONARY, WHEEL
DIRECTION OF POSITIVE WHIRL
α_{g1}
$Q/kr_{g1} \cot\alpha_{g1}$
C
C
r_{s3}
RESULTANT TANGENTIAL
ENTRANCE VELOCITY $= Q/kr_{s3} \cot\beta_{s3} - \omega_s r_{s3}$
Q/kr_{s3}
α'_{g3}
$Q/kr_{s3} \cot\beta_{s3} + \omega_s r_{s3}$
END VIEW
CUT OUT TO SHOW
ENTRANCE FLOW TO GUIDE

The total *drop* in head across the turbine rotor

$$H_2 - H_3 = \Delta H_S + H_{L(2-3)}, \qquad (12)$$

where

$$\Delta H_S = \frac{1}{\rho Q} \cdot \Phi_S \omega_S = \frac{1}{\rho}[A\omega_P + B'Q - C'\omega_S]\omega_S.$$

The total *drop* in head across the guide blades is

$$H_3 - H_1 = H_{L(3-1)}. \qquad (13)$$

Since the total head or pressure drop is nil for the complete circuit, then

$$\begin{aligned} H_2 - H_1 &= (H_2 - H_3) + (H_3 - H_1); \\ \therefore \quad \Delta H_P - \Delta H_S &= H_{L(1-2)} + H_{L(2-3)} + H_{L(3-1)}, \qquad (14) \end{aligned}$$

which is another form for the total energy components of the system.

The fluid flow through the various passages is subjected to friction and turbulent losses which are difficult to estimate due to the complexity of the flow in the curved and relatively short blade system. Due to the varying speed requirements of the secondary or turbine rotor, discontinuity in velocities occur at entrance to blade channels, which in turn give rise to eddying and large turbulent losses. Such losses are known as the entrance shock losses. Moreover the lack of uniformity of the entrance and exit velocities both in magnitude and direction across these sections, and the deviations of the mean velocity from that indicated by the blade paths, limits the accuracy of the various formulae based on the simple Euler Theory.

Likewise the following estimation of the losses can only be regarded as a rough approximation. These losses are characterized by entrance shock losses between blade systems and friction losses in the blades themselves. The former are taken proportional to the square of the abrupt change in tangential whirl velocities and the latter are conveniently measured by the square of the relative exit velocities of the respective blade systems.

The performance characteristics of the converter can be greatly improved by reducing these losses; particularly, the

V.
19

entrance shock losses at the lower and higher speeds of the output shaft. This may be interpreted in the following analysis either by the use of more favorable entrance blade angles at other than optimum speeds, or by introducing a coefficient ξ less than unity in the shock loss expression.

(1-2) Loss of head, $H_{L(1-2)}$, across pump impeller.

The loss of head divides into two components, the entrance shock loss and the friction loss in the pump blades.

a. Entrance Shock Loss: Since the mean velocity normal to the peripheral area is unaffected by shock losses, we are concerned with the abrupt change in tangential velocity from the exit stationary guides to the entrance to pump rotor. The velocity head corresponding to this loss is, approximately,

$$H_{LS(1-2)} = \frac{1}{2g}\left\{\frac{Q}{F_{g1}}\cot\alpha_{g1} - \left[\frac{Q}{F_{P1}}\cot\beta_{P1} + \omega_P r_{P1}\right]\right\}^2.$$

b. Friction Loss in Impeller Blades: This is measured by the *relative* velocity at pump exit and the corresponding head is

$$H_{Lf(1-2)} = \frac{\xi_P}{2g}\left(\frac{\csc\beta_{P2}}{F_{P2}}\right)^2 Q^2, \qquad (\xi = 0.2 \text{ roughly}).$$

Hence,

$$H_{L(1-2)} = H_{LS(1-2)} + H_{Lf(1-2)}. \tag{15}$$

(2-3) Loss of head, $H_{L(2-3)}$, across turbine rotor.

Again the loss of head divides into two components, the entrance shock loss and the friction loss in the turbine blades.

a. Entrance Shock Loss: The abrupt change in tangential velocity is the exit tangential velocity from the pump rotor minus the entrance tangential velocity just within the turbine blade, the latter being compounded of the relative and peripheral velocity of the blades at entrance. The velocity head for the turbine entrance shock loss is

$$H_{LS(2-3)} = \frac{1}{2g}\left[\left(\omega_P r_{P2} + \frac{Q}{F_{P2}}\cot\beta_{P2}\right) - \left(\omega_S r_{S2} + \frac{Q}{F_{S2}}\cot\beta_{S2}\right)\right]^2.$$

b. Friction Loss in Turbine Blades: This is measured in terms of the exit relative velocity of the turbine and the loss of head is

$$H_{Lf(2-3)} = \frac{\xi_S}{2g}\left(\frac{\csc\beta_{S3}}{F_{S3}}\right)^2 Q^2;$$

$$\therefore\quad H_{L(2-3)} = H_{LS(2-3)} + H_{Lf(2-3)}. \qquad (16)$$

(3–1) Loss of head, $H_{L(3-1)}$, across guide blades.

The exit tangential velocity from the turbine is $\omega_S r_{S3} + Q/F_{S3} \cot\beta_{S3}$ and the entrance tangential velocity within the guide vanes is $Q/F_{g3}\cot\alpha_{g3}$. Hence, the entrance shock loss head to the guide vanes is

$$H_{LS(3-1)} = \frac{1}{2g}\left[\omega_S r_{S3} + \left(\frac{\cot\beta_{S3}}{F_{S3}} - \frac{\cot\alpha_{g3}}{F_{g3}}\right) Q\right]^2$$

and the friction loss drop in head is

$$H_{Lf(3-1)} = \frac{\xi_g}{2g}\left(\frac{\csc\alpha_{g1}}{F_{g1}}\right)^2 Q^2;$$

$$\therefore\quad H_{L(3-1)} = H_{LS(3-1)} + H_{Lf(3-1)}. \qquad (17)$$

Compatibility Relation: On substituting the above values for the various drops along the circuit in equation (14) we have a quadratic function for the Q's and speeds. Noting that, approximately,

$$\begin{aligned} r_{g1} &= r_{P1} = r_1 &\quad\text{and}\quad F_{P1} &= F_{g1} = F_1,\\ r_{P2} &= r_{S2} = r_2 & F_{P2} &= F_{S2} = F_2,\\ r_{S3} &= r_{g3} = r_3 & F_{S3} &= F_{g3} = F_3,\end{aligned}$$

then the compatibility condition is

$$\begin{aligned}\frac{\omega_P^2}{2g}[r_2^2 - r_1^2] + \frac{\omega_S^2}{2g}[r_3^2 - r_2^2] = \frac{Q}{g}\Bigg[\left(\omega_P\frac{r_1}{F_1}\cot\beta_{P1} - \omega_S\frac{r_3}{F_2}\cot\alpha_{g3}\right)\\ -(\omega_P - \omega_S)\frac{r_2}{F_2}\cot\beta_{S2}\Bigg] + \frac{Q^2}{2g}\Bigg[\frac{1}{F_1^2}\left\{\xi_g\csc^2\alpha_{g1} + (\cot\alpha_{g1} - \cot\beta_{P1})^2\right\}\\ + \frac{1}{F_2^2}\left\{\xi_P\csc^2\beta_{P2} + (\cot\beta_{P2} - \cot\beta_{S2})^2\right\}\\ + \frac{1}{F_3^2}\left\{\xi_S\csc^2\beta_{S3} + (\cot\beta_{S3} - \cot\alpha_{g3})^2\right\}\Bigg]. \qquad (18)\end{aligned}$$

The left term is the centrifugal head corresponding to the work of the centrifugal forces in the rotating channel.

An alternate form for the derivation of this equation is of interest in that the pressure drops are expressed entirely in the form of velocity heads.

The rate of energy transfered to the fluid by the impeller is

$$\Phi_P\omega_P = \frac{W}{g}\left[V_{P2}r_2\cos\beta_{P2} + \omega_P r_2^2 - C_1 r_1 \cos\alpha_{g1}\right]\omega_P, \qquad (19)$$

where V_{P2} = the *exit relative* velocity of the impeller, C_1 = the *absolute entrance* velocity to the impeller, α_{g1} = the exit velocity from the fixed blades, ω_P = angular velocity of the impeller, W = flow rate of the circulating fluid (lbs./sec.).

Let C_2 = the exit absolute velocity from the impeller which is likewise the entrance absolute velocity to the turbine; then, since

$$C_2^2 = V^2_{P2} + \omega_P^2 r_2^2 + 2V_{P2}\cdot\omega_P r_2 \cos\beta_{P2},$$

$$V^2_{P1} = C_1^2 + \omega_P^2 r_1^2 - 2C_1\omega_P r_1 \cos\alpha_{g1},$$

$$\therefore \quad \Phi_P\omega_P = P_P$$

$$= \frac{W}{g}\left[\left(\frac{C_2^2 - C_1^2}{2}\right) - \left(\frac{V^2_{P2} - V^2_{P1}}{2}\right) + \frac{\omega_P^2(r_2^2 - r_1^2)}{2}\right] \qquad (20)$$

Since

$$\Delta H_P = P_P/W = \left(\frac{p_2}{\rho} + \frac{C_2^2}{2g}\right) - \left(\frac{p_1}{\rho} + \frac{C_1^2}{2g}\right) + H_{L(1-2)},$$

$$\therefore \quad \Delta H_P = \frac{1}{2g}\left[(C_2^2 - C_1^2) - (V^2_{P2} - V^2_{P1}) + \omega_P^2(r_2^2 - r_1^2)\right] \qquad (21)$$

and

$$\frac{1}{\rho}(p_1 - p_2) = \frac{1}{2g}\left[\omega_P^2(r_2^2 - r_1^2) - (V^2_{P2} - V^2_{P1})\right] - H_{L(1-2)}. \qquad (22)$$

The rate of energy transferred from the fluid to the turbine is

$$\Phi_S\omega_S = \frac{W}{g}\left[C_2 r_2 \cos\alpha_2 - V_3 r_3 \cos\beta_{S3} - \omega_S r_3^2\right]\omega_S, \qquad (23)$$

where V_3 and β_3 are the exit *relative* velocity and exit blade angle of the turbine, and ω_S = ang. velocity of rotor.

Again, noting

$$C_2^2 + \omega_S^2 r_2^2 - 2C_2\omega_S r_2 \cos\alpha_2 = V^2_{S2}$$

and

$$V^2_{S3} + \omega_S^2 r_3^2 + 2V_3 r_3 \omega_S \cos\beta_{S3} = C_3^2,$$

then

$$\Phi_S\omega_S = P_S = \frac{W}{2g}[(C_2^2 - C_3^2) + (V^2_{S3} - V^2_{S2}) + \omega_S^2(r_2^2 - r_3^2)]; \quad (24)$$

since

$$\Delta H_S = P_S/W = \left(\frac{p_2}{\rho} + \frac{C_2^2}{2g}\right) - \left(\frac{p_3}{\rho} + \frac{C_3^2}{2g}\right) - H_{L(2-3)},$$

$$\therefore\ \frac{1}{\rho}(p_2 - p_3) = \frac{1}{2g}[(V_{S3} - V_{S2})^2 - \omega_S^2(r_3^2 - r_2^2)] + H_{L(2-3)}. \quad (25)$$

Finally the pressure drop in the guide vanes is

$$\frac{1}{\rho}(p_3 - p_1) = H_{L(3-1)} + \frac{C_1^2 - C_3^2}{2g}. \quad (26)$$

It is important to note that in equations (22), (25) and (26), due to entrance shock losses, the relative velocities V_{P1} and V_{S2} in general do not coincide with entrance blade angles of pump and turbine. Further, the exit absolute velocity C_3 does not coincide with entrance guide angle α_{g3}. The *entrance relative* velocities should be defined by the vector relation,

$$\overline{V_{P1}} = \overline{C_1} - \overline{\omega_P r_1} \qquad \text{and} \qquad \overline{V_{S2}} = \overline{V_{P2}} + \overline{(\omega_P - \omega_S)r_2},$$

for the pump and turbine respectively.

On combining equations (22), (25) and (26) we obtain the compatibility conditions for the complete circulation of the fluid,

$$\frac{1}{2g}[\omega_P^2(r_2^2 - r_1^2) + \omega_S^2(r_3^2 - r_2^2)]$$
$$= \frac{1}{2g}[(V^2_{P2} - V^2_{P1}) + (V^2_{S3} - V^2_{S2}) + (C_1^2 - C_3^2)]$$
$$+ H_{L(1-2)} + H_{L(2-3)} + H_{L(3-1)}. \quad (27)$$

The condition for continuity is,

$$C_1 \sin\alpha_{g1} = Q/F_1, \qquad V_{P2}\sin\beta_{P2} = Q/F_2, \qquad V_{S3}\sin\beta_{S3} = Q/F_3,$$

so that

$$V^2_{P1} = (Q/F_1 \cot\alpha_{g1} - \omega_P r_1)^2 + Q^2/F_1^2,$$
$$V^2_{S2} = (Q/F_2 \cot\beta_{P2} + (\omega_P - \omega_S)r_2)^2 + Q^2/F_2^2,$$
$$C_3^2 = (Q/F_3 \cot\beta_{S3} + \omega_S r_3)^2 + Q^2/F_3^2.$$

V.2
194

Thus the velocity heads are expressed directly in terms of the flow rate, the blade speeds and the geometrical blade angles. On substituting these values in (27) together with the losses we obtain (18).

3. TORQUE CONVERTER CHARACTERISTICS.

In the application of the torque converter we are concerned with the variation in turbine torque and secondary output against speed for various conditions of primary torque, speed and input.

The overall hydraulic efficiency is given by the relation

$$\epsilon = \frac{\Phi_S \omega_S}{\Phi_P \omega_P} = \frac{[AQ\omega_P + B'Q^2 - CQ\omega_S]\omega_S}{[A\omega_P Q + BQ^2]\omega_P} \tag{28}$$

subjected to the compatibility relations of the circulation with impeller and turbine speeds, given in equation (18) which may be expressed as an implicit function,

$$F(Q, \omega_P, \omega_S) = 0. \tag{29}$$

We may consider Q, ω_P and ω_S (and the blade angles if they can be made to vary) as the coördinates of the systems. From eq. (29), we note, only two can be regarded as independent. Thus if we choose ω_P and ω_S as independent coördinates, then Q is determined by (29), that is, by eq. (18), from which we calculate the efficiency from eq. (28), the turbine torque from eq. (6) and the corresponding output from eq. (7), then the impeller torque from eq. (4) and the required engine input from eq. (5).

A. If we hold the ***engine speed constant***, i.e., ω_P = constant, then the circulation Q varies with the secondary or output speed ω_S, according to the compatibility equation (29) or (18). Since both the secondary and primary torques are quadratic functions of Q, we find the secondary torque ***modified*** from a linear relation with secondary speeds, while the primary torque cannot be constant throughout the range of secondary speeds, so that the input itself must vary with secondary speed.

B. If we hold the ***engine torque constant***, then

$$\Phi_P = A\omega_P Q + BQ^2 = \text{Constant}, \qquad (= \Phi_{PC}). \tag{30}$$

Thus Q is directly related with the engine speed ω_P, i.e.,

$$Q = f(\omega_P) = \frac{-A\omega_P + \sqrt{A^2\omega_P{}^2 + 4B\Phi_{PC}}}{2B}.$$

On substituting in the compatibility eq. (29) or (18) we find ω_P directly related with ω_S, that is, the impeller speed must also vary with the turbine speed. At constant torque, the impeller speed increases nearly linearly with the turbine speed.

However, in a first approximation, the characteristics of the torque converter are not greatly modified by assuming a constant circulation Q at constant impeller speed ω_P for a wide range of turbine or output speeds ω_S. In other words the characteristic performance is mainly that of the turbine supplied at constant flow rate. Since the impeller speed is assumed constant, this implies constant input. From eqs. (9) and (5) the overall hydraulic efficiency must be

$$\epsilon = \frac{P_S}{P_P} = \frac{(M - N\omega_S)\omega_S}{\Phi_P\omega_P}, \tag{31}$$

which reaches a maximum when $\omega_{SR} = M/2N$, the parabolic efficiency, falls to zero, at starting, and at $\omega_{SM} = M/N$. If we define ω_{SR} as the *rated speed*, i.e., that speed corresponding to maximum output and efficiency, then the maximum speed, corresponding to zero torque, is just twice the rated speed.

One difficulty with a direct application of the torque converter is the rapid drop in the efficiency with increasing overspeeds relative to its rated speed. If we limit the useful speed range to 50 per cent. over its rated value, then the efficiency falls to $\frac{3}{4}$ of its maximum value at rated speed. Thus if the maximum efficiency at rated speed is 85 per cent., this means the efficiency at 50 per cent. overspeed is such that a change over to direct drive is desirable with no further torque amplification. For this reason, the relation of secondary torque to primary torque is such that the secondary torque falls to the value of the primary torque at approximately 1.5 × rated speed of the converter.

Plate 2 shows a linear output torque Φ_S against secondary speed ω_S, at constant primary torque Φ_P and primary speed ω_P. For this case the secondary output P_S is a parabolic

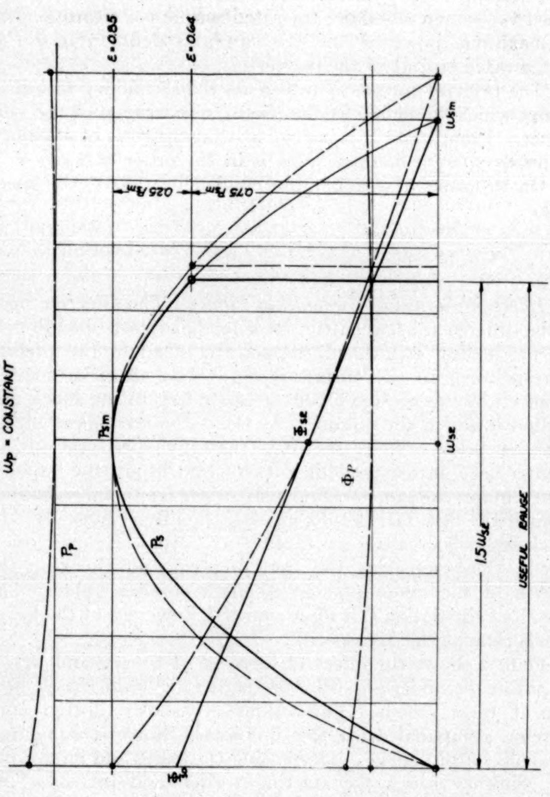
ω_p = CONSTANT
E = 0.85
E = 0.64
0.25 P_{sm}
0.75 P_{sm}
ω_{sm}
P_{sm}
Φ_{se}
ω_{se}
Φ_p
P_p
P_s
Φ_{so}
1.5 ω_{se}
USEFUL RANGE

PLATE #2

curve, with its maximum value at rated speed $\omega_{SR} = \frac{1}{2}\omega_{SM}$. The stalling torque or maximum torque at zero secondary speed Φ_{SO} is then just twice the rated torque Φ_{SR} corresponding to maximum power P_{SM}. We can also define $P_{SR} = P_{SM}$ = the rated output of the converter.

The primary torque Φ_P intersects the secondary torque at $1.5\omega_{SR}$ which we define as the useful speed range of the converter. From Plate 2, it is evident that the *ratio* of *secondary* to *primary torque at rated speed* is in the order of $\Phi_S/\Phi_P = 2$.

On the basis of a maximum efficiency at 0.85, the speed ratio

$$\gamma = \omega_P/\omega_S = \frac{1}{\epsilon}\,(\Phi_S/\Phi_P) = 2.35 \text{ at rated speed.}$$

Effect of Change of Circulating Flow Q: The effective head is the difference between the impeller head corresponding to the mechanical input and the counter head of the turbine corresponding to the output power. The effective head is balanced by the friction head corresponding to the shock and friction losses in the circuit. As the secondary speed either decreases below or increases above the rated speed, the output counter head decreases, while, at constant input, the impeller head remains the same. Obviously, if the frictional resistance is small the flow rate would increase rapidly. Actually, the shock losses increase very rapidly at both lower and overspeeds, thus increasing the friction head and checking the growth of the circulation to a much smaller value. The growth of circulation Q is more marked, however, at the lower speeds than at the overspeeds.

Plate 2 shows the effect of increase of torque and power output at the under and overspeeds due to the increased flow rate at these speeds. The values are shown dotted and, thereby, compared with the previously linear torque and parabolic output curve. Decreasing the losses and improving the efficiency raises the starting torque and increases the useful operating speed range of the converter.

The ratio of starting torque to rated torque at the output end is increased to 2.5 approx., i.e., $\Phi_{SO}/\Phi_{SR} = 2.5$.

Efforts have been made to extend the speed range and improve the efficiency to a more flat top curve at the under

V.2
194

and overspeeds, by reducing the losses and through multi-reaction stages. Shock losses at the unfavorable speeds have been reduced by blunt or round shaped blades at entrance as in the Lysholm Smith Torque Converter. This combination of special designed blades with multi-reaction stages has resulted in a considerable increase in speed range with a more flat top efficiency curve combined with augmented starting torque.

Plate 3 shows a typical reaction stage velocity diagram. C_1 and C_2 are entrance and exit absolute velocities and V_1 and V_2 are corresponding relative velocities. The entrance angle, of the absolute entrance velocity to the moving blade, is the exit angle α_1 of the fixed guide blade, while the relative velocity angle at exit from the moving blade is β_2. In a typical reaction stage the pressure drop in the moving blade results in an increase in relative velocity from V_1 to V_2. With multiple stages V_2 is made equal to C_1 and the relative velocity angle at exit β_2 is made equal to the exit guide vane α_1 i.e., the angle of the absolute entrance velocity. Let W = lbs. fluid/sec. for the flow rate. Then the torque is (Plate 3)

$$\begin{aligned}\Phi_S &= \frac{W}{g}[C_1 \cos \alpha_1 + (V_2 \cos \beta_2 - U)]r \\ &= \frac{W}{g}[2C_1 \cos \alpha_1 - U]r, \qquad \text{since} \quad \left\{\begin{array}{l} V_2 = C_1, \\ \beta_2 = \alpha_1. \end{array}\right. \end{aligned} \tag{32}$$

Since the peripheral velocity $U = \omega r$, the output per stage is

$$P_S = \frac{W}{g}[2C_1 \cos \alpha_1 - U]U \tag{33}$$

and the rated speed Ur occurs when $\dfrac{dP_S}{dU} = 0$;

$$\therefore \quad U_R = C_1 \cos \alpha_1 \qquad \text{or} \qquad \cos \alpha_1 = \frac{U_R}{C_1}.$$

Since

$$\left.\begin{array}{r} V_2^2 - 2V_2U \cos \beta_2 + U^2 = C_2^2, \\ C_1^2 - 2C_1U \cos \alpha_1 + U^2 = V_1^2, \end{array}\right\}$$

then

$$P_S = \frac{W}{2g}[(V_2^2 - V_1^2) - (C_2^2 - C_1^2)] = W \cdot \Delta H_S, \tag{34}$$

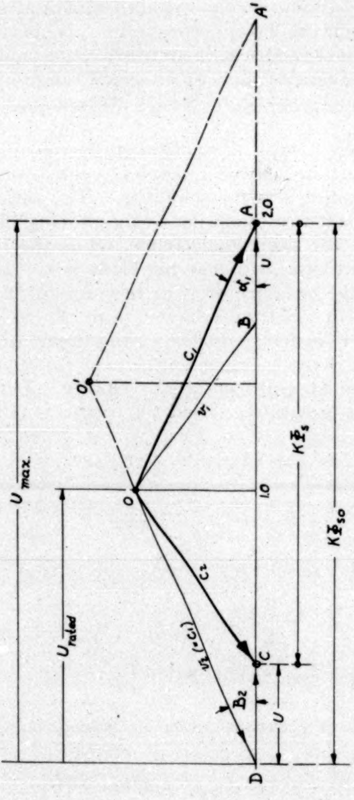
A'
A
2.0
u
α_1
B
C_1
O'
v_1
$K\Phi_s$
$U_{max.}$
O
1.0
$K\Phi_{so}$
C_2
U_{rated}
$v_2(=c_1)$
C
β_2
U
D

PLATE #3

where ΔH_S = the *counter head* due to the *energy transfer* at the reaction stage. The total head includes a friction loss head.

Referring to the velocity diagram (Plate 3), the entrance shock loss head is

$$\Delta H_{fS} = \frac{f_S}{2g}[(C_1 \cos \alpha_1 - U) - C_1 \sin \alpha_1 \cot \beta_1]^2$$

$$= \frac{f_S}{2g}\left[\frac{\sin(\beta_1 - \alpha_1)}{\sin \beta_1} C_1 - U\right]^2 = \frac{f_S}{2g}[k'C_1 - U]^2,$$

where β_1 = the entrance moving blade angle.

The friction loss in the blade itself has the form

$$\Delta H_{fV} = \frac{f_V}{2g} V_2^2 = \frac{f_V}{2g} C_1^2 \qquad \text{since} \qquad V_2 = C_1.$$

Hence the total friction head is

$$\Delta H_f = \Delta H_{fS} + \Delta H_{fV} = \frac{f_S}{2g}[k'C_1 - U]^2 + \frac{f_V}{2g} C_1^2. \qquad (35)$$

In variable speed operations the first term, by far, is the most important, so that when U is nil, ΔH_f reaches its maximum value.

The total drop in head across a moving reaction blade is

$$\Delta H_t = \Delta H_S + \Delta H_f,$$

i.e.,

$$\frac{p_1 - p_2}{\rho} + \frac{C_1^2 - C_2^2}{2g} = \left\{\frac{V_2^2 - V_1^2}{2g} - \frac{C_2^2 - C_1^2}{2g}\right\} + \Delta H_f.$$

Since $V_2 = C_1$, we have for the pressure drop

$$\Delta H = \frac{p_1 - p_2}{\rho} = \frac{C_1^2 - V_1^2}{2g} + \Delta H_f. \qquad (36)$$

From the velocity diagram $(C_1^2 - V_1^2)/2g$, which is the pressure drop corresponding to the mechanical output, reaches its maximum value when

$$U = U_{\text{rated}} = C_1 \cos \alpha_1$$

and becomes nil when $U = 0$. On the other hand, the friction head ΔH_f is a minimum when $U = U_{\text{rated}}$ and reaches its maximum value when $U = 0$ or U = Max.

By cutting down the friction head, when U is small or at overspeeds, the *total head is reduced over its optimum value at rated speed.*

Now assuming a constant energy supply from the impeller, we have

$$W \Sigma \Delta H = \text{constant}. \tag{37}$$

Therefore, when U is either below or above the optimum or rated speed, the flow rate W (lbs./sec.) must increase. This has the effect of increasing all the velocities as shown in the enlarged vector diagram, Plate 3. The entire speed range is increased *particularly at the lower and higher values of U.* It does not greatly modify the optimum value of U for maximum efficiency, since the total drop in head is then effected principally by the counter head ΔH_S (ΔH_f being small since $k'C_1 - U$ is a minimum). Thus the diagram should be enlarged only for small and high values of U.

The effect of reducing friction and shock losses on the performance of the converter is shown in Plate 4, where f max. refers to a converter with large friction losses and f min. refers to a converter with small losses.

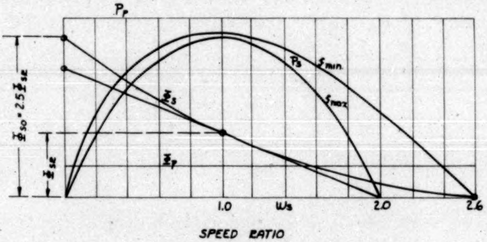

PLATE # 4

Reducing the losses improves the low and high speed performance and increases the useful speed range.

FLUID COUPLING.

The fluid coupling is essentially a hydraulic clutch operating with small slippage between primary and secondary wheels.

V.2
194

The mutual torque between primary and secondary is

$$\Phi_P = -\Phi_S = \frac{\rho Q}{g}\left\{\left[\omega_P r_{P2} + \frac{Q}{F_{P2}}\cot\beta_{P2}\right] r_{P2} - \left[\omega_S r_{S1} + \frac{Q}{F_{S1}}\cot\beta_{S1}\right] r_{S1}\right\},$$

where ω_P and ω_S are the primary and secondary speeds, Q is the circulation flow rate, $F_{P2} = F_2$ = upper annular; $F_{S1} = F_1$ = lower annular; $r_{P2} = r_2$ and $r_{S1} = r_1$ are their corresponding mean radius, and β_{P2} and β_{S1} are the exit blade angles of primary and secondary wheels.

With radial blades, the expression for torque reduces to

$$\Phi = \frac{\rho Q}{g}[\omega_P r_2^2 - \omega_S r_1^2]. \qquad (1)$$

In the fluid coupling, the variation in torque is influenced primarily by the circulating flow rate Q and this in turn depends upon the effective head ΔH_U and the shock and friction losses.

With straight blades, the effective head due to energy transfer to the blades is

$$\Delta H_U = \frac{1}{g}[\omega_P r_2^2 - \omega_S r_1^2](\omega_P - \omega_S). \qquad (2)$$

The total friction and shock loss head ΔH_L is

$$\Delta H_L = \frac{1}{2g}[(\omega_P - \omega_S)^2 r_2^2 + (\omega_S - \omega_P)^2 r_1^2] + \frac{\xi}{2g}\frac{Q^2}{A^2}\cdot \qquad (3)$$

Since $\Delta H_U = \Delta H_L$ for an energy balance,

$$\frac{1}{2g}[\omega_P^2(r_2^2 - r_1^2) - \omega_S^2(r_2^2 - r_1^2)] = \frac{\xi}{2g}\frac{Q^2}{A^2} \qquad (4)$$

in agreement with Eq. 18, which is thus seen to be a special case of the torque converter analysis.

Since $\omega_S = (1 - S)\omega_P$ on substituting in (4),

$$\frac{1}{2g}(r_2^2 - r_1^2)(2 - S)S\omega_P^2 = \frac{\xi}{2g}\frac{Q^2}{A^2},$$

so that

$$Q = K\omega_P\sqrt{(r_2^2 - r_1^2)(2 - S)S} = K\omega_P F(S). \qquad (5)$$

On substituting in (1)

$$\Phi = \frac{\rho Q}{g}[r_2^2 - (1 - S)r_1^2]\omega_P = K'\omega_P^2 f(S), \qquad (6)^*$$

where

$$\begin{aligned} f(S) &= [r_2^2 - (1 - S)r_1^2][(r_2^2 - r_1^2)(2 - S)S]^{\frac{1}{2}} \\ &= \sqrt{2}(r_2^2 - r_1^2)^{\frac{1}{2}}\sqrt{S} \quad \text{(roughly)}. \end{aligned}$$

Thus $f(S)$ depends not only on the slip but also on the size and proportions of the coupling. However the efficiency $\epsilon = 1 - S$ always varies linearly with the slip. On the other hand, to maintain a small slip and high efficiency will require excessive proportions for transmitting large torques. The size of the coupling can be considerably reduced by transmitting the torque at high rotative speeds.

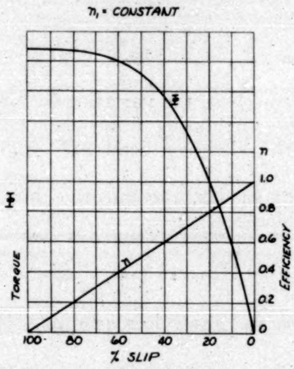

PLATE #5

Plate 5 shows the experimental trend of $f(S)$ that is the variation of torque with slip. Likewise the efficiency varies as a linear function with the slip.

---

[*] Otherwise, since $Q = k\sqrt{H}$ approx. and $\Delta H = 1/g[\omega_P r_2^2 - \omega_S r_1^2](\omega_P - \omega_S) = 1/g[r_2^2 - (1 - S)]\omega_P^2 S$, $\therefore \Phi = \kappa[r_2^2 - (1 - S)r_1^2]^{\frac{1}{2}}\omega_P^2\sqrt{S}$ (approx.).

From dynamic similarity, the time rate of change of angular momentum has the form

$$\Phi = k_1 \frac{\rho}{g} Q \omega d^2 f_1(S),$$

where *d* is a linear dimension as a diam., but the circulation *Q* is the product of a *velocity* and *area*, where the velocity depends on the $\sqrt{g \cdot \Delta H}$.

$$\therefore \quad Q = K d^2 \sqrt{g \cdot \Delta H},$$

but from the previous analysis, ΔH has the form

$$\Delta H = \frac{1}{g} d^2 \omega^2 f_2(S); \; \therefore \quad Q = K d^3 \omega (f_2(S))^{\frac{1}{2}}.$$

Therefore,

$$\left.\begin{aligned} \Phi &= k \frac{\rho}{g} \omega^2 d^5 f(S), \\ P &= k \frac{\rho}{g} \omega^3 d^5 f(S). \end{aligned}\right\} \tag{7}$$

Since

$$\Phi = F(\rho, g, \omega, d, S) \equiv \left| \frac{ML^2}{T^2} \right|,$$

$$\frac{\rho}{g} = \left| \frac{M}{L^3} \right|, \qquad \omega = \left| \frac{1}{T} \right|, \qquad d = |L|, \qquad S = \text{numeric}.$$

$$\Phi = k \left(\frac{\rho}{g} \right)^{\alpha} \cdot (\omega)^{\beta} \cdot (d)^{\gamma} = \left| \frac{M}{L^3} \right|^{\alpha} \cdot \left| \frac{1}{T} \right|^{\beta} \cdot |L|^{\gamma} \equiv \left| \frac{ML^2}{T^2} \right|$$

$$\alpha = 1, \qquad \beta = 2, \qquad \gamma = 5,$$

which agrees with the exponents in (7).

THE FLUID COUPLING AS A VIBRATION DAMPENER.

The fluid coupling when placed in a torsional vibration system is an effective dampener. When vibrating about the mean load position,

$$\Phi = K' \omega_P{}^2 f(S) \qquad (= K' \omega_P{}^2 \sqrt{S} \text{ approx.}),$$

and

$$\omega_P = \dot{\theta}_1, \qquad \omega_S = \dot{\theta}_2 = (1 - S)\omega_P.$$

For small oscillations, let ω mean angular velocity of *the primary shaft* and S_0 the mean slip corresponding to the mean load. Then $\omega = \omega_{P0}$,

$$\theta_1 = \omega t + \phi_1, \qquad \theta_2 = (1 - S_0)\omega t + \phi_2,$$

$$\therefore\ \dot{\theta}_1 = \omega + \dot{\phi}_1 = \omega_P = \omega_{P0} + \Delta\omega_P,$$

$$\dot{\theta}_2 = (1 - S_0)\omega + \dot{\phi}_2 = \omega_S.$$

Since the torque can always be expressed as an explicit function " F " of the primary speed ω_P and the slip S, then

$$\Phi = K'F(\omega_P, S) = K'\omega_P{}^2 f(S), \tag{8}$$

where

$$F(\omega_P, S) = F_0 + \left(\frac{\partial F}{\partial \omega_P}\right)_0 \Delta\omega_P + \left(\frac{\partial F}{\partial S}\right)_0 \Delta S,$$

$$F_0 = \omega^2 f(S)_0, \qquad \left(\frac{\partial F}{\partial \omega_P}\right)_0 = 2\omega f(S)_0, \qquad \left(\frac{\partial F}{\partial S}\right)_0 = \omega^2 f'(S)_0.$$

We note, however,

$$\Delta\omega_P = \dot{\phi}_1, \qquad \omega_P - \omega_S = S\omega_P = (S_0 + \Delta S)(\omega + \dot{\phi}_1)$$

and

$$\omega_P - \omega_S = S_0\omega + (\dot{\phi}_1 - \dot{\phi}_2) = S_0\omega + \omega\Delta S + S_0\dot{\phi}_1;$$

hence,

$$\omega\Delta S = (1 - S_0)\dot{\phi}_1 - \dot{\phi}_2 = \dot{\phi}_1 - \dot{\phi}_2 \quad \text{(approx.)}.$$

Since

$$\Phi = \Phi_0 + \Delta\Phi = K'\left[F_0 + \left(\frac{\partial F}{\partial \omega_P}\right)_0 \dot{\phi}_1 + \left(\frac{\partial F}{\partial S}\right)_0 \Delta S\right],$$

$$\therefore\quad \Delta\Phi = 2K'\omega f(S)_0\dot{\phi}_1 + K'\omega(\dot{\phi}_1 - \dot{\phi}_2)\left(\frac{\partial F}{\partial S}\right). \tag{9}$$

The first term can be neglected since $f(S)\phi_1$ is small. Hence the damping torque due to the coupling is

$$\Phi_D = \Delta\Phi = K\left(\frac{\partial F}{\partial S}\right)_0 \omega(\dot{\phi}_1 - \dot{\phi}_2) = B(\dot{\phi}_1 - \dot{\phi}_2) \tag{10}$$

where

$$B = K\omega\left(\frac{\partial F}{\partial S}\right)_0 \left(= \frac{K'\omega}{\sqrt{S_0}} \text{ approx.}\right)$$

V.2
194

ϕ_1 and ϕ_2 = the vibration coordinates of the primary and secondary wheels.

The coupling separates a dynamic system into two distinct parts with equilibrium angular velocities ω and $\omega(1 - S_0)$ respectively. The two systems oscillate relative to their respective mean positions; where the vibratory coordinate of the primary relative to its mean position is ϕ_1, and the vibratory coordinate of the primary relative to its mean position is ϕ_2.

As an example, consider the vibration system shown in Plate 6, Fig. 1, which consists of two, two mass systems,

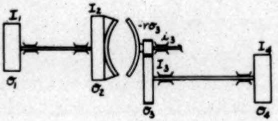
I_1
I_2
$-\gamma\sigma_3$
i_3
I_4
I_3
σ_1
σ_2
σ_3
σ_4

FIG. #1

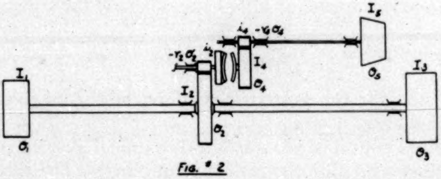
I_5
i_4
$-\gamma_4\sigma_4$
$-\gamma_2\sigma_2$
i_2
I_1
I_2
I_4
σ_4
σ_5
I_3
σ_1
σ_2
σ_3

FIG. # 2

PLATE #6

coupled by a fluid dampener. The second system has a reduction gear with inertias i_3, I_3 and I_4, and gear ratio γ between i_3 and I_3, with i_3 including the secondary rotor of the coupling. The shaft constant between I_3 and I_4 is C_{34}. The primary system consists of the inertias I_1 and I_2 with shaft constant C_{12}.

Let $\Phi_1 e^{ipt}$ = the applied torque on mass I_1. The Lagrangian functions are

$$\left.\begin{aligned} T &= \tfrac{1}{2}[I_1\dot{\theta}_1^2 + I_2\dot{\theta}_2^2 + (I_3 + \gamma^2 i_3)\dot{\theta}_3^2 + I_4\dot{\theta}_4^2], \\ V &= \tfrac{1}{2}C_{12}(\theta_1 - \theta_2)^2 + \tfrac{1}{2}C_{34}(\theta_3 - \theta_4)^2, \end{aligned}\right\} \qquad (11)$$

while the dissipation function is assumed entirely concentrated at the coupling, and is

$$F = \tfrac{1}{2}B(\dot{\theta}_2 + \gamma\dot{\theta}_3)^2. \tag{12}$$

The equations of motion are, therefore,

$$\left.\begin{aligned} I_1\ddot{\theta}_1 + C_{12}(\theta_1 - \theta_2) &= \Phi_1 e^{ipt}, \\ I_2\ddot{\theta}_2 + C_{12}(\theta_2 - \theta_1) + B(\dot{\theta}_2 + \gamma\dot{\theta}_3) &= 0, \end{aligned}\right\} \text{System I}$$
$$\left.\begin{aligned} (I_3+\gamma^2 i_3)\ddot{\theta}_3 + C_{34}(\theta_3-\theta_4) + \gamma B(\gamma\dot{\theta}_3+\dot{\theta}_2) &= 0, \\ I_4\ddot{\theta}_4 + C_{34}(\theta_4-\theta_3) &= 0, \end{aligned}\right\} \text{System II} \tag{13}$$

with $\theta_1 = \theta_{10}e^{ipt}$, $\theta_2 = \theta_{20}e^{ipt}$, etc.

Let $D(ip)$ be the determinate

$$\begin{vmatrix} -I_1p^2+C_{12} & -C_{12} & 0 & 0 \\ -C_{12} & -I_2p^2+C_{12}+iB & iBr & 0 \\ 0 & iBr & -I_3'p^2+C_{34}+\gamma^2B & 0 \\ 0 & 0 & -C_{34} & -I_4p^2+C_{34} \end{vmatrix}$$

where $I_3' = I_3 + \gamma^2 i_3$, and D_{rS} be the minor of the rth column and Sth row;

$$\therefore \quad \theta_{r0} = \frac{\sum_1^n D_{rS}(ip)\Phi_S}{D(ip)}, \tag{14}$$

where $S = 1$ for the system considered and θ_{r0} equals either θ_{10}, θ_{20}, θ_{30}, θ_{40} and $n = 4$.

The fluid coupling separates a dynamical system *into component systems* on either side of the coupling. The interaction between the systems is the coupling damping torque. For effective damping, the motion at the coupling must be large, and therefore its location should be away from nodal points of either system. When the coupling is located in the proximity of a node, the vibration of the system for the corresponding mode is practically unaffected by the coupling.

The importance of reducing gear vibrations in a system, as in Plate 6, Fig. 2, shows the location of the coupling at the intermediate gear set. Let I_1, I_2 (with pinion i_2) and I_3 be a component system (I) on one side of the coupling. Let I_4 plus pinion i_4 and I_5 be a separate system (II) on the other side of the coupling. Let C_{12} and C_{23} be the elastic shaft constants of system (1) and γ_2 = the gear ratio for pinion i_2. Likewise C_{45} and γ_4 are the elastic shaft constant and gear ratio for system (II).

We may select the normal coördinates for each system on either side of the coupling. For the 1st system, let ϕ_{r1}, ϕ_1 and ϕ_2 be the rigid and normal vibration coördinates. Let ϕ_{r2} and ϕ_4 be the rigid and normal coördinates for the 2nd system. Then if $\theta_1, \theta_2, \theta_3, \theta_4, \theta_5$ are the coördinates of the several masses, we have

$$\begin{array}{ll}
\text{1st System} & \text{2nd System} \\
\theta_1 = \phi_{r1} + \phi_1 + \phi_2, & \theta_4 = \phi_{r2} + \phi_4, \\
\theta_2 = \phi_{r1} + k_2'\phi_1 + k_2''\phi_2, & \theta_5 = -\gamma_4\phi_{r2} + k_5'''\phi_4, \\
\theta_3 = \phi_{r1} + k_3'\phi_1 + k_3''\phi_2, &
\end{array}$$

where k' is the amplitude ratio of the first mode for any given mass *corresponding* to the natural frequency n_1; likewise k'' is the amplitude ratio of mode two at frequency n_2. For the *second system* (a free two mass system) we have only one mode at frequency n_4 with the amplitude ratio k_5''' for mass I_5.*

The *total* kinetic energy for the two systems in terms of rigid and normal coördinates of the separate systems is

$$\begin{aligned}
T = \{&\tfrac{1}{2}[I_1+(I_2+\gamma_2^2 i_2)+I_3]\dot\phi^2_{r1}+\tfrac{1}{2}[I_1+(I_2+\gamma_2^2 i_2)k_2'^2+I_3k_3'^2]\dot\phi_1^2 \\
&+\tfrac{1}{2}[I_1+(I_2+\gamma_2^2 i_2)k_2''^2+I_3k_3''^2]\dot\phi_2^2\}_{\mathrm{I}} \\
&+\{\tfrac{1}{2}[(I_4+\gamma_4^2 i_4)+\gamma_4^2 I_5]\dot\phi^2_{R2}+\tfrac{1}{2}[(I_4+\gamma_4^2 i_4)+I_5k_5'''^2]\dot\phi_4^2\}_{\mathrm{II}};
\end{aligned}$$

$$\therefore \quad T=\tfrac{1}{2}[(A_{r1}\dot\phi^2_{r1}+A_1\dot\phi_1^2+A_2\dot\phi_2^2)_{\mathrm{I}}+(A_{r2}\dot\phi^2_{r2}+A_4\dot\phi_4^2)_{\mathrm{II}}], \qquad (15)$$

where the A_r's are the inertia coefficients for the rigid coördi-

---

* *For system I*

$$k_2' = \frac{C_{12} - n_1^2 I_1}{C_{12}}, \qquad k_3' = \frac{C_{23}(C_{12} - n_1^2 I_1)}{C_{12}(C_{23} - n_1^2 I_3)}, \qquad \textit{1st Mode}$$

$$k_2'' = \frac{C_{12} - n_2^2 I_1}{C_{12}}, \qquad k_3'' = \frac{C_{23}(C_{12} - n_2^2 I_1)}{C_{12}(C_{23} - n_2^2 I_3)}, \qquad \textit{2d Mode}$$

where n_1^2 and n_2^2 are the roots of the frequency equation

$$\frac{I_1 I_2' I_3}{C_{12} \cdot C_{23}} n^4 - \left[\frac{I_1(I_2' + I_3)}{C_{12}} + \frac{I_3(I_1 + I_2')}{C_{23}}\right] n^2 + (I_1 + I_2 + I_3) = 0$$

and

$$I_2' = I_2 + i_2 r_2^2$$

For system II

$$k_5''' = \frac{r_4 C_{45}}{n_4^2 I_5 - C_{45}} \quad \text{and} \quad n_4^2 = \frac{[I_5 + I_4 + r_4^2 i_4]C_{45}}{I_5(I_4 + r_4^2 i_4)}.$$

nates and the A_n's are the inertia coefficients for the normal coördinates for the two systems.

The interaction between the two systems can be expressed in terms of a dissipation function,

$$\begin{aligned} F &= \tfrac{1}{2}B(\dot{\theta}_4 + \gamma_2\dot{\theta}_2)^2 \\ &= \tfrac{1}{2}B[(\dot{\phi}_{r2} + \dot{\phi}_4) + \gamma_2(\dot{\phi}_{r1} + k_2'\dot{\phi}_1 + k_2''\dot{\phi}_2)]^2. \end{aligned} \tag{16}$$

We have damping coupling terms between the otherwise independent normal coördinates of the two independent systems.

Assuming the disturbing torque $\Phi_3 e^{ipt}$ to act on Mass I_3 we have the following equations for the vibration of the system:

$$\left.\begin{aligned} \ddot{\phi}_{r1} + B\frac{\gamma_2}{A_{r1}}[\dot{\phi}_{r2} + \dot{\phi}_4 + \gamma_2(\dot{\phi}_{r1} + k_2'\dot{\phi}_1 + k_2''\dot{\phi}_2)] &= \frac{\Phi_3 e^{ipt}}{A_{r1}}, \\ \ddot{\phi}_1 + n_1^2\phi_1 + B\frac{\gamma_2 k_2'}{A_1}[\dot{\phi}_{r2} + \dot{\phi}_4 + \gamma_2(\dot{\phi}_{r1} + k_2'\dot{\phi}_1 + k_2''\dot{\phi}_2)] &= \frac{k_3'\Phi_3 e^{ipt}}{A_1}, \\ \ddot{\phi}_2 + n_2^2\phi_2 + B\frac{\gamma_2 k_2''}{A_2}[\dot{\phi}_{r2} + \dot{\phi}_4 + \gamma_2(\dot{\phi}_{r1} + k_2'\dot{\phi}_1 + k_2''\dot{\phi}_2)] &= \frac{k_3''\Phi_3 e^{ipt}}{A_2}, \\ \cdots\cdots\cdots\cdots\cdots\cdots\cdots\cdots & \\ \ddot{\phi}_{r2} + B/A_{r2}[\dot{\phi}_{r2} + \dot{\phi}_4 + \gamma_2(\dot{\phi}_{r1} + k_2'\dot{\phi}_1 + k_2''\dot{\phi}_2)] &= 0, \\ \ddot{\phi}_4 + n_4^2\phi_4 + B/A_4[\dot{\phi}_{r2} + \dot{\phi}_4 + \gamma_2(\dot{\phi}_{r1} + k_2'\dot{\phi}_1 + k_2''\dot{\phi}_2)] &= 0, \\ \text{with} \qquad & \\ \phi_{r1} = \phi_{r10}e^{ipt}, \qquad \phi_1 = \phi_{10}e^{ipt}, \qquad \text{etc.} & \end{aligned}\right\} \tag{17}$$

A solution is easily effected provided we know the free normal modes for each system in order to compute the k's.

It is apparent that the use of normal coördinates offers no simplification over ordinary coördinates, when a complete solution is required. Some approximations, however, can best be shown through normal coördinates.

The rigid displacements can be assumed small compared with normal vibrations of an excited mode. Further, we will assume the 2nd mode of system (1) excited and k_2'' large for this mode. This means a large oscillation at the gear. Therefore, the system approximates to

$$\left.\begin{aligned} \ddot{\phi}_2 + n_2^2\phi_2 + B\frac{\gamma_2 k_2''}{A_2}[\dot{\phi}_4 + \gamma_2 k_2''\dot{\phi}_2] &= \frac{k_3''}{A_2}\Phi_3 e^{ipt}, \\ \ddot{\phi}_4 + n_4^2\phi_4 + B/A_4[\dot{\phi}_4 + \gamma_2 k_2''\dot{\phi}_2] &= 0. \end{aligned}\right\} \tag{18}$$

V.2 194

Therefore,

$$\left.\begin{aligned} \ddot{\phi}_2 + \frac{b_{22}}{A_2}\dot{\phi}_2 + n_2{}^2\phi_2 + \frac{b_{24}}{A_2}\dot{\phi}_4 &= \frac{k_3{}''}{A_2}\Phi_3 e^{ipt}, \\ \ddot{\phi}_4 + \frac{b_{44}}{A_4}\dot{\phi}_4 + n_4{}^2\phi_4 + \frac{b_{42}}{A_4}\dot{\phi}_2 &= 0, \end{aligned}\right\} \qquad (19)$$

where

$$b_{24} = b_{42} = B\gamma_2 k_2{}'',$$
$$b_{22} = B\gamma_2{}^2 k_2{}''^2, \qquad b_{44} = B,$$

and we have a simple two degree damped vibration system. This shows the nature of the physical interaction of the coupling.

Let

$$\phi_2 = \phi_{20}e^{ipt}, \qquad \phi_4 = \phi_{40}e^{ipt},$$

$$\left.\begin{aligned} \left(n_2{}^2 - p^2 + ip\frac{b_{22}}{A_2}\right)\phi_{20} + ip\frac{b_{24}}{A_2}\phi_{40} &= \frac{k_3{}''}{A}\Phi_3, \\ ip\frac{b_{42}}{A_4}\phi_{20} + \left(n_4{}^2 - p^2 + ip\frac{b_{44}}{A_4}\right)\phi_{40} &= 0; \end{aligned}\right\} \qquad (20)$$

$$\left.\begin{aligned} \therefore \quad \phi_{20} &= \frac{\left(n_4{}^2 - p^2 + ip\dfrac{b_{44}}{A_4}\right)\dfrac{k_3{}''}{A_2}\Phi_3}{D}, \\ \phi_{40} &= \frac{-\,ip\dfrac{b_{24}}{A_4}\dfrac{k_3{}''}{A_2}\Phi_3}{D}, \end{aligned}\right\} \qquad (21)$$

where

$$D = \left(n_2{}^2 - p^2 + ip\frac{b_{22}}{A_2}\right)\left(n_4 - p^2 + ip\frac{b_{44}}{A_4}\right) + p^2\frac{b^2{}_{24}}{A_2A_4}\cdot$$

Now in our approximation, we have assumed the 2d mode of the first system to be excited by the torque $\Phi_3 e^{ipt}$. This means that we assume $n_2 = p$ nearly. Hence the factor $n_2{}^2 - p^2 + ip\dfrac{b_{22}}{A_2}$ approaches $ip\dfrac{b_{22}}{A_2}$ and D reduces to

$$D = ip\frac{b_{22}}{A_2}\left(n_4{}^2 - p^2 + ip\frac{b_{44}}{A_4}\right) + p^2\frac{b^2{}_{24}}{A_2 \cdot A_4},$$

so that the vibration torque transmitted through the coupling is,

$$\Phi_{C0} = B[\dot{\phi}_{40} + \gamma_2 k_2''\dot{\phi}_{20}] = Bip[\phi_{40} + \gamma_2 k_2''\phi_{20}]$$

$$\therefore \quad \Phi_{C0} = \frac{B}{D}\left[p^2\frac{b_{24}}{A_4} + i\gamma_2 k_2'' p\left(n_4^2 - p^2 + ip\frac{b_{44}}{A_4}\right)\right]\frac{k_3''}{A_2}\Phi_3$$

$$= \frac{B\left[p\dfrac{b_{24}}{A_4} + i\gamma_2 k_2''\left(n_4^2 - p^2 + ip\dfrac{b_{44}}{A_4}\right)\right]k_3''\Phi_3}{p\dfrac{b^2_{24}}{A_4} + ib_{22}\left(n_4^2 - p^2 + ip\dfrac{b_{44}}{A_4}\right)}$$

since

$$b_{24} = B\gamma_2 k_2'', \qquad b_{22} = B\gamma_2^2 k_2''^2$$

$$\therefore \quad \Phi_{C0} = \frac{k_3''\Phi_3}{\gamma_2 k_2''}, \qquad \text{when } n_2 \text{ approaches } p.$$

If we isolate system I, the work of the applied torque Φ_3 must balance the work of the damping torque Φ_{C0} at the coupling, i.e.,

$$\Phi_3 \cdot k_3''\delta\phi_2 - \Phi_{C0} \cdot \gamma_2 k_2''\delta\phi_2 = 0,$$

at resonance for the second mode of this sytem.

The corresponding angular displacements at the coupling, are,

$$\phi_2 = \frac{\left(n_4^2 - p^2 + ip\dfrac{b_{44}}{A_4}\right)\dfrac{k_3''}{A_2}\Phi_3 e^{ipt}}{ip\dfrac{b_{22}}{A_2}\left(n_4^2 - p^2 + ip\dfrac{b_{44}}{A_4}\right) + p^2\dfrac{b^2_{24}}{A_2 A_4}}$$

since $b^2_{24} - b_{22}b_{44} = 0$ for excitation of the second mode, therefore,

$$\therefore \quad \phi_2 = \left[1 + i\left(\frac{p \cdot \dfrac{b_{44}}{A_4}}{n_4^2 - p^2}\right)\right]\frac{k_3''\Phi_3 e^{i(pt-\pi/2)}}{pb_{22}}$$

and,

$$\phi_4 = -\frac{\dfrac{b_{24}}{A_4} \cdot k_3''\Phi_3 e^{ipt}}{b_{22}(n_4^2 - p^2)} = -\frac{k_3''\Phi_3 e^{ipt}}{\gamma_2 k_2'' A_4(n_4^2 - p^2)}$$

$$\therefore \quad \phi_4 = -\frac{\Phi_{C0}e^{ipt}}{A_4(n_4^2 - p^2)}, \qquad \text{since} \qquad \Phi_{C0} = \frac{k_3''\Phi_3 e^{ipt}}{\gamma_2 k_2''}$$

that is, the *external* torque exciting system II is the coupling torque Φ_{C0}.

When the second system is not excited, then ϕ_2 approaches

$$\frac{k_3''\Phi_3 e^{i(pt-\pi/2)}}{pb_{22}} \quad \text{and} \quad \phi_4 \doteq 0.$$

When, in addition, the frequency of the second system is in close proximity with the exciting frequency, then $n_4 = p$ nearly, so that both the amplitudes ϕ_2 and ϕ_4 are large and the damping of the coupling becomes ineffective.

In general, however, the coupling acts as an effective dampener for any mode of vibration of the systems on either side of the coupling, and in particular for those modes whose nodes are away from the coupling.

COMBINATION OF TORQUE CONVERTER WITH FLUID COUPLING.

Very satisfactory torque characteristics and high efficiencies are obtained by combining the torque converter with the fluid coupling. The combination can be done in two ways. The one way is to arrange two circuits, one for the converter and another one for the clutch. By filling or emptying the one or the other, a change over from converter to coupling is effected. The other way is that used in the Trilok Gear. This contains only one casing, in which the guide wheel for converter drive remains stationary. As a coupling, the guide vane rotates with the turbine. The change over is caused when the secondary torque approaches the primary one and is effected automatically through a free wheel drive.

The change over occurs approximately at 1.5 times the rated speed, i.e., the speed corresponding to maximum converter output. If the converter output curve drops to $\frac{3}{4}$ the maximum output at 1.5 rated speed, this means an overall efficiency at change over at $\frac{3}{4} \times 0.85 = 0.64$.

After change over from converter to coupling, there is no further torque amplification. The transmission therefore operates directly on the torque-speed characteristics of the engine.

Assuming constant engine torque, the change over from converter to coupling (or clutch) requires a reduction in engine speed consistent with torque-speed-slippage characteristics. Let Φ_P = primary or engine torque and ω_P = primary speed. Let Φ_S = secondary or output torque and ω_S = secondary speed. Let ϵ_R = transmission efficiency at rated output speed. Let x = relative efficiency at change over compared with rated output. Then at change over the overall efficiency is $\epsilon = x\epsilon_R = 0.64$ (approx.).

Let ω_{PR} = normal or rated *engine* speed. Then, *just before change over,* the secondary or output speed of the converter is $\omega_{SM} = 1.5\omega_{SR}$ approx. or in general,

$$\epsilon\Phi_P\omega_{PR} = \Phi_{SM}\omega_{SM}; \qquad \therefore \quad \omega_{SM} = \frac{\epsilon\Phi_P\omega_{PR}}{\Phi_{SM}}.$$

Since $\Phi_{SM} = \Phi_P$ approx. for *the turbine torque, at change over,* therefore $\omega_{SM} = \epsilon\omega_{PR}$ (approx.).

After change over, operating with the coupling, $\Phi_P = \Phi_S$ *always,* and $\omega_S = (1 - S)\omega_P$. With the coupling, just after change over let $\omega_P = \omega_{P2}$ where ω_{P2} is the *lowered* engine speed. The output shaft has the previous converter speed ω_{SM}. The efficiency of the coupling is $1 - S$, at change over. Hence,

$$\Phi_S\omega_{SM} = (1 - S)\Phi_P\omega_{P2};$$

$$\therefore \quad \omega_{P2} = \frac{\omega_{SM}}{1 - S}, \qquad \text{since} \qquad \Phi_S = \Phi_P,$$

and the drop in engine speed, noting $\omega_{SM} = \epsilon\omega_{PR}$,

$$\omega_{PR} - \omega_{P2} = \left[1 - \frac{\epsilon}{1 - S}\right]\omega_{PR} \text{ (approx.).} \qquad (23)$$

The slip S and the reduced engine speed ω_{P2} are not independent. Assuming constant engine torque Φ_{PR},

$$\Phi_{PR} = K\omega^2{}_{P2}f(S) = K\omega^2{}_{PR}f(S)_0;$$

$$\therefore \quad (1 - S)\sqrt{\frac{f(S)_0}{f(S)}} = \epsilon \text{ approx.,} \qquad (24)$$

or alternately,

$$S = F\left(\frac{\Phi_{PR}}{\omega_P{}^2}\right) = F\left[\left(\frac{\Phi_{PR}}{\omega^2{}_{PR}}\right)\left(\frac{\omega^2{}_{PR}}{\omega_P{}^2}\right)\right],$$

where the function F depends upon the coupling size.

The change over from converter to coupling occurs at roughly two-thirds the maximum speed range. To extend the speed range two couplings can be used with the converter. The primary parts of converter and the two couplings are driven at the same speed. The secondary part of the first coupling is connected with a speed reduction gear while the secondary part of the second coupling is in direct drive. In this way the range of operation of the converter can be reduced to less than 50 per cent. of the maximum speed range. At each change over the engine speed is dropped in the order of 25 per cent.

The future of the torque converter is to improve the efficiency at both over and under speeds relative to its rated value. In this way (1) the entire speed range is materially extended, (2) the torque amplification at starting is increased, (3) the drop in power and engine speed at converter to coupling change over is reduced and (4) weight reduction and simplification are then further possible. The use of improved entrance blade design, with a tendency toward multiple stages, appears helpful, while a simple mechanism for varying the blade angles of the impeller should prove most promising.

Acknowledgment: The author is particularly indebted to Prof. W. Spannhake, who critically reviewed the preliminary manuscript with helpful suggestions, and later to Dr. T. D. Cope for his careful review of the paper in its final form. Acknowledgment is also due to Dr. James Barnes for sugfestions and to Mr. Walter Hammer and Mr. F. S. Chaplin for aiding the author.

APPENDIX.

1. Flow of Fluid in Stationary Channel.

Let C_r and C_U be the radial and tangential velocities, ρ the density, p the pressure, r, z and θ the cylindrical coordinates of a particle, and C_z the velocity in the axial direction. Then

$$\frac{dC_r}{dt} - \frac{C_U^2}{r} = q_r - \frac{1}{\rho}\frac{\partial p}{\partial r}, \qquad \text{(1) radial motion,}$$

$$\frac{d(C_U r)}{dt} = \left(q_U - \frac{1}{\rho}\frac{\partial p}{r\partial\theta}\right) r = \text{change in Ang. Momentum;}$$

$$\therefore \frac{dC_U}{dt} + \frac{C_U C_r}{r} = q_U - \frac{1}{\rho}\frac{\partial p}{r\partial\theta}, \qquad \text{(2) tangential motion,}$$

$$\frac{dC_z}{dt} = q_z - \frac{1}{\rho}\frac{\partial p}{\partial z}, \qquad \text{(3) axial motion,}$$

with the equation of continuity,

$$\frac{\partial(\rho C_r r)}{\partial r} + \frac{\partial(\rho C_U r)}{r\partial\theta} + \frac{\partial(\rho C_1 r)}{\partial z} + r\frac{\partial\rho}{\partial t} = 0$$

or

$$\frac{\partial(C_r r)}{\partial r} + \frac{\partial(C_U r)}{r\partial\theta} + \frac{\partial(C_z r)}{\partial z} = 0 \qquad (4) \text{ for const. } \rho.$$

Since the motion is irrotational, we have the rotations about the r, z and the normal to the plane of rz, at a particle, nil. That is the respective circulations are

$$\left.\begin{aligned} \frac{\partial C_z}{r\partial\theta} - \frac{\partial C_U}{\partial z} &= 0, \\ \frac{1}{r}\frac{\partial(C_U r)}{\partial r} - \frac{\partial C_r}{r\partial\theta} &= 0, \\ \frac{\partial C_r}{\partial z} - \frac{\partial C_z}{\partial r} &= 0. \end{aligned}\right\} \qquad (5)$$

Thus, for the circulation at a point around the z axis we have

$$C_r dr + \left(C_U + \frac{\partial C_U}{\partial r}dr\right)(r + dr)d\theta - \left(C_r + \frac{\partial C_r}{r\partial\theta}\cdot rd\theta\right)dr - C_U rd\theta = 0;$$

$$\therefore \frac{\partial C_U}{\partial r} + \frac{C_U}{r} - \frac{\partial C_r}{r\partial\theta} = \frac{1}{r}\frac{\partial(C_U r)}{\partial r} - \frac{\partial C_r}{r\partial\theta} = 0.$$

2. Flow of Fluid in a Rotating Channel.

The relative velocities are v_r and v_U, where $v_r = C_r$ and $v_U = C_U - \omega r$. On substituting these values in the previous equations, noting $\theta = \phi + \omega t$,

$$\frac{dv_r}{dt} - \frac{v_U^2}{r} - 2v_U\omega - \omega^2 r = q_r - \frac{1}{\rho}\frac{\partial p}{\partial r}, \qquad (6)$$

$$\frac{dv_U}{dt} + \frac{v_U v_r}{r} + 2v_r\omega = q_U - \frac{1}{\rho}\frac{\partial p}{r\partial\phi}, \qquad (7)$$

$$\frac{dv_z}{dt} = q_z - \frac{1}{\rho}\frac{\partial p}{\partial z}, \qquad (8)$$

where $2v_U\omega$ and $2v_r\omega$ are the components of the Coriolis acceleration due to the *relative* motion in the rotating channel. Since the *absolute* rotation is nil, on substituting $C_U = v_U + \omega r$, $C_z = v_z$, $C_r = v_r$, we have

$$\left.\begin{aligned} 2w_r &= \frac{\partial v_r}{r\partial\theta} - \frac{\partial v_U}{\partial z} = 0, \\ 2w_z &= \frac{\partial v_U}{\partial r} + \frac{v_U}{r} - \frac{\partial v_r}{r\partial\phi} = -2\omega, \\ 2w_n &= \frac{\partial v_r}{\partial z} - \frac{\partial v_z}{\partial r} = 0, \end{aligned}\right\} \qquad (9)$$

where w_r, w_z and w_n are the corresponding rotations. The *relative* rotation about the z axis, i.e., the axis of rotation of the channel, is then

$$w_z = -\omega.$$

3. Applied Acceleration Components.

H. Lorenz introduced the acceleration components q_r, q_U and q_z, as an equivalent system of forces per unit volume, equal to the unbalanced surface pressures of the blades on the fluid. Since the channel exerts a torque on the fluid, the streamlines are subjected to lateral unbalanced pressures, which are exactly equivalent to applied acceleration components normal to the stream flow. Therefore, for the applied acceleration components to be equivalent to the torque reaction of the blades, the moment of the tangential acceleration components must be equal to the rate of change of the angular momentum of the particles, while the summation of these moments is equal to the change of angular momentum of the entire fluid flowing through the blades, and, therefore, to the total torque exerted by the blades on the fluid.

Hence,

$$\frac{d(C_U r)}{dt} = \frac{dv_U}{dt} + \frac{v_U v_r}{r} + 2v_r\omega = q_U \cdot r, \tag{11}$$

where

$$\int \rho q_U dV \cdot r = \int \rho \frac{d(C_U r)}{dt} dV = \Phi \tag{12}$$

and $1/\rho \dfrac{\partial p}{r\partial\phi}$ is omitted, since it is already included in q_U.

Another condition is that the total work of the applied acceleration components must be equivalent to the torque per unit mass times the angular velocity of the channel. Using relative velocity, we have, since $v_r = C_r$, $v_z = C_z$,

$$q_r v_r + q_z v_z + q_U(v_U + \omega r) = \omega \frac{d(C_U r)}{dt}. \tag{13}$$

Since

$$q_U r \cdot \omega = \frac{d(C_U r)}{dt} \cdot \omega, \tag{14}$$

therefore,

$$q_r v_r + q_z v_z + q_U v_U = 0,$$

which shows the *applied acceleration components must be normal to the relative flow streamlines*. This condition is also evident since the resultant is due to the normal pressure of the channel wall surfaces.

4. Relative Streamline Functions.

On multiplying equations (6), (7) and (8) by v_r, v_U and v_z noting $\dfrac{1}{\rho}\dfrac{\partial p}{r\partial\phi} = 0$ and $q_r v_r + q_U v_U + q_z v_z = 0$, we have

$$v_r dv_r + v_U dv_U + v_z dv_z - \omega^2 r dr = -1/\rho\left[\frac{\partial p}{\partial r}dr + \frac{\partial p}{r\partial\phi}\cdot r d\phi + \frac{\partial p}{\partial z}dz\right]; \tag{16}$$

$$\therefore \quad \frac{v^2}{2} - \frac{\omega^2 r^2}{2} + \frac{p}{\rho} = C, \tag{17}$$

where C varies for each streamline.

Let us now consider the stream function ψ defined as

$$v_z r = \frac{\partial\psi}{\partial r}, \qquad v_r \cdot r = -\frac{\partial\psi}{\partial z}. \tag{18}$$

Since $\dfrac{\partial v_z}{\partial r} - \dfrac{\partial v_r}{\partial z} = 0$ for the irrotational motion,

$$\therefore \quad \frac{\partial^2\psi}{\partial z^2} + \frac{\partial^2\psi}{\partial r^2} - \frac{1}{r}\frac{\partial\psi}{\partial r} = 0. \tag{19}$$

Obviously ψ itself is a function of ϕ, and for a given ϕ, $\psi = C\phi$. The significance of ψ can be shown as follows. Since the channel walls are tangent to the streamlines, then if ψ_1 and ψ_2 are the corresponding stream functions, we have

$$2\pi(\psi_1 - \psi_2) = Q; \qquad \therefore \quad d\psi = \frac{1}{2\pi}dQ, \tag{20}$$

where Q is the total flow rate through a channel, and the torque is,

$$\Phi = \rho\frac{Q}{g}[(C_Ur)_2 - (C_Ur)_1] \text{ per channel.} \tag{21}$$

In terms of the stream function, $\psi(z, r)$

$$\Phi = \frac{\rho}{g}\int\frac{\partial(C_Ur)}{dt}\cdot dV, \qquad dV = 2\pi rdrdz$$

$$\therefore \quad \Phi = \frac{2\pi\rho}{g}\int\int\left[\frac{\partial(C_Ur)}{\partial z}\cdot v_z + \frac{\partial(C_Ur)}{\partial r}\cdot v_r\right]rdr\cdot dz$$

Since

$$v_zr = \frac{\partial\psi}{\partial r}, \qquad v_rr = -\frac{\partial\psi}{\partial r}$$

$$\therefore \quad \Phi = \frac{2\pi\rho}{g}\int\int\left[\frac{\partial(C_Ur)}{\partial z}\cdot\frac{\partial\psi}{\partial r} - \frac{\partial(C_Ur)}{\partial r}\cdot\frac{\partial\psi}{\partial z}\right]dr\cdot dz \tag{22}$$

but,

$$\Phi = \frac{\rho}{g}\int\int dQ\cdot d(C_Ur) = \frac{2\pi\rho}{g}\int\int d\psi\cdot d(C_Ur)$$

$$\therefore \quad \frac{\partial(C_Ur)}{\partial z}\cdot\frac{\partial\psi}{\partial r} - \frac{\partial(C_Ur)}{\partial r}\cdot\frac{\partial\psi}{\partial z} = d\psi\cdot d(C_Ur) \tag{23}$$

This equality suggests the transformation of r and z to new variables ψ and C_Ur i.e., $r = f_1(\psi, C_Ur)$ and $z = f_2(\psi, C_Ur)$.

The improvement in efficiency of the torque converter requires a reduction in shock losses at speeds differing from the optimum speed.

If we take for the *control* surfaces those sections between any two blade systems, the momentum transferred across such sections is complicated by the irregularity of the flow due to eddying.

For a circumferential control surface, let s the circumference distance (or arc); then the angular momentum transferred per unit time per unit width is

$$\text{A.M.} = \rho\int^{s}\overline{C_r\cdot C_Ur}ds = \rho\int_0^{s}\overline{v_r\cdot(v_U + \omega r)}rds,$$

where C_r = radial velocity ⊥ to control surface, C_U = tangential velocity, and v_r and v_U are the corresponding relative values. Now both C_r and C_U are functions of s depending upon the nature of the eddying across the section.

The flow across the control surface may be considered as the resultant of velocity components of three stream functions:

- ψ_1 a relative radial potential flow, which has no effect on causing torque on the blades.
- ψ_2 a circulation flow, which accounts for the mean torque on the blades in combination with
- ψ_3 a relative eddying flow with a circulation corresponding to the *negative* rotation of the wheel. Se eq. (9).

V.2
194

Then the resultant potential is, ($\psi' = f(r, rd\phi)$)

$$\psi' = \psi_2 + \psi_1 + \psi_3,$$

$$v_r = -\frac{\partial\psi'}{rd\phi}, \qquad v_U = \frac{\partial\psi'}{\partial r}, \qquad rd\phi = dS_{\text{rel}}.$$

Now at each control surface between blade systems, we have a circumferential circulation Γ_1, Γ_2 and Γ_3 where $\Gamma = 2\pi r\bar{C}_U$ and $\bar{C}_U$ is the mean tangential velocity. Further the circulation flow is $Q = 2\pi r\bar{C}_r \cdot l$ where l depth of blades, and C_r is the mean normal (or radial) velocity.

The circulation around each bucket blade, where number of blades, is defined as

$$n_P\Gamma_P = \Gamma_2 - \Gamma_1 \qquad \text{and} \qquad n_S\Gamma_S = \Gamma_2 - \Gamma_3,$$

where Γ_P and Γ_S are the bucket circulations for impeller and turbine. Therefore,

$$\Phi_P = \frac{\rho Q}{g}(r_2C_{U2} - r_1C_{U1}) = \frac{\rho Q}{2g\pi}n_P\Gamma_P, \tag{24}$$

which is the reaction on the flow, due to pump impeller.

$$\Phi_S = \frac{\rho Q}{g}(r_2C_{U2} - r_3C_{U3}) = \frac{\rho Q}{2g\pi}n_S\Gamma_S, \tag{25}$$

Which is the *counter* reaction on the flow due to turbine rotor, since $\Gamma_2 > \Gamma_3$.

In addition, we have a *positive* reaction on the flow due to the guide blades, since $\Gamma_1 > \Gamma_3$

$$\Phi_g = \frac{\rho Q}{g}(r_1C_{U1} - r_3C_{U3}) = \frac{\rho Q}{2g\pi}n_g\Gamma_g \tag{26}$$

Evidently;

$$n_P\Gamma_P + n_S\Gamma_S + n_g\Gamma_g = (\Gamma_2 - \Gamma_1) + (\Gamma_3 - \Gamma_2) + (\Gamma_1 - \Gamma_3) = 0$$

that is, the total circulation corresponding to the total change in Ang. momentum, about the shaft axis is nil.

For the function which accounts for the relative eddying flow, we have the *negative* circulation for the *relative* flow in any rotating blades channel given by

$$\omega_z = \frac{\partial v_U}{\partial r} + \frac{v_U}{r} - \frac{\partial v_r}{r\partial\phi} = -2\omega \qquad \text{(see eq. 9)}$$

$$\therefore \quad \frac{\partial^2\psi^1}{\partial r^2} + \frac{1}{r}\frac{\partial\psi^1}{\partial r} + \frac{\partial^2\psi^1}{r^2\partial^2\phi} = -2\omega$$

where $\omega_z = -\omega$ is the *relative* induced vortex motion due to the rotation ω about the shaft axis.

Transferring to rectangular coordinates, this equation as suggested by Kurcharski, becomes identical to that of a stretched membrane with initial tension to per unit run and a pressure so adjusted that the *slopes* of the membrane then correspond to the relative velocities, with boundaries along the blades.

The resultant flow is obtained by superimposing the radial, the eddying or rotational flow and the circulation.

It is important to note that detachment of the flow from the driving face of the blade in the impeller pump takes place when the velocity along the blade surface due to the relative counter eddy caused by the wheel rotation exceeds the velocity due to the radial potential flow. The eddy velocity is roughly proportioned to the angular velocity of the wheel times the blade width, while the radial velocity is proportional to the flow rate. Thus a minimum flow rate is required for a given speed of rotation. Due to the increasing width of widely spaced blades away from the axis, the eddying velocity is increased requiring increased flow rate.

REFERENCES.

Handbuch der Physik, Band VII, by R. Grammel.
Technische Hydromechanik, by H. Lorenz.
Steam and Gas Turbines, by A. Stodola.
Centrifugal Pumps, Turbines and Propellers, by W. Spannhake.

ELIHU THOMSON—IN RETROSPECT.

BY

EMILY DUANE WALLACE.

Just ninety years after the birth of Elihu Thomson, let us stop momentarily to review a few of the highlights in his versatile life.

Although his name is not generally known to the millions of people whose lives have been made easier by his devices, there are few homes and cities in America which have been unaffected by the results of his experiments.

Most of the electrical apparatus he invented for peacetime comforts have now been transformed to meet the demands of war. Well constructed dynamos, made from his principles, are supplying the power for machinery in our production plants, and also for Edison's light bulbs, trains, traffic signals, meters, as well as many treasured household products.

He also gave us the process of electric resistance welding by which pieces of metal are united by the passing of an electric current through the joint. This method was previously used in the automobile industry, and is now essential in assembling tanks and planes, and other war necessities.

Many people who do know of him associate his name with the arc lighting system which is used in many parts of the world, but this is just one of his contributions.

At The Franklin Institute, where he first presented a number of his scientific discoveries, there is an historical collection of some models of his early apparatus. These include transformers of the shell and core types, spherical, and 2-coil armatures, as well as T-H regulator. There is also a model of the first dynamo, which he made in 1873, for which he used asphalt cement to hold the parts together.

Born in Manchester, England, in 1853, Elihu Thomson came to Philadelphia with his family five years later. After graduating from the Boys' Central High School with high honors, he became Assistant Professor of Chemistry at the school, without ever attending college. When he was 22, he was given a full Professorship in chemistry and mechanics.

In the school building at Broad and Green Streets, he made the first successful experiments on which our modern methods of radio broadcasting and receiving are based. With Edwin J. Houston, the Science Professor, the first experiments were also completed in the transmission of electrical magnetic waves, ten years before Hertz proved their existence. (Hertz was the German inventor who is usually accredited with the recognition of the electric waves, which were named in his honor. This was the ground work that enabled Marconi to follow on, and develop our present system of wireless communications.) Although Thomson had succeeded in sending signals by wireless, he left the job of commercializing these investigations to others, and continued to develop other electrical phenomena.

During his student years, there was a jobbing shop known as the Harrison Machine Works on what is now Ludlow Street, and the proprietor allowed the youthful scientist to use his tools and equipment. Here he made his first Bi-phase dynamo, although they were later referred to as Alternators. He made his own wood patterns, operated the crude machines that were then available, and did all the winding of the armature, and fields. This dynamo has been preserved, and is now in The Franklin Institute.

In 1883, he gave up teaching to devote his time exclusively to the development and manufacture of electrical apparatus. His prime interest was in developing things to be useful to mankind and to enable them to be produced at less cost. It has been estimated that he held over 700 patents during his life, which ended on March 13, 1937, having received his first one when he was eleven. With Professor Houston as his partner, he organized the Thomson-Houston Electric Co., which later merged with the Edison General Electric Co., and is now the General Electric Co.

Always profoundly interested in the safety of his inventions, Thomson would never permit their production until devices had been made to eliminate the obvious dangers. It was this never failing interest which led him to make possible the use of alternating current. Even after the entire arc lighting system had been worked out successfully, he would not allow it to be installed until he had invented devices, which minimized the possibility of injuries from fire, or from the fatal shock, which might result from contact with the high voltage.

He applied his inventive genius to his numerous hobbies and made many noteworthy contributions. He was the first to take X-ray stereoscopic pictures, and the builder of the original high frequency machine. Also he made a microscope containing ten lenses, a long range telescope, and an electric pneumatic pipe organ, with 25 stops, which he played.

A member of The Franklin Institute for 64 years, he was a frequent contributor to the JOURNAL. At the age of 23, he gave a course of five lectures on Electricity. From 1878 to 1881, he served on the Board of Managers, and was four times the recipient of Institute awards. Twice winner of the Scott medal, once of the Cresson, and in 1928 he was the first Philadelphian to receive the Franklin medal, the highest award given by the Institute for scientific achievement.

Twin Drydocks Constructed Under Water.—(*Engineering News-Record*, Vol. 129, No. 21.) Adjacent drydocks are being built at an eastern navy yard for construction of large ships of war. Supported on steel H piles, these shipbuilding drydocks are huge concrete boxes with bottom, inshore end and sides of tremie-placed concrete, the outshore end being closed by a floating caisson. Thus a large part of the work is done under water, and what makes the job more difficult, it is located in an area congested with all manner of other construction work that cannot be delayed or interfered with. These drydocks therefore constitute a construction job of first magnitude. Although drydocks have been used for many years for repair and maintenance of ships, it is only recently that the Navy and the Maritime Commission have built such basins for ship construction purposes. In a drydock a ship can be built on a level keel, which simplifies the framing and assembling of the steel structure and eliminates the time consumed in computations and measurements necessary to insure members being in proper relation to each other as is necessary on inclined ways. The speed of erection is also accelerated as less bolting and bracing are required to hold parts in true position while the riveting or welding is completed. Nor do temporary structural members have to be put into the ship to resist launching stresses as is necessary on way building. Finally when ships are built in basins, the big guns and superstructures can be installed (limited only by the capacity of the dock cranes), whereas the use of ways requires that the addition of such heavy pieces be postponed until after the ship is launched. Launching from basins merely requires letting water in through tunnels, which are built into the side walls, after which the completed ship merely floats off the keel blocks. Another advantage of building in a drydock rather than on inclined ways is the simpler and less expensive materials-handling equipment that is required. Full revolving cranes on low gantries can service the ship construction, eliminating the high and elaborate overhead structure used for building ships on conventional ways. Also, the cranes are on wide gage tracks and are designed to move around much of the yard, thus reducing the total equipment necessary.

R. H. O.

THEORY OF THE HALFTONE PROCESS. II. THE DIFFRACTION THEORY—CALCULATION OF THE LIGHT DISTRIBUTION.

BY

J. A. C. YULE.

Communication No. 916 from the Kodak Research Laboratories, Rochester, N. Y.

SUMMARY.

An approximate method of calculating the light distribution in the dots formed behind a halftone screen from the Fresnel diffraction theory is described, and in a typical case, the distribution is found to check closely with that determined experimentally, being very different from that calculated from geometrical optics.

In a previous paper [1] the observed light distribution in the dots formed behind a halftone screen, under typical conditions used in making halftone negatives, was found to be very different from the distribution calculated from the penumbra theory (geometrical optics). It remains to calculate the light distribution from the theory of diffraction.

This calculation, if carried out in an exact and generalized manner, appears to involve a laborious and complicated mathematical analysis and may even be impossible. However, a simplified method is satisfactory for the calculation in a special case, and it is found experimentally that deviations from the conditions applying to this special case do not lead to discrepancies of any importance in halftone work. Probably, the reason for this is that the lens aperture used in practical halftone work is not a point source of light, but is relatively large so that all fine details of the diffraction pattern are completely lost.

The calculation is carried out in three steps:

1. The light distribution behind a parallel-line screen with a very small lens aperture, i.e., a point source of light, is calculated.

2. The result of crossing two parallel-line screens at right angles is found, a point source of light again being used.
3. Regarding the normal lens aperture as consisting of a large number of incoherent point sources of light, each of which independently produces a diffraction pattern slightly displaced relative to the others, all these diffraction patterns are added up to produce the total light distribution. This is the method of approach used by Fruwirth and Mertle.[2]

The Theory of Diffraction:

A brief description of Fresnel's theory of diffraction will first be given. For further details, see C. F. Meyer's textbook on diffraction or any advanced treatise on light.[3]

In Fig. 1, L is a point source of light, S is a screen with an aperture in it, and P is the so-called "field point" at which the intensity of light is to be found. Each point in the aperture, for instance, the point A, is regarded as a secondary light source, from which secondary waves originate. The amplitude of light reaching P is the resultant of the waves from all points in the screen aperture. However, the waves which do not travel in a straight line from L to P go along a somewhat longer path, and hence arrive at P a little later. Those which arrive just half a wave apart, so that the crest of one wave arrives at the same moment as the trough of another, exactly neutralize each other. When the effects of all these waves are added, it is found that the light at the point P is bright if the waves mostly reinforce each other.

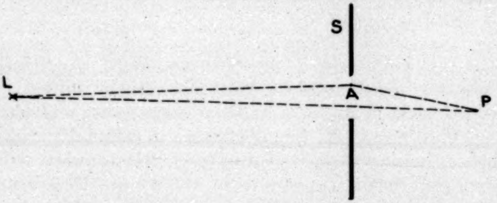

FIG. 1. Diffraction by a small opening in a screen S.

On the other hand, if most of the waves reaching this point neutralize each other, the light at *P* is relatively weak.

Waves which arrive simultaneously, or exactly one, two, three, etc., wave lengths apart, reinforce each other. Those which arrive 0.5, 1.5, 2.5, etc., wave lengths apart neutralize each other. In most positions in the geometrical shadow behind the screen, they tend to neutralize each other, and behind the clear portions of the screen, they reinforce each other. This is the reason for the formation of a shadow, and means that light appears to travel in approximately straight lines. Waves arriving at intermediate times may partly reinforce or partly neutralize each other, and the total effect may be found by calculation or by the use of a so-called vibration curve. The Cornu spiral, Fig. 2, may be used as a vibration curve for determining the light distribution behind a straight edge, a slit, or a series of parallel slits, such as a parallel-line screen. It does not apply, however, to openings at a considerable distance from the direct ray, which are

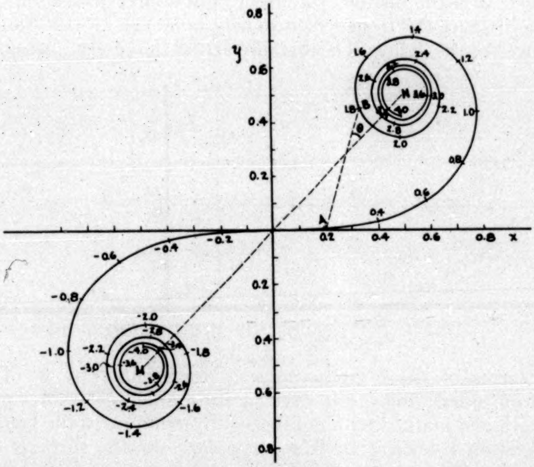

FIG. 2. Cornu spiral.

found to have a negligible effect in comparison with the nearest openings in the typical case under consideration.

The curve is used as follows: In an optical system, such as Fig. 3, a straight line drawn from light source to field point passes through the screen at O. A line is drawn across the screen through O at right angles to the edges of the slit (greatly enlarged in the diagram) and is divided into equal parts, the length of each unit being equal to $\sqrt{\frac{ab\lambda}{2(a+b)}}$, where a is the distance LO from light source to screen, b is the distance OP from screen to field point, and λ is the wave length of the light. The distance across the screen, measured in terms of these graduations, is represented by v. The Cornu spiral, Fig. 2, is divided into small parts of equal length and marked with numbers corresponding to the graduations on the slit. In this particular case the slit extends from $v = 0.2$ to 1.8, P being a point in the geometrical shadow of the screen near the edge of the slit.

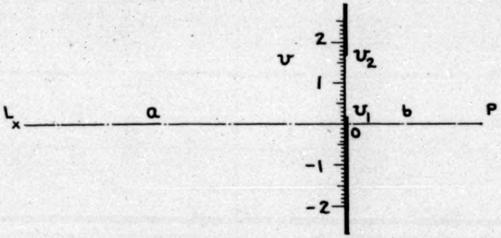

FIG. 3. Calibration of a slit in terms of v.

The points of the Cornu spiral marked thus are joined by a straight line AB. The length of this line represents the amplitude of the light reaching the point P. The amplitude with no screen present, which is the same as that with an infinitely wide slit, is represented by the length of the line MN. The change of phase of the light due to the screen is given by the angle θ between these lines. The amplitude and phase of the light reaching the point P from other parallel slits can be found in the same way. Under normal conditions of use of a halftone screen, it is found experimentally that the nearest three slits of a parallel-line screen are the only ones which have an important influence on the light distribution at the point *P*. In Fig. 4, *A* is a diagram of the optical system. The lines representing the three slits of the screen, *a*, *b*, and *c*, nearest to the field point, are shown on the Cornu spiral. It is not sufficient merely to add the amplitudes of the light arriving from different slits, since, if the phases are opposite, they will tend to neutralize each other. Their amplitudes and phases, i.e., the lengths and directions of the lines, must be combined vectorially by placing the lines end to end, as in Fig. 4*C*, in which the narrow lines representing the three slits combine to give the resultant shown as a heavy line. After the amplitude has been found in this way at a single point *P*, the process is repeated until a sufficient number of points have been found.

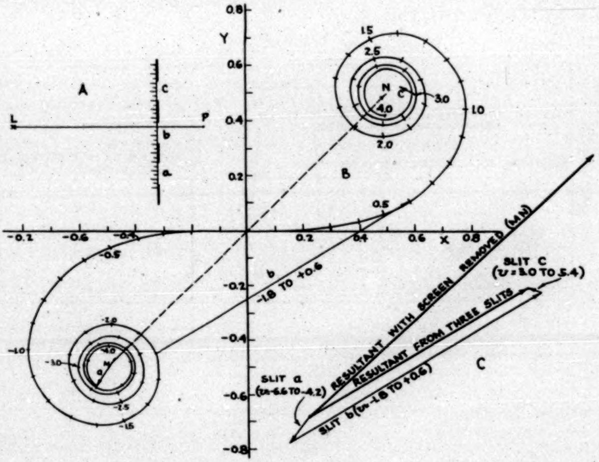
A
L
P
c
b
a
0.8
Y
0.6
0.4
0.2
-0.2
-0.4
-0.6
-0.8
-0.2
-0.6
-0.4
0.2
0.4
0.6
X
0.8
1.5
2.5
N
C
3.0
4.0
1.0
2.0
B
0.5
-0.5
b
-1.8 TO +0.6
-2.0
-1.0
-3.0
-4.0
N
a
-2.5
-1.5
(MN)
RESULTANT WITH SCREEN REMOVED
SLIT C
(v = 3.0 TO 5.4)
RESULTANT FROM THREE SLITS
C
SLIT a
(v=-6.6 TO -4.2)
SLIT b (v=-1.8 TO +0.6)

FIG. 4. Diffraction by a parallel-line screen: *A*—optical system (not to scale); *B*—Cornu spiral showing effects of three slits; *C*—determination of resultant from three slits.

In actual computations it is often more convenient to solve the problem by calculation instead of graphically, as will be shown in the mathematical part.

The resulting light distribution behind a parallel-line screen with equal lines and spaces, the width of each of which is 2.4 in terms of v (for instance, with distance from light source to screen = 23.5 in., screen separation = 0.413 in., wave length = 435 mμ, and screen ruling = 120 lines per inch), is shown in Fig. 5.

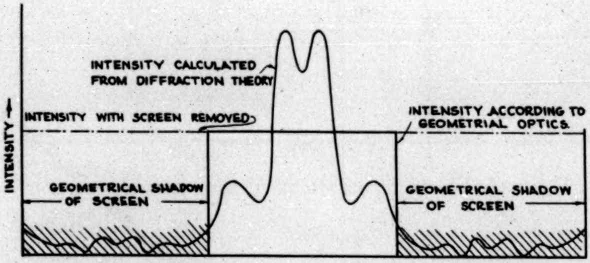

FIG. 5. Calculated diffraction pattern behind a 1 : 1 parallel-line screen, with a small light source, under conditions such that the width of one screen opening equals 2.4 in terms of v.

Crossed Screens:

For the special case which we are considering, it will be shown (see mathematical part) that, with a point source of light, the intensity at a given point of observation, due to two parallel-line screens crossed at right angles, is equal to the product of the intensities which would be produced by each of the screens taken separately, the intensity in the absence of any screen being taken as unity.

This has a superficial similarity to the familiar law of additivity of density of two superimposed layers of any light-absorbing material, although it must be remembered that for diffracting screens it is only true under the restricted conditions under consideration. Each screen may be regarded as having a certain apparent optical density with reference to a point source of light and point of observation. The apparent density of the crossline screen is then equal to the sum of the apparent densities of the two parallel-line screens of which it is composed. This does not refer only to the average intensity observed under conditions where the individual lines of the screen are indistinguishable, but also to the brightness at individual points in the diffraction pattern.

The diffraction pattern for a crossline screen with a point source of light, calculated in this way from the results for a parallel-line screen shown in Fig. 5, is given in Table I.

TABLE I.

Calculated light distribution in the diffraction pattern behind a crossline screen with equal lines and spaces, at such a distance that $v_1 - v_2$, for the two sides of a single opening, equals 2.4, with a point source of light. The two points given in heavy type represent the center and the corner of one screen element. Values are expressed as a percentage of the intensity with the screen removed.

212	262	144	63.0	82.4	83.3	32.7	19.8	9.6	16.2	2.0	22.9	11.4
	324	177	77.8	102.0	103.0	40.3	24.5	13.2	20.0	2.5	28.2	14.0
		97.1	42.6	55.6	56.4	22.1	13.4	6.5	10.9	1.4	15.5	7.7
			18.6	24.4	24.6	9.7	5.9	2.8	4.8	.6	6.8	3.4
				31.9	32.3	12.7	7.7	3.7	6.3	.79	8.9	4.4
					32.7	12.8	7.8	3.8	6.4	.8	9.0	4.5
						5.0	3.0	1.5	2.5	.31	3.5	1.7
							1.8	.9	1.5	.19	2.1	1.1
								.44	.73	.09	1.0	.52
									1.2	.15	1.7	.83
										.02	.22	.11
											2.5	1.2
												.61

Only one-eighth of the pattern corresponding to a unit screen element has been tabulated, since the pattern is symmetrical and the rest of the pattern merely duplicates the figures in this table.

Diffraction Pattern Due to a Large Light Source:

The light distribution just given is produced by a point source of light. In halftone practice, the light source is a lens which may be regarded as being made of a large number of small sources of light. Dividing the aperture into 49 elements was considered sufficient for this calculation. The relative proportions of screen and aperture, as they would be seen from a point in the plane of observation immediately behind the center of a screen opening, are shown in Fig. 6. The 49 elements of the aperture produce 49 diffraction patterns, identical but slightly displaced with regard to each other. For each point in the plane of the emulsion, the intensities of the appropriate points in these diffraction patterns are added together to give the total intensity. In this case, it is not necessary to take phase relationships into account, if the light sources are independent.

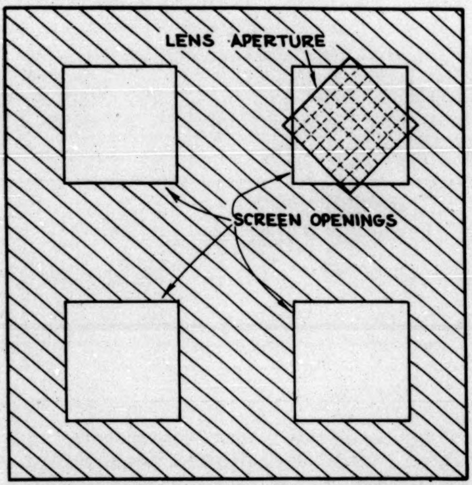

FIG. 6. Illustrating the division of the lens aperture into 49 elements which may be regarded as point sources of light.

If the lens aperture were illuminated by a uniform light source placed close to the lens, the 49 elements of the lens aperture would obviously be independent, since they would arise from different points on the light source. However, in practice, the copy, which may be regarded as a light source, is imaged on the plane of observation, which would mean that the light from all points of the lens aperture is coherent, i.e., in the same phase. In spite of this, it was found experimentally that, with a large uniform light source, the light distribution in the plane of observation was the same, within the limits of experimental error, whether the light source was imaged on the film or was immediately in front of the lens. This unexpected result is considered sufficient justification for regarding the lens aperture as a collection of independent light sources. The calculation has been simplified by choosing an aperture of such size (0.196 in.) that its projection, as seen from the plane of observation, bears a simple relationship to the size of a screen element. In this case, the projected width of the aperture was 7/24 times the width of a single screen element.

The resulting light distribution, calculated under the conditions of screen distance, etc., just given, is shown in Table II.

TABLE II.

Light distribution behind a crossline screen with a light source equal in size to the lens aperture illustrated in Fig. 6, calculated from the diffraction pattern tabulated in Table I.

96.2		90.8		73.9		47.2		24.2		15.8		10.3
	93.5		81.5		61.1		33.5		18.4		12.0	
		82.5		65.0		38.4		20.8		12.8		9.37
			65.4		42.8		22.9		13.2		8.56	
				43.4		25.9		13.7		8.48		6.86
					27.8		15.1		7.88		6.05	
						15.2		7.25		4.83		4.08
							7.21		4.15		3.13	
								3.79		2.34		2.08
									2.26		1.80	
										1.62		1.43
											1.40	
												1.14

By joining points of equal brightness, and completing the pattern for one or more complete screen elements, the light distribution may be mapped as shown in Fig. 7. This may be contrasted with the results of the penumbra theory calculation given in Fig. 8. The shape of the isolux lines is very different in the two cases.

The method of determining the light distribution experimentally was given in the previous paper. The optical conditions are slightly different from those chosen in the former case, so as to simplify the diffraction calculation.

The light distribution in the halftone dot, found by experiment in this way, is shown in Fig. 9. It is seen that the shapes of the isolux lines shown in Fig. 9 correspond well with those calculated by the diffraction theory, Fig. 7, and not at all with the penumbra calculations, Fig. 8.

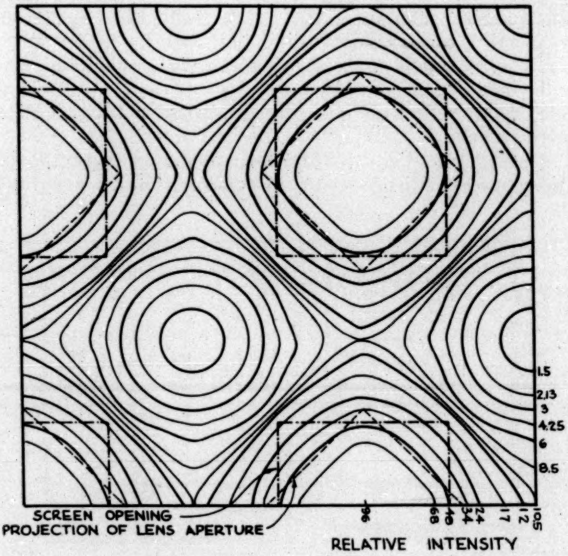

FIG. 7. Light distribution behind halftone screen, calculated from diffraction theory.

The values for light intensity are more easily compared by plotting the area of the dot against the relative intensity at its boundary (see Fig. 10). Here again, the diffraction, but not the penumbra calculation, agrees well with experimental results, except that a little too much light has penetrated to the dark regions. This may be attributed to the scattering of light by imperfections in the screen and optical system, which it is very difficult to measure, to the low resolving power of the emulsion, and partly to the approximations used in making the diffraction calculations.

Mathematical Part:

For those who wish to follow the analysis in greater detail, the following more complete description is given.

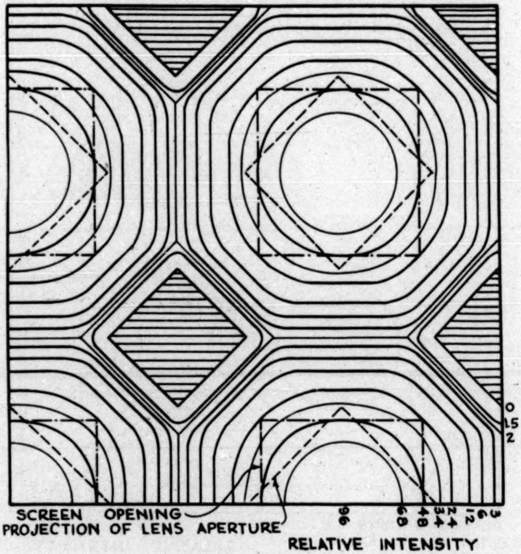
0
1.5
2
SCREEN OPENING
PROJECTION OF LENS APERTURE
96
68
48
34
24
12
6
3
RELATIVE INTENSITY

FIG. 8. Light distribution behind halftone screen, calculated from geometrical optics (penumbra theory).

ASSUMPTIONS.

The calculations given in this paper are based on Fresnel's integrals, from which the Cornu spiral is plotted, and which are accurate only when rays close to the straight line *LP* from light source to point of observation are considered. The halftone screen, on the other hand, extends over a large area. However, it has been found experimentally that under the chosen conditions, with a parallel-line screen, only the three screen openings close to the direct ray have a measurable effect. Near the center of the screen, the greatest error consists in neglecting third-order terms. This involves phase errors of considerably less than one hundredth of a wave length. Amplitude errors, due to the assumptions that the inclination factor for all the rays equals unity and that loss of amplitude according to the inverse square law because of the greater path length of the less direct rays is negligible, are even less important. At the edges of the screen, phase errors due to the obliquity of the screen might be thought to be appreciable, but in photographic experiments under the conditions of use of a halftone screen, it has not been possible to observe any effects that might be ascribed to a difference

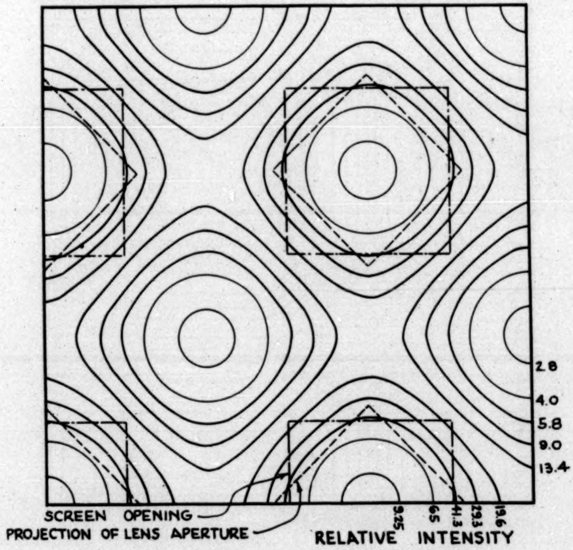

FIG. 9. Light distribution behind halftone screen, determined experimentally.

V.2
194

in diffraction pattern when images formed near the edges of the screen are compared with images produced on the axis.

If these assumptions are made, it follows that indirect rays of light from equal elemental areas of the screen are equal in amplitude and are retarded in phase in proportion to the square of their distance, in the plane of the screen, from the line joining light source and point of observation.

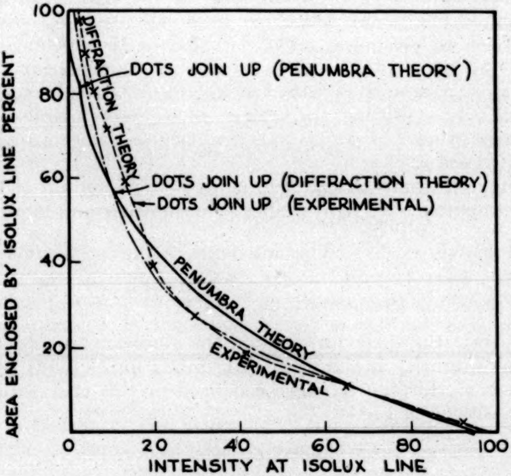

FIG. 10. Relationship between the intensity at an isolux line and the area enclosed within it.

PARALLEL-LINE SCREEN.

Instead of carrying out the computation graphically with the help of the Cornu spiral, the values were calculated from Fresnel's integrals, from which the Cornu spiral is plotted. These are available [4] up to a value of $v = 8.5$.

In the particular example we are studying, the screen distance has been chosen with respect to screen ruling and wave length, so that the width of the slit $(v_1 - v_2)$ equals 2.4. Taking as an example a field point one-fourth of a screen element away from the center of a screen opening, slits will extend from $v = -1.8$ to $+0.6$, from 3.0 to 5.4, and on the other side from $v = -6.6$ to -4.2. Openings corresponding to values of v further than 7.2 or -7.2 are neglected. This is the problem which was solved graphically in Fig. 4.

If x and y are the values of Fresnel's integrals corresponding to a given value of v, we subtract values of x at the left-hand side of a slit from those at the right, and doing the same for y, we get $x_1 - x_2 = 0.581 + 0.334 = 0.915$ and $y_1 - y_2 = 0.111 + 0.451 = 0.562$ for the opening from $v = -1.8$ to $+0.6$. Values for the other two openings are $x_1 - x_2 = .072$ and $-.048$, and $y_1 - y_2 = -.101$ and $.019$, respectively. Adding the values of $x_1 - x_2$ for the three openings gives $x = 0.795$ and, similarly, a value of 0.480 is obtained for y.

The amplitude at this field point is the resultant of these two components at right angles to each other and is proportional to $\sqrt{\dfrac{x^2 + y^2}{2}}$. The intensity, being proportional to the square of the amplitude, equals $\dfrac{x^2 + y^2}{2}$, or for this point 0.432 times the intensity in the absence of a screen.

The intensity is similarly determined for as many points as desired, thirteen having been used in this case with the results shown in Fig. 5.

CROSSED SCREENS.

The Fresnel-Kirchhoff equation for the disturbance at P, when the wave length is very short compared with the distances involved, reduces to the following form when LP is normal to the screen:

$$U_P = \frac{ik}{4\pi}\frac{e^{-ik(a+b)}}{ab}\int\int e^{-ik\Delta}dxdy,$$

where Δ is the increase in path length for the ray going through (x, y) compared with the direct ray LP, so that

$$\Delta = (x^2 + y^2)\left(\frac{a + b}{2ab}\right).$$

The double integral term then becomes

$$\int\int e^{-ik(x^2+y^2)(a+b)/2ab}dxdy$$

or

$$\int\int e^{-ikx^2(a+b)/2ab}e^{-iky^2(a+b)/2ab}dxdy.$$

The screen openings of a 90-degree crossline screen are rectangular, so that if x and y are measured in directions parallel to the rulings, the values of x and y and the limits of integration with respect to x and y are independent of each other. The integral may, therefore, be resolved into the product of two integrals, giving the equation

$$U_P = \frac{ike^{-ik(a+b)}}{4\pi ab}\int dxe^{-ikx^2(a+b)/2ab}\int dye^{-iky^2(a+b)/2ab}.$$

Each of these integrals represents the effect of one of the parallel-line screens of which the crossline screen may be considered to be composed. The disturbance at P due to the crossline screen is therefore equal to the product of the disturbances due to the two parallel-line screens.

CONCLUSIONS.

Under typical conditions, the light distribution, which controls dot shape and tone reproduction curve, corresponds well with that calculated from the diffraction theory and disagrees with computations from geometrical optics.

In the next section of this paper, further qualitative evidence of the effects of diffraction and a discussion of the types of diffraction patterns formed at different screen distances, and their effects on halftone negatives, will be given.

ACKNOWLEDGMENT.

My thanks are due to Dr. F. Kottler of these Laboratories, for his helpful criticisms and suggestions.

ROCHESTER, N. Y.
February 24, 1943.

REFERENCES.

1. YULE, J. A. C., J. FRANKLIN INST., **231**, 23–38 (1941).
2. FRUWIRTH, A., and MERTLE, J. S., *American Photo-Engraver*, **27**, 291–297 (1935).
3. DRUDE, P. K. L., "Theory of Optics," Longmans, Green and Co., New York, 3rd ed., 1912.
   MEYER, C. F., "The Diffraction of Light, X-Rays, and Material Particles," pp. 1–111, University of Chicago Press, Chicago, 1934.
4. JAHNKE, E., and EMDE, F., "Funktionentafeln mit Formeln und Kurven." p. 26, B. G. Teubner, Leipzig und Berlin, 1909.

V.2
194

DETERMINATION OF LATERAL PASSIVE SOIL PRESSURE AND ITS EFFECT ON TUNNEL STRESSES.

BY

M. A. DRUCKER,

Designer-in-Charge, Board of Transportation, City of New York.

Generally, as soon as a tunnel is constructed it tends to become distorted so that its horizontal diameter is increased and its vertical diameter is correspondingly reduced. In order to have the tunnel retain its theoretical shape, it is erected, wherever possible, so that its vertical diameter is larger than the horizontal. Also, wherever it is considered necessary and found feasible, temporary horizontal tie rods are employed until either the soil is considered to have filled the voids left by the shield or the space is filled with gravel and grout forced in under pressure. Where the vertical loading is greater than the active side pressures, the horizontal diameter becomes larger until sufficient lateral passive soil resistance is developed. The difference between the vertical and active horizontal loading is greater in non-plastic soils than in silt or soft clay and also varies with the amount of earth cover over the tunnel.

For large earth covers the vertical loads are considerably greater than the active lateral pressures resulting in large moments. It, therefore, becomes desirable to consider the relieving effect of the lateral passive soil pressures produced by the tunnel deformation caused by the active loads and pressures. The amount of this passive resistance that may be developed will depend upon the horizontal deformation of the tunnel and upon the resistance of the soil to being compressed. As the measured lateral deflections of tunnels are less than the computed values due to assumed active forces, it is apparent that the passive pressures are brought into play.

Various methods of stress calculations for tunnels considering active forces and pressures have been presented in books and other technical publications. But so far as the writer is aware a discussion of the effects of the passive soil resistance has not yet found its way into print.

In the following analysis formulas will be developed from which the lateral passive soil pressure and its effect on the thrusts, shears, and moments, may be readily obtained for any given set of conditions. The method here presented could be used in conjunction with any procedure employed for determining the effects of the active forces and their vertical reactions. The only result of such calculations that is necessary for determining the lateral passive pressure is the deflection, at the horizontal diameter of the tunnel, due to the assumed active forces.

Let Curve C, Fig. 1 (a), represent the undeformed tunnel; Curve D, the tunnel after deformation due to all the active forces; and Curve E, the final position of the tunnel after the passive pressures were brought into action. And let d_1 represent the lateral deflection at the horizontal diameter of the tunnel due to all the active forces while d_2 represents the deflection at the same point after the passive pressures were brought into play. Then d_3 would represent the reduction in the maximum deflection due to the final passive resistance of the soil. So that $d_3 = d_1 - d_2$. Also let the pressure curve, whose ordinates vary approximately as the lateral deflection of the tunnel with the maximum ordinate = p, Fig. 1 (b),

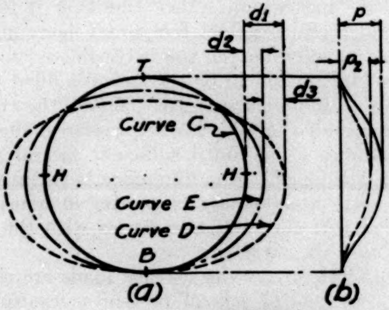

FIGURE 1

represent the lateral pressures that would be necessary to bring the tunnel back to its original position, i.e., to deflect it back through the distance d_1 at the horizontal diameter. It may be noted that the pressure represented by the curve whose maximum ordinate is p is used only for reference purposes; p is not equal to Kd_1, as d_1 is the theoretical deflection without considering any passive pressure; and, also, that the ratio p_2/p is equal to d_3/d_1 and not to d_2/d_1. (K is the soil constant to be defined later.)

It will be convenient, and sufficiently accurate, to assume that the resultant lateral deflection due to all the active vertical and horizontal forces is due to a uniform vertical loading acting downward above the entire horizontal diameter and resisted by an equal uniform pressure acting upward below this diameter. And, that the intensity of the passive lateral pressures are proportional to the lateral deflections of the tunnel subject to such uniform loading. That this approximation will have little effect on the results may be seen from the fact that due to all the active forces acting on a tunnel the deflections at points 45° above and below the horizontal diameter were found to be 0.349 and 0.360, respectively, of that at the horizontal diameter while due to uniform vertical loading the deflections at these points are 0.354 of that at the horizontal diameter.

From Equation (B) it may be seen that for a uniform loading to cause a deflection, d_1, at the horizontal diameter,

$$w = \frac{d_1EI}{144r^4}, \tag{1}$$

where w is the uniform load in pounds per sq. ft.; d_1 is the deflection at the horizontal diameter in inches; I is the moment of inertia of the tunnel ring per foot of tunnel length in inches^4; E is the modulus of elasticity of the tunnel material in pounds per sq. in.; and r is the radius of the tunnel ring, at its neutral axis, in feet.

If, now, K represent the soil constant, which is the pressure in pounds per sq. ft. that would cause the soil, through which the tunnel is to be built, to compress 1 inch, then d_2K would be the final maximum intensity of the passive pressure that would push the tunnel back through a maximum distance

d_3, so that, by proportion,

$$\frac{d_2K}{p} = \frac{d_3}{d_1} = \frac{d_1 - d_2}{d_1},$$

from which

$$d_1d_2K = d_1p - d_2p, \quad \text{or} \quad d_2(d_1K + p) = d_1p,$$

and

$$d_2 = \frac{d_1p}{d_1K + p}, \tag{2}$$

also

$$p_2 = Kd_2. \tag{3}$$

Equation (H) shows that the maximum intensity, p, of a lateral pressure which varies as the deflection caused by a uniform vertical loading, w, must be equal to $1.28w$ in order that the lateral pressure should cause the same deflection at the horizontal diameter as the vertical loading. Such theoretical pressure would be sufficient to bring the tunnel back to its theoretical shape. So that $1.28w$ could be substituted for p in Equation (2). Equation (F) shows that due to such lateral pressure the moments at top and bottom of tunnel would be equal to $-0.182pr^2$. As the final passive pressure, whose maximum intensity is p_2, would vary proportionately to that whose maximum intensity is p, then due to such final pressure, $M_T = M_B = -0.182p_2r^2$. The minus sign denotes compression at intrados of tunnel. For p_2 in pounds per sq. ft. and r in feet, M would be in foot pounds.

Substituting for p_2 its equivalent Kd_2 and for d_2 its equivalent $pd_1/(Kd_1 + p)$, then

$$M_T = M_B = -0.182Kd_2r^2 = -0.182Kr^2\frac{pd_1}{Kd_1 + p}. \tag{4}$$

As $p = 1.28w$, and, for any deflection d_1, the value of $w = (d_1EI/144r^4)$, as given by Equation (1), then,

$$p = \frac{1.28d_1EI}{144r^4} = \frac{0.0089EId_1}{r^4}. \tag{5}$$

This would be a constant for any tunnel ring having a maximum deflection d_1 due to all the active forces.

Using the moment coefficient from Equation (G), the

V.2
194

moments at points H, due to the passive pressures were found to be

$$M_H = +\,0.208Kr^2 \frac{pd_1}{Kd_1 + p}. \qquad (6)$$

The plus sign denotes tension at intrados of tunnel.

Also, the thrusts at T and B, due to the passive pressures, would be

$$H_T = H_B = 0.59Kr \frac{pd_1}{Kd_1 + p} \qquad (7)$$

and

$$p_2 = K \frac{pd_1}{Kd_1 + p}. \qquad (8)$$

To illustrate the application of the foregoing analysis and formulas, the following examples will be worked out:

Example 1:

Radius of tunnel ring at neutral axis is 8.5 feet; I is 136 in.^{4} for cast iron tunnel ring per foot of tunnel length; E, the modulus of elasticity for cast iron, will be taken as 12,000,000 pounds per sq. in.; the deflection d_1, of points H, due to all the active forces was found to be 0.52 in. Substituting these values in Equation (5), we get

$$p = \frac{0.0089 \times 0.52 \times 12{,}000{,}000 \times 136}{(8.5)^4} = 1{,}430,$$

so that, in terms of the soil constant, K, the moments due to the passive soil resistance would be

$$M_T = M_B = -\,0.182(8.5)^2K \frac{0.52 \times 1430}{0.52K + 1430} = \frac{-\,9800K}{0.52K + 1430}.$$

For r in feet and K in pounds per sq. ft., M will be in foot pounds.

Substituting values for K from 1,000 to 25,000 lbs. and bearing in mind that

$$M_H = \frac{+\,0.208}{-\,0.182} M_T = -\,1.14M_T,$$

the values in Table 1 were obtained.

It may readily be seen from this table that the relieving moments due to the passive pressures are far from varying in direct proportion to the values of the soil constant. This is illustrated even more clearly by the curve on Fig. 2 which shows the ratio of the relieving moments for values of K up to 25,000 lbs. compared with those for $K = 10{,}000$ lbs. It may be seen that for $K = 5{,}000$ lbs. the relieving moment would be as much as 82 per cent of that for $K = 10{,}000$ lbs., while for $K = 20{,}000$ lbs. the relieving moment would be only 12 percent greater than for $K = 10{,}000$ lbs. These percentages would vary slightly for different tunnels.

TABLE 1
MOMENTS DUE TO PASSIVE SOIL PRESSURES

SOIL CONSTANT K	MOMENTS	
	$M_T = M_B$	M_H
1000 lbs.	-60,500″#	+69,000″#
5000 "	-146,500 "	+167,000 "
10000 "	-178,500 "	+204,000 "
15000 "	-192,000 "	+219,000 "
20000 "	-200,000 "	+228,000 "
25000 "	-205,000 "	+234,000 "

For the problem under consideration the moments at points T, H, and B, due to all the active forces, to be designated as M_T', M_H', and M_B', were found to be, respectively, $+250''^{k}$, $-244''^{k}$, and $+229''^{k}$. Table 2 gives the net moments resulting from combining the above moments, due to all the active forces, with those obtained for passive pressures based on several values of K.

The thrusts at T and B, due to the passive pressures, can be obtained by substituting in Equation (7) which gives,

$$H_T = H_B = 0.59 \times 8.5K \, \frac{0.52 \times 1430}{0.52K + 1430}.$$

For $K = 4{,}000$; 8,000; and 12,000 lbs., the values of H_T

and H_B were found to be 4,250; 5,200; and 5,800 lbs., respectively. The lateral pressures cause neither thrust nor shear at points H. For computations of stresses in the tunnel ring the thrusts and moments, for the assumed values of K, should be combined algebraically with those due to the active forces.

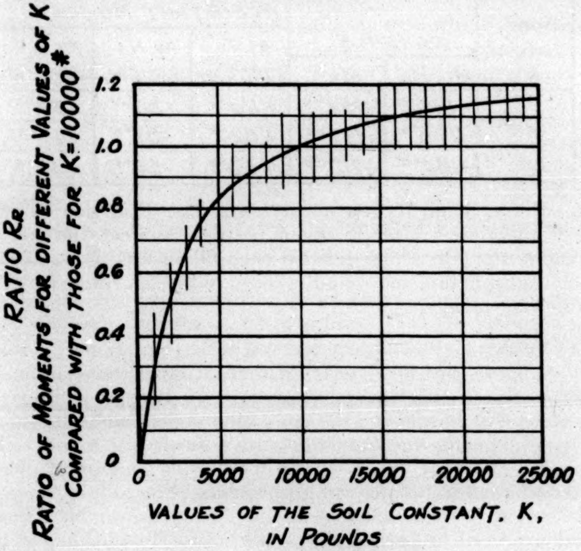

FIGURE 2

Also, the value for the maximum passive pressure intensity p_2 could be found from Equation (8). Substituting values in that equation, p_2 was found to be 845; 1065; and 1,160 lbs., respectively, for values of K equal to 4,000; 8,000; and 12,000 lbs. per sq. ft.

Values for the soil constant are generally assumed more or less arbitrarily depending upon the judgment of the engineer. By means of the analysis here presented, however, the values of this constant may be determined, if any data exists for tunnels of any size having been constructed through the same soil or through a soil similar to that through which the new tunnel is to pass. The only information needed, in addition to the assumed active forces, is the horizontal deflection, d_2, which should represent the horizontal distortion of one-half the tunnel after it began to press against the soil or against the gravel and grout if such filling was used. From such information the value of K may be determined in the following manner:

TABLE 2

SOIL CONSTANT K	MOMENTS		RESULTANT MOMENTS		
	$M_T = M_B$	M_H	AT $T = +250''^{K} - M_T$	AT $H = -244''^{K} + M_H$	AT $B = +229''^{K} - M_B$
4^K	$-135''^{K}$	$+154''^{K}$	$+115''^{K}$	$-90''^{K}$	$+94''^{K}$
8^K	$-168''^{K}$	$+192''^{K}$	$+82''^{K}$	$-52''^{K}$	$+61''^{K}$
12^K	$-184''^{K}$	$+210''^{K}$	$+66''^{K}$	$-34''^{K}$	$+45''^{K}$

Example 2:

Suppose that for a 30 ft. diameter tunnel whose moment of inertia is 1,000 in.^4 per foot of tunnel length; radius at neutral axis is 14.6 ft.; the computed deflection at the horizontal diameter due to all the active forces was found to be 1.0 in.; and that the measured increase in horizontal diameter was 0.8 in. This would mean that the actual average deflection at each side was 0.4 in. From Equation (1), the uniform vertical loading that would cause a deflection of 1.0 in. would be

$$w = \frac{1.0 \times 12{,}000{,}000 \times 1{,}000}{144 \times (14.6)^4} = 1{,}830 \text{ lbs.}$$

For this value of w, the maximum intensity, p, of the theoretical passive pressure necessary to bring the tunnel back to its original position, would be $1.28w$, as previously indicated. So that p would be $1.28 \times 1{,}830 = 2{,}350$ lbs. per sq. ft. As the measured value of d_2 is 0.4 in., then d_3 would be $1.0 - 0.4 = 0.6$ in. By proportion the value of p_2 would have had to be equal to $(0.6/1.0) \times 2{,}350 = 1{,}410$ lbs. As this passive pressure was developed by a compression of 0.4

V.23
1943

in., then, by proportion again, the value of the soil constant would be (1.0/0.4) × 1,410 = 3,500 lbs. per sq. ft.

If the actual deflection at each side of the tunnel had been 0.2 in., then d_3 would be 1.0 − 0.2 = 0.8 in.; p_2 would be (0.8/1.0) × 2,350 = 1,880 lbs. and the soil constant would be (1.0/0.2) × 1,880 = 9,400 lbs. per sq. ft.

By following the method of analysis here outlined, existing data may serve as a basis for design and a check can be obtained by measuring the deflections at the horizontal diameter of the tunnel during construction. In this manner the tunnel may be made use of as a full scale model under actual conditions and the information so obtained could be preserved for future use.

Example 3:

It will now be assumed that the tunnel of Example 2 was considered satisfactory for the portion under a river. For the land portions, however, where the earth cover is large, the tensile stresses were found to be excessive when considering only the active loadings and pressures. For the intrados at point T, where the tensile stresses are generally a maximum, the stress was found to be 6,000 lbs. per sq. in. larger than permissible. It would, therefore, be desirable to determine the necessary soil constant, K, so that the developed passive resistance would cause a compressive stress of 6,000 lbs. at this point. This may readily be done with the aid of the diagram on Fig. 2 by first finding the relieving stress due to a soil constant of 10,000 lbs. Assuming that the computed value for d_1, due to all the active forces, was 1.0 in., then, substituting in Equation (5) the values given in Example 2,

$$p = \frac{0.0089 \times 1.0 \times 12{,}000{,}000 \times 1{,}000}{(14.6)^4} = 2{,}350$$

and from Equation (4)

$$M_T = -\,0.182 \times 10{,}000 \times (14.6)^2 \frac{1.0 \times 2{,}350}{10{,}000 \times 1.0 + 2{,}350}$$

$$= -\,388{,}000 \times 0.191 = -\,74{,}200 \text{ ft. lbs.}$$

$$= -\,890{,}000 \text{ in. lbs.}$$

From Equation (7)

$$H_T = 0.59 \times 10{,}000 \times 14.6 \times 0.191 = 16{,}500 \text{ lbs.}$$

As the area of the cast iron lining is 50 sq. in. and the section modulus for the intrados is 100 in.[4] per foot of tunnel length when the combined compressive stress for $K = 10{,}000$ lbs. would be $890{,}000/100 + 16{,}500/50 = 8{,}900 + 330 = 9{,}230$ lbs. per sq. in. For a desired stress reduction of 6,000 lbs., the value of R_R for the diagram on Fig. 2 would be $6{,}000/9{,}230 = 0.65$. It may be seen that for this value of R_R the necessary soil constant would have to be about 3000 lbs. For the condition of a large earth cover at the land portion of a tunnel, after grout and gravel have been forced in to fill the void left by the shield, it could reasonably be expected that the soil constant would be considerably larger than the required 3000 lbs.

For this K value the maximum deflection could be obtained by first finding the value of p_2 from Equation (8).

$$p_2 = K\frac{pd_1}{Kd_1 + p} = 3000 \times \frac{2350 \times 1}{3000 \times 1 + 2350} = 1320,$$

$$d_3 = \frac{p_2}{p} = \frac{1320}{2350} = 0.56 \quad \text{and} \quad d_2 = 1.0 - 0.56 = 0.44 \text{ in.}$$

If the actual deflection be less than this it would show that the soil was firmer than one having a constant of 3,000 lbs.

DERIVING COEFFICIENTS.*

The coefficients 1.28; -0.182; $+0.208$; and 0.59 were obtained by employing the standard deflection equations. The equations used are those that give $\Delta\phi$, the change in angle between the tangents at any two points, and Δx, the horizontal shift in position of any point. The general equations for these are:

$$\Delta\phi = \int M ds \quad \text{and} \quad \Delta x = \int M(y - b)ds$$

For any point e on Fig. 3, $M = M_T + H_T y + V_T x + M_e$, where H_T is the thrust and V_T is the vertical shear at T while M_e is the cantilever moment of the loading between points T and e about point e; $y = r(1 - \cos\phi)$; $b = r(1 - \cos\alpha)$; $y - b = r(\cos\alpha - \cos\phi)$; and $ds = rd\phi$.

---

* In deriving these coefficients, N. Raboy, Structural Designer, Board of Transportation, New York City, collaborated in the mathematical work.

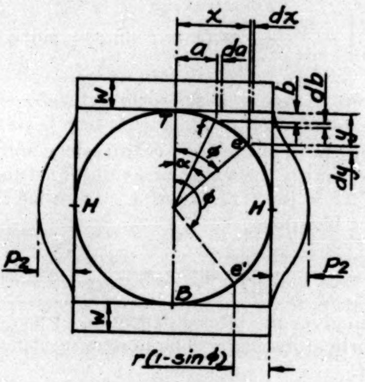

FIGURE 3

For a uniform vertical loading only, H_T and $V_T = 0$, and $M_e = -(wr^2/2)\sin^2\phi$ for points above the horizontal diameter and $M_{e'} = -(w/2)[r(1-\sin\phi)]^2 + wr(1-\sin\phi)$ for points below the diameter. So that for points on the upper half of the tunnel

$$\Delta x = \frac{1}{EI}\left\{\int_{\alpha}^{\pi/2}(M_T + M_e)(y-b)rd\phi \right.$$
$$\left. + \int_{\pi/2}^{\pi}(M_H + M_{e'})(y-b)rd\phi\right\}.$$

For a uniform loading w per sq. ft., $M_T = +(wr^2/4)$ and $M_H = -(wr^2/4)$, giving

$$\Delta x = \frac{1}{EI}\left\{\int_{\alpha}^{\pi/2}\left(\frac{wr^2}{4} - \frac{wr^2}{2}\sin^2\phi\right) r(\cos\alpha - \cos\phi)rd\phi \right.$$
$$+ \int_{\pi/2}^{\pi}\left[-\frac{wr^2}{4} - \frac{wr^2}{2}(1 - 2\sin\phi + \sin^2\phi)\right.$$
$$\left.\left. + wr(1-\sin\phi)r\right] r(\cos\alpha - \cos\phi)rd\phi\right\}.$$

For points below the horizontal diameter,

$$\Delta x = \frac{1}{EI}\int_{\alpha}^{\pi} (M_H + M_{e'})(y - b)r\,d\phi$$

$$= \frac{1}{EI}\int_{\alpha}^{\pi}\left[-\frac{wr^2}{4} - \frac{wr^2}{2}(1 - 2\sin\phi + \sin^2\phi) + wr(1 - \sin\phi)\right] r(\cos\alpha - \cos\phi)r\,d\phi.$$

Integrating both of the above expressions and substituting the indicated limits, the value of Δx obtained from each was found to be $\Delta x = (wr^4/12EI)\sin^3\alpha$. In order that Δx be in inches while r is in feet,

$$\Delta x = \frac{1728wr^4}{12EI}\sin^3\alpha = \frac{144wr^4}{EI}\sin^3\alpha. \qquad \text{(A)}$$

This equation gives the lateral deflection at any point due to a uniform vertical loading. The maximum deflection, which is at point H,

$$= \frac{144wr^4}{EI}\sin^3\frac{\pi}{2} = \frac{144wr^4}{EI}. \qquad \text{(B)}$$

For the passive lateral pressures to be proportional to the horizontal deflections caused by uniform vertical loading, the pressure at any point would be equal to $(144wr^4/EI)\sin^3\phi C_1K$, where K is the soil constant and C_1 represents the ratio of the final deflection of a point on the tunnel after the passive pressure is brought into action to the deflection that would be caused by the vertical loading alone. Also, the term $(144wr^4/EI)$ would be constant for any tunnel with a uniform loading w, which may be represented by C_2, so that the unit pressure at any point would be $C_1C_2K\sin^3\phi = C_3\sin^3\phi$, where $C_3 = C_1C_2K$.

Now $y = r - r\cos\phi$ and the increment $dy = r\sin\phi d\phi$. The pressure on such increment $= C_3\sin^3\phi r\sin\phi d\phi = rC_3\sin^4\phi d\phi$.

$$H_T = rC_3\int_0^{\pi/2}\sin^4\phi d\phi = \frac{3\pi}{16}rC_3.$$

As $C_3\sin^3\phi$ is the pressure at any point, it would also apply to point H where $\sin^3\phi = 1$, so that C_3 may be said to

V.2
194

represent the unit pressure at that point which was previously designated as p_2.

Therefore,

$$H_T = \frac{3\pi}{16} p_2 r = 0.589 p_2 r. \tag{C}$$

In order to obtain the moments due to the lateral passive soil resistance use may be made of the fact that due to this symmetrical loading the tangents at points T and B will remain horizontal, so that the change in slope between them will be zero, or

$$\Delta\phi = \frac{1}{EI}\int_0^{\pi} (M_T + H_T y + V_T x + M_e) r d\phi. \tag{D}$$

$H_T = 0.589 p_2 r$; $V_T = 0$; and M_e will have to be determined. $b = r - r\cos\alpha$ and increment $db = r\sin\alpha d\alpha$. The pressure on this increment $= p_2 r \sin^3\alpha \sin\alpha d\alpha$. The moment of this pressure about another point distant y below $T = p_2 r \sin^4 \alpha d\alpha (y - b) = p_2 r \sin^4 \alpha d\alpha (\cos\alpha - \cos\phi) r$. The moment of the pressures between T and e about e

$$= - p_2 r^2 \int_0^{\phi} \sin^4 \alpha (\cos\alpha - \cos\phi) d\alpha.$$

This reduces to

$$M_e = -\frac{p_2 r^2}{40}(-2\sin^5\phi - 5\sin^3\phi + 15\sin\phi - 15\phi\cos\phi). \tag{E}$$

Substituting this value for M_e in Equation (D), we get

$$\frac{1}{EI}\int_0^{\pi}\Bigg[M_T + 0.589 p_2 r(1 - \cos\phi) r$$
$$- \frac{p_2 r^2}{40}(-2\sin^5\phi - 5\sin^3\phi + 15\sin\phi - 15\phi\cos\phi\Bigg] d\phi = 0.$$

Integrating, substituting the limits and equating,

$$M_T = - p_2 r^2 (0.589 - 0.407) = - 0.182 p_2 r^2, \tag{F}$$

$$M_H = M_T + H_T r - \int_0^{\pi/2} M_e d\phi = -0.182 p_2 r^2 + 0.589 p_2 r^2$$
$$- \frac{p_2 r^2}{40}\left(-2\sin^5\frac{\pi}{2} - 5\sin^3\frac{\pi}{2} + 15\sin\frac{\pi}{2}\right)$$
$$= p_2 r^2 (-0.182 + 0.589 - 0.199) = +0.208 p_2 r^2. \tag{G}$$

In order to obtain the ratio between the maximum pressure intensity, p, and the uniform vertical loading, w, that would cause the same horizontal deflections, but in opposite direction, of points H, the deflection due to the side pressure will have to be determined.

The horizontal movement of any point, f, with reference to a point, e, may be obtained from the expression

$$\Delta x = \frac{1}{EI}\int_{\alpha}^{\phi}[M_T + H_T r(1-\cos\phi) + M_e]r^2(\cos\alpha - \cos\phi)d\phi$$

$$= \frac{1}{EI}\Big\{ M_T\phi r^2\cos\alpha - M_T r^2\sin\phi + H_T\phi r^3\cos\alpha$$

$$- H_T r_3 \sin\phi\cos\alpha - H_T r^3\sin\phi + H_T r^3$$

$$\times\left(\frac{\phi}{2} + \frac{\sin\phi\cos\phi}{2}\right) + \frac{p_2 r^4}{40}\cos\alpha$$

$$\times\left(-\frac{2}{5}\sin^4\phi\cos\phi - \frac{11}{5}\sin^2\phi\cos\phi - \frac{128}{5}\cos\phi + 15\phi\sin\phi\right)$$

$$-\frac{p_2 r^4}{40}\Big[\frac{1}{3}\sin^6\phi + \frac{5}{4}\sin^4\phi - \frac{15}{2}\sin^2\phi + 15$$

$$\times\left(\frac{\phi^2}{4} + \frac{\phi}{4}\sin 2\phi - \frac{\sin^2\phi}{4}\right)\Big]\Big\}\Big|_{\alpha}^{\phi}.$$

If point B be taken as the fixed point, then $\phi = \pi$; substituting $\pi/2$ for α to obtain the horizontal movement of point H; reducing and multiplying by 1,728 so that the deflection would be in inches while r is in feet, the deflection at H was found to be $= -(112p/EI)$.

As the horizontal deflection at H due to a uniform vertical loading, w, $= (144wr^4/EI)$, then for an equal and opposite deflection to be caused by lateral pressures varying as $\sin^3\phi$, the maximum pressure intensity, p, would have to be equal to

$$\frac{144}{112}w = 1.28w. \tag{H}$$

A GENERAL STRESS-STRAIN-TIME FORMULA.

BY

P. G. NUTTING,

Geophysicist, U. S. Geological Survey.

In 1921 the writer advanced a simple general law of deformation to represent the behavior of a number of semisolid substances under stress, studied at that time. Although this formula, representing strain as a simple exponential function of time and stress, was arrived at by empirical methods, it was found to cover the whole range from elastic solids to viscous fluids so well that it was adopted as sufficient for practical work and as probably the most important term in the complete theoretical relation. The classical laws of elasticity and of fluid flow are but special cases. The same formula was shown to cover electrical conduction in leaky dielectrics in such a way that Ohm's Law is a special case.

The general formula has in recent years found much favor in technologic research on such materials as paints, plastics, asphalts and food products, particularly in Great Britain. However, interviews and correspondence with the users of this formula indicate the need of a more detailed discussion and clarification of the subject than was given in the original papers.

The general law of deformation in question [1, 2] is a relation between strain S, stress F, time t and a constant a, which may be written

$$(1)\qquad S = at^n F^m,$$

$$(2)\qquad \log S = \log a + n \log t + m \log F,$$

$$(3)\qquad \frac{dS}{S} = n\frac{dt}{t} + m\frac{dF}{F}.$$

For plotting observed data, (2) is the most convenient form, giving the constants a, n and m from the plot. A plot of m against n in the first quadrant [5] is useful for spotting the characteristic properties of a substance. The differential form (3) is preferred for some work because every term has zero dimensions.

For compression or extension, the strain S is the change in length or volume per unit length or volume, i.e., $\delta l/l$ or $\delta v/v$, caused by the stress F as pressure or force per unit area, the ratio giving the moduli. For shear, S is the dimensionless angle of shear. The constant a represents the ease of yielding to stress or deformability. Its reciprocal, representing firmness, is preferred by some British writers. It is meaningless unless the units of stress, strain and time are specified.

For $n = 0$ and $m = 1$, the above equations represent the deformation of a perfectly elastic body $S :: F$. The work done on such a body *all* goes to free energy, is completely recoverable. For $n = 1$ and $m = 1$, they represent perfect fluids, *no* energy is stored and recoverable, the deformation is a pure shear. While no perfectly elastic bodies nor perfect fluids exist, there are many close approximations to each and theoretical works on elasticity and hydrodynamics have sufficed for most practical work. These are based on the assumption that terms of second and higher order are negligible. It was the investigation of semifluid substances (such as pitch) by the writer in 1920 that lead to the above formulas.

Several attempts to bridge the gap between fluids and solids have been made. Seventy years ago Maxwell introduced the "time of relaxation" to account for the steady yield of near-solids under long continued stresses. This permitted a decided advance in theory and found some practical application. However it does not represent observed data well and Maxwell himself remarked that time of relaxation probably varies with strain. Many substances show the opposite effect (a stiffening) and both effects must evidently be included in a general theoretical derivation. E. C. Bingham[3] in recent years has developed a formula for plastics which assumes in effect that such bodies are elastic solids up to the yield point but are fluids under higher stresses. The curved portion of the stress-strain diagram, representing intermediate and in some cases the most important properties of a body, is simply ignored. de Waele[4] and others have modified the Bingham formula somewhat to make it fit data better.

V.2
194

The same substance may be a fluid under one deformation and possess high elasticity under another. A gas under adiabatic compression is nearly perfectly elastic ($n = 0$, $m = 1$) but shears like a nearly perfect fluid ($n = 1$, $m = 1$). Many other fluids are highly elastic to compression but most solids flow slightly under high pressures and high shearing stresses. The compressibility ($S : F$) of most solids decreases with applied stress (m less than unity) while under tension they weaken near the elastic limit unless given time for molecular rearrangement.

For shearing stresses the writer found values of n from 0.4 to 0.9 for pitches and of m from 0.8 to 3.5. The alignment of data on the logarithmic plot showed no systematic departures from a straight line over large ranges of time and applied force so that formula (1) must be at least a good first order approximation. Inertia effects at the start and deformations involving rupture are not represented.

It is at first difficult to associate the familiar properties of a body (hard, rubbery, tacky, jelly-like—) with the values of m and n which quantitatively define them. In a recent paper Scott-Blair [5] gives a graphic plot which is very helpful. This is simply a coordinate plot of $m(y)$ against $n(x)$ as shown in Fig. 1. Perfect fluids and perfectly elastic solids are each represented by a point on this diagram. Other known values are given. No values of n greater than unity have yet been found.

Other means of visualizing m and n may be mentioned. Rigidity and viscosity are well established concepts and if these are defined in terms of general deformation (Eq. 1), their variation with n and m may be graphed as desired. The reciprocals of these properties, elastic yield E and mobility or fluidity B give simpler algebraic forms,

$$(4) \qquad \text{Elastic yield } E = S : F = at^n F^{m-1}$$
$$= a \quad \text{for} \quad n = 0 \quad \text{and} \quad m = 1.$$

$$(5) \qquad \text{Mobility } B = \frac{dS : dt}{F} = ant^{n-1}F^{m-1}$$
$$= a \quad \text{for} \quad n = 1 \quad \text{and} \quad m = 1.$$

Both the elastic yield and mobility concepts depend primarily on the constant a. Thus a in (4) is large for rubber and very small for steel while in (5) it is large for water and gases but small for tar and glasses.

The variation of either E or B with either n, m, t or F may of course be obtained at once by differentiation but it is

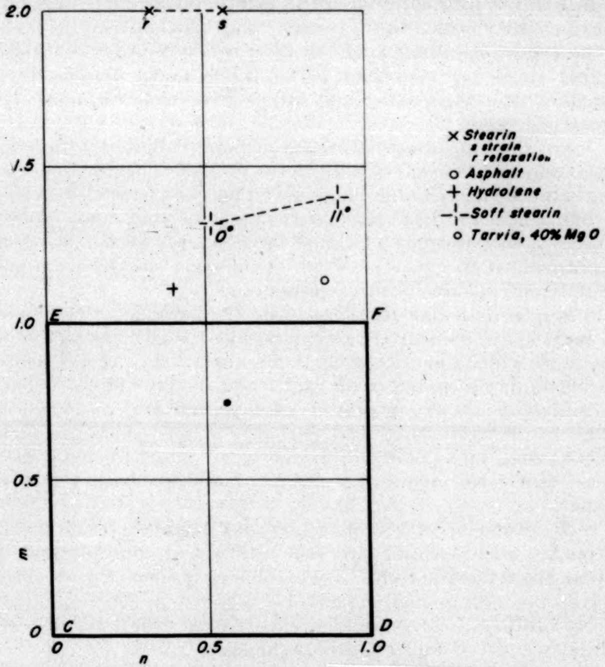

FIG. 1. Deformation fields. The coördinates are m and n of equation (1). The point $E(n = 0, m = 1)$ indicates a perfectly elastic body or $S :: F$. The point $F(n = 1, m = 1)$ corresponds to a perfect fluid, $S :: Ft$. Along the line E to F, elastic solid to fluid, both elastic yield E and mobility B are independent of the force applied but both vary with time. Along the line DF, $n = 1$, mobility varies with force applied, increasing for $m > 1$, decreasing for $m < 1$. To the right of the line $DF (n > 1)$ no substances have been found. They would be more-than-perfect fluids. Between the ordinates $n = 0$ and $n = 1$, various substances have been spotted from $m = 0.77$ up to $m = 2.0$. The largest m, 3.5 (not shown) was for a ZnO-linseed-oil paint.

simpler to deal with (4) and (5) as they stand. A hard stearine pitch studied by the writer showed an increase of ten fold in mobility as the force applied was increased from 1 to 10 kg. The value of m found was 2.0 while n was 0.56, the mobility decreased with time, since $n - 1 = -0.44$. Another hard pitch (140° Hydrolene) showed little variation of viscosity with force applied ($m = 1.14$) but was far from being a true fluid for n was only 0.40. The viscosity of paints (zinc oxide and linseed-oil) was studied by Bingham and Green (A. S. T. M., 1919) using a long capillary, a wide range of pressures and mixtures ranging from very thin to thick pastes. Their data fit formula (2) very well indeed over the whole range of both pressures and concentrations, with $m = 3.50$. These data fit the Bingham formula (rate of flow: : $F - F_0$) as well as an exponential curve fits two straight lines. Some forms of absolute viscosimeter have been discredited because they show a variation of viscosity with force and velocity. Obviously the assumption of perfect fluidity, not the instruments, are in error. An oil studied by the writer with a MacMichael instrument gave $m = 0.77$. Capillary tubes of the same diameter and length (ordinary viscosimeters) of course always flow the same quantity of a fluid at the same temperature in the same time, if a variation in pressure (head) is carefully avoided.

Interest centers in values of n near 0 and 1 and half way between, say $n = 0.1$, 0.5 and 0.9 and for $m = 0.5$, 1.0 and 2.0. These represent nearly perfectly elastic solids, nearly perfect fluids and substances far removed from either. From (4) and (5), for

$m = 0.5$	$n = 0.1$	$E = at^{0.1}F^{-0.5}$	$B = 0.1at^{-0.9}F^{-0.5}$
	0.5	$at^{0.5}F^{-0.5}$	$0.5at^{-0.5}F^{-0.5}$
	0.9	$at^{0.9}F^{-0.5}$	$0.9at^{-0.1}F^{-0.}$
$m = 1$	$n = 0.1$	$E = at^{0.1}$	$B = 0.1at^{-0.9}$
	0.5	$at^{0.5}$	$0.5at^{-0.5}$
	0.9	$at^{0.9}$	$0.9at^{-0.1}$
$m = 2$	$n = 0.1$	$E = at^{0.1}F$	$B = 0.1at^{-0.9}F$
	0.5	$at^{0.5}F$	$0.5at^{-0.5}F$
	0.9	$at^{0.9}F$	$0.9at^{-0.1}F.$

These 18 equations may be graphed or translated into words by way of illustration. For $m = 1$, both the elastic yield E and the mobility B are independent of the force F applied, but both vary with time, E increasing and B decreasing. Such a substance would become more elastic and more viscous as deformed by any steady force. For m less than 1, the time relations are similar but both elastic yield and mobility decrease with increase in applied force, the body becomes stiffer, like quicksand. On the other hand for m greater than unity both E and B increase with F. This is a very common behavior corresponding perhaps to molecular breakdown under strain.

For paints, easy spreading requires a fairly low viscosity (a large). But also it must not run down an inclined surface under the gentle shearing stress of gravity. This means that it should have a small n with perhaps a large m. A fusible pitch, to stay put when cold, should have both a and n as small as possible. For bread dough, the requirements are similar and if m is large it will be easy kneading. For lubricants, a high fluidity coupled with a high resistance to squeezing out of a bearing under high pressures, is desired. These conditions indicate a large value of a, $n = 1$ and m as small as possible. No attempt to investigate lubricants from this angle has yet been made though it is a large and important field. For a cup grease on the other hand, a should be moderate, n nearly zero and m large.

Test instruments in which one of the three variables S, F and t (strain, stress and time) is held constant while the other two are observed, have been discussed. Two additional types of methods for studying deformation are possible, namely those in which stress is applied at a fixed rate (dF/dt = constant) and others in which dS/dt = constant. Then there is the notched bar test, in which the (measured) momentum (Ft) is increased until fracture occurs.

For studying the properties of asphalts, Traxler[10] has developed a test instrument in which rate of shear dS/dt between two concentric cylinders, is kept constant by a motor drive while the resultant torque (stress F) is observed at various time intervals. When the fixed rate of shear is not too great, the shear is uniformly distributed and no rupture occurs.

Typical results for asphalt are reproduced in Fig. 2 for the details of the initial stages of deformation which they give.

In judging consistency by *touch*, it is *stress* not strain that is estimated, hence it is held by some that F and S in (1) should be interchanged to make force a function of strain and time. However, there can be no question but that strain is the effect of force applied acting for a given time, therefore S is properly a function of t and F as written in (1). Using apparent elastic yield (or rigidity) and apparent viscosity (or fluidity or mobility) as here defined, the gap between purely

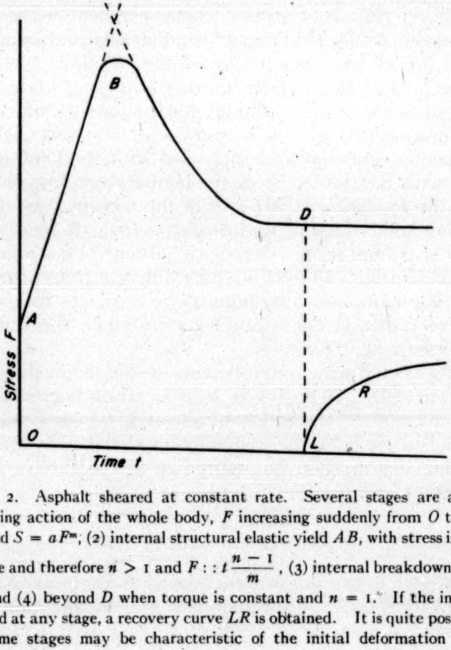

FIG. 2. Asphalt sheared at constant rate. Several stages are apparent; (1) a spring action of the whole body, F increasing suddenly from O to A with $n = 0$ and $S = aF^m$; (2) internal structural elastic yield AB, with stress increasing with time and therefore $n > 1$ and $F : : t\frac{n-1}{m}$, (3) internal breakdown BD with $n < 1$ and (4) beyond D when torque is constant and $n = 1$. If the instrument is stopped at any stage, a recovery curve LR is obtained. It is quite possible that these same stages may be characteristic of the initial deformation of every substance.

physical and purely psychological concepts may be readily bridged.

For many metals, building stones and other crystalline solids, n and a are so small that large stresses and long times are necessary to produce an observable deformation not reversible on release of stress. Some excellent work on rock deformation by David Griggs [6] is under way and some fundamental theory has been developed by Goranson.[7]

For a steel tape under tension, the 1907 data of Van Orstrand taken in the Washington Monument (unfortunately still unpublished) give $n = .0928$ and $m = 1.011$, thus the yield per kilogram of load increased with the load and very slowly with the time. From the temperature drop caused by strain the four internal stresses in the tape may be derived.[8]

Other solids such as lead or putty dissipate nearly all the energy of deformation. Some are hardened by strain, others soften indicating values of m, quite different from unity. For measuring hardness, instruments are designed to give it in terms of either stress, strain or time while the other two variables are kept constant.

Relaxation during and following strain obviously plays an important role. It begins as soon as strain begins and continues even after the stress is released. A slow relaxation observed in pitch by the writer followed the same law as the preceding deformation but with two of the three constants different.

$$(6)\quad \begin{aligned} \text{Strain } S &= 0.28t^{0.56}F^{2.0} \\ \text{Relaxation } &= 0.24t^{0.33}F^{2.0}. \end{aligned}$$

The stress F in the relaxation equation is that operating just previous to release. The constant $m = 2.0$ is the same for the two cases but a and n are different. For a fixed deformation, the (internal) stress-time curve could perhaps be observed in some materials but this has not been done to the writer's knowledge. Observed strain relaxations indicate the absence of a definite time limit, rather it trails off like a decay curve, possibly with the tail end chopped off as though relaxation ceased below a finite strain. Griggs used the formula $S = a + b \log t + ct$ to represent the slow yield of rocks to stress with time.[6] This formula tacitly assumes that the deformation is made up of three additive components; elastic yield a, plus a steady flow ct and an intermediate slowly increasing yield $b \log t$. The rate of strain, $dS : dt = b/t + c$ or $t(\dot{S} - c) =$ constant. Griggs' data on a compressed limestone show an application of his formula and the writer's (Fig. 3). Both formulas fit the observations well but the simpler $S = at^n$ gives a straight line.

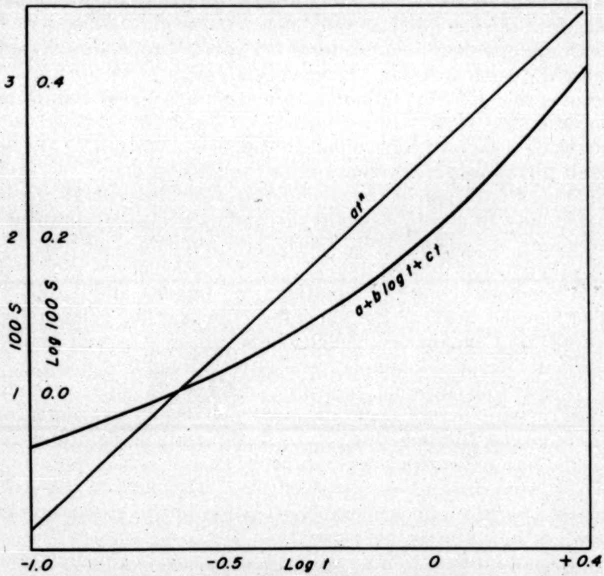

FIG. 3. Strain-time in deformed limestone. Solenhofen limestone under 5500 kg./cm.^{2} compression while compressed by a hydrostatic pressure of 10,000 atmospheres. 100 S (in per cent.) is plotted against log t (in hours) for the Griggs formula and log 100 S against log t for the writer's.

Splitting the stress F into two fractions, one producing elastic the other viscous deformation, is both illogical and useless since such changes would be included in the values of the constants a and m. The same may be said of the time factor and the constants a and n. Any deformation may be resolved into a compression and a shear, hence it seems logical to split the stress F in two fractions kF and $(1 - k)F$ but such a procedure affects only the value of a in (1) hence does not change its form. If a strain is considered made up of one elastic and one viscous component, these may be added if both are expressible in the form (1) and the constants m and n are the same for each. However the elastic strain, instantly recoverable is very different from the relaxation requiring considerable time. It seems more logical to decrease the stress by a factor proportional to the rate of shear $dS : dt$ but even this procedure does not alter the form of (1).

The separation of the free energy from the energy dissipated may be accomplished if thermal as well as strain measurements are made. With such data available, all four internal pressures may be found for each applied stress as shown in a previous paper[8] in equations (4) and (5) and Table 2. The specific heat of the substance, its specific volume (or length) and expansion coefficient are required as well as the adiabatic change of temperature with each applied stress.

These four internal pressures, deduced in this instance from the stretch of a steel tape and its change in temperature, are of course fundamental in any basic study of deformation for the formulation of a general theory as well as for separating elastic from dissipative energy effects. This field of research appears worthy of considerable attention but its discussion is beyond the scope of this paper.

It is of interest to note that the stress-strain-time relation (1) is consistent with the general equation of motion $a\ddot{x} + b\dot{x} + cx = f$ and with the LaGrange equation in generalized coordinates of which it is a special case. Neither equation of course adds to the theory of deformation or to the interpretation of results.

Objections to (1) have been raised on the grounds that it does not conform to classical theories of elasticity and hydrodynamics and that it does not "dimension." As to the first objection, it has been abundantly proved that there are a great many materials that are far from being either perfectly elastic or perfectly fluid. The older theories apply only to substances possessing ideal properties, but never to actual materials in more than a first order approximation.

As to dimensions, it may be pointed out that every term of a Taylor or Maclaurin expansion of any function has different dimensions, yet such a series is just as legitimate an expression of observed facts as the function itself. Relations (1), (2) and (3) are mathematically identical yet each term in (3) has zero dimensions. If any one of these is capable of representing observed facts, so must the other two.

The velocity of water in a stream does not increase in proportion to distance upward from the bed but approaches a parabolic or logarithmic rather than a linear relation.[9] In other words, while the shear stress is uniform the rate of shear is not. From this it might be supposed that shear (flow) is not uniformly distributed between two parallel planes moving at different rates in any viscous fluid. While such properties would account for the forms of (1) and (5) very nicely and cannot be ruled out as impossible at present, they appear improbable since they would mean a distributed source or sink of energy not due to the bounding walls. In the case of water ($m = 1$ and $n = 1$, very nearly) in a stream bed, the observed variation of rate of shear is more likely due to the mixing of slower moving bed water with that above.

Consideration of the thermodynamic potential (*RT* log concentration) of the structural units (molecular or unit cells) of a body gives at once the logarithmic relation (1) between stress and strain for hydrostatic compression, a scalar quantity. But for extension and shear, vector quantities must be considered and the potential varies, even in sign, in different directions as shown by Goranson.[7] This point of attack is helpful in theory and in understanding such properties as strain hardening, aging and hysteresis by deduction but most observations must be made on sizable bodies of materials though strains in lattice cells may be observed by X-ray diffraction.

While there is a considerable accumulation of engineering observations on the deformation of materials, this important field of research has been left severely alone by physicists. What is most needed at present is a wide range of scouting preliminary work, a broad survey of the field based on actual facts rather than on centuries old assumptions. This would provide the basis for precision work in selected fields with specially designed instruments, from which may come the data required for a comprehensive theory of deformation in all its details.

REFERENCES.

1. P. G. NUTTING. "A New General Law of Deformation." JOUR. FRANKLIN INST., **191**, 679, 1921
2. P. G. NUTTING. "A Study of Elastic Viscous Deformation." *Proc. A. S. T. M.*, **21**, 1162, 1921.
3. E. C. BINGHAM. "Fluidity and Plasticity." McGraw-Hill, 1922.
4. A. DE WAELE. "Interfacial Forces in Dispersed Systems." *J. Am. Chem. Soc.*, **48**, 2760, 1926.

   N. A. DE BRUYNE. "Viscous and Plastic Flow." *Proc. Physical Soc. (London)*, **53**, 251, 1940.
5. G. W. SCOTT-BLAIR. "Rheological Properties of Industrial Materials." *J. Sci. Inst.*, **19**, 89, 1942.
6. DAVID GRIGGS. "Creep of Rocks." *Journal of Geology*, **47**, 225, 1939.
7. ROY W. GORANSON. "Flow in Stressed Solids." *Bull. Geol. Soc. Am.*, **51**, 1023, 1940.
8. P. G. NUTTING. "Deformation and Temperature." *J. Wash. Acad.*, **19**, 109, 1929.
9. A. B. COX. "A New Theory of Fluid Flow." J. FRANK. INST., **198**, 769, 1924.
10. R. N. TRAXLER. "A Rotary Viscometer for High Consistencies." *Ind. & Eng. Chem.*, **14**, p. 340, April 1942. Also *Proc. A. S. T. M.* 1936, 1937 and 1940.

Published by permission of the Director, Geological Survey, Department of the Interior.

NOTES FROM THE NATIONAL BUREAU OF STANDARDS.*

SOURCES OF ERROR IN PRECISE COMMERCIAL REFRACTOMETRY.

Certain modifications of the Abbe-type refractometer, which have extended its field of application to precise measurements, make it advisable to examine possible sources of error in order that greater accuracy may accompany increases in precision. In the April *Journal of Research* (RP1535) Leroy W. Tilton points out that the quality of optical surfaces on lenses and prisms must be high because, in general, the symmetrical use of all apertures is not possible. Approximate corrections for different performance of the instrument at different temperatures are not adequate at water-jacket temperatures differing widely from those of the room, but it is seldom necessary to distinguish between index of sample referred to air at water-jacket temperature or to air at room temperature. When using solid samples the prismatic effect of contact liquid must be carefully eliminated; only 1/3 interference fringe per centimeter along the contact surface is permissible, as viewed in the exit pupil of the telescope.

For refractometry of liquids certain compromises seem necessary. The illuminating prism should be set very close to the refracting prism in order to retain the sample and admit light at truly grazing incidence. On the other hand, the separation should be somewhat larger to eliminate troublesome interference fringes which can cause masking of the critically-refracted rays. The surface of the illuminating prism should be polished or fine ground to facilitate cleanings and to allow maximum transmission when working with spectral sources of low intensity. On the other hand, a rough-ground surface eliminates the interference fringes that cause masking.

CLASSIFICATION OF CARBOHYDRATES.

A system for classifying the carbohydrates has been proposed by Weidenhagen, and, although it has considerable value, it also has a number of obvious deficiencies. In the *Journal of Research* for April (RP1531), William Ward Pigman shows that many of these difficulties may be obviated by considering the individual enzymes of Weidenhagen, e.g., α-glucosidase, as classes of enzymes of similar action but varying according to the source. The results of more recent studies of the specificity of the carbohydrates are considered and the action of enzymes on pentoses, hexoses, and heptoses of similar ring conformations is interpreted. These results and the conception of the complex nature of Weidenhagen's individual enzymes are utilized in the establishment of a provisional system for the classification of the carbohydrates.

---

* Communicated by the Director.

OFNER'S METHOD FOR THE DETERMINATION OF INVERT SUGAR.

The Ofner method for determining the small invert sugar content of refined sugars has recently been subjected to critical study by Richard F. Jackson and Emma J. McDonald and has been found greatly superior to the Herzfeld method which it is intended to replace. At the low alkalinity of the copper reagent, sucrose has but little reducing action. This correction has been determined for weights of sample varying from 1 to 10 grams. The reducing powers of invert sugar for the range from zero to 25 mg. have been determined. It is concluded that the method is satisfactory for the analysis of refined sugar. The complete report on this work has been submitted for publication in the *Journal of Official Agricultural Chemists*.

REVISED COMMERCIAL STANDARD FOR DOUGLAS FIR PLYWOOD.

A new printed edition of Douglas Fir Plywood, Commercial Standard CS45-42, is now available. A number of changes have been made since the previous edition issued in 1940, so as to bring the standard in line with present manufacturing practice as influenced by war conditions.

A very large percentage of the total output of Douglas fir plywood is required by the war program, and it has been necessary for the plywood plants to go on a mass production basis to fill these needs. Consequently, adjustments had to be made in the grades and standard sizes in order to keep a balanced relation to the veneer grades produced, and to prevent a critical shortage in those grades and sizes of plywood most commonly needed for construction purposes.

The major changes made in the standard are the elimination of the grades "Good 2 Sides" and "Good 1 Side" and the addition of a new grade "Sound 1 Side" for moisture-resistant stock. Also, a considerable reduction was made in the number of standard thicknesses and widths.

The present edition of the standard covers detail requirements for six grades of "Moisture-Resistant" type and seven grades of "Exterior Type" Douglas fir plywood, as well as tests for those two types of bonding. For those unfamiliar with the product, a chart is included, showing the types and grades that are generally suitable for a long list of uses, and a section covering nomenclature and definitions.

Printed copies of CS45-42 are obtainable from the Superintendent of Documents, Government Printing Office, Washington, D. C. The price is 10 cents.

MICROSCOPICAL EXAMINATION OF PORTLAND CEMENT CLINKER.

In the microscopical examination of portland cement clinker by the metallographic method, a prismatic phase which is readily etched by water is frequently observed. A report on the nature of this phase is presented by William C. Taylor in the April *Journal of Research* (RP1536).

This prismatic material has been observed only in relatively rapidly cooled clinkers containing K_2O or Na_2O, or both. However, the results of a series of phase equilibrium studies show that K_2SO_4 and $K_2O \cdot 23CaO \cdot 12SiO_2$ are the only compounds containing K_2O that may exist when a mixture of K_2O, CaO, MgO, Al_2O_3, Fe_2O_3, SiO_2 and SO_3, in the proportions occurring in portland cement clinker, is heated and cooled under equilibrium conditions. Neither of these compounds has properties similar to those of the prismatic phase.

The results of microscopical examinations by other investigators on commercial clinkers were analyzed, and these results indicated that a very close chemical relationship existed between the prismatic phase and $3CaO \cdot Al_2O_3$.

Accordingly, the relation of the prismatic phase to the system $K_2O\cdot 23CaO\cdot 12SiO_2$-$CaO$-$5CaO\cdot 3Al_2O_3$, and to other systems involving K_2O, was studied. The phase in question was found to have no range of real stability, and was produced only under conditions of rapid cooling. The observed thermal and compositional requirements for its formation suggest that it may be a metastable form of $3CaO\cdot Al_2O_3$ and monotropic with respect to the stable, isotropic, rectangular $3CaO\cdot Al_2O_3$. The exact composition of the prismatic phase was not established definitely because of certain experimental difficulties, which are outlined in the report. That portion of K_2O combined as K_2SO_4 in clinker was found to have no effect in inducing the formation of the prismatic material.

In conclusion, the conditions necessary for the formation of the prismatic phase are briefly set forth and it is recommended that this phase be referred to as "prismatic $3CaO\cdot Al_2O_3$" instead of the indefinite term, "prismatic dark interstitial material."

MODULUS OF ELASTICITY OF CONCRETE.

In a recent investigation at the Bureau, Rudolph C. Valore, Jr., and Jason C. Yates observed the gain in dynamic modulus of elasticity, E, of concretes made with various brands of normal, white, and high-early-strength portland cements, cured in various ways, over periods up to 635 days. They also determined the effect of calcium chloride admixtures upon this modulus over the same periods of time.

Two groups of 4 by 4 by 30 inch prisms were cast from a concrete proportioned 1 : 2 : 4 by weight and with a water content of 6½ gallons per bag of cement. In each group, for each of 8 standard, 1 high-early-strength, and 2 white portland cements, triplicate specimens were cast for each calcium chloride admixture content (1, and 2 per cent. by weight of cement) and for plain concrete.

Initial determinations of dynamic E were made on one group of specimens 24 hours after casting; the specimens were then placed in a moist room at 70°F. Additional determinations were made thereafter up to 270 days, after which the specimens were placed in dry storage at constant temperature

(70° F.) for an additional 365 days and readings made periodically.

The second (duplicate) group of specimens was subjected to continuous dry storage (temperature and humidity not controlled) immediately after the 24-hour age determinations were made.

The results showed that the dynamic *E* can be determined with good reproducibility with the type of specimen used, as early as 24 hours after casting.

For most of the concretes calcium chloride markedly increased the dynamic *E* at early ages but not as much as compressive strengths at corresponding ages were increased by calcium chloride in tests reported by Rapp in 1934. The dynamic *E* for concretes containing calcium chloride generally remained higher than that of reference concrete to the end of each test series.

Changes in moisture content of concrete markedly affect the dynamic modulus of elasticity. Comparisons between concretes of different moisture contents on a basis of values of dynamic moduli may therefore be misleading.

The complete account of this work has been submitted for publications in the *Proceedings* of the Highway Research Board.

SIMPLIFIED PRACTICE RECOMMENDATION FOR WIRE ROPE.

Simplified Practice Recommendation R198-43, Wire Rope, was initiated at the request of the Steel Division of the War Production Board. It was developed by engineers of the wire rope industry to serve as a war-time conservation measure, immediately, and as a basis for recognized practice after the war.

This simplification program is concerned primarily with a reduction in the number of different sizes, varieties, and grades of wire rope produced for stock purposes. For the convenience of all concerned, the technical details "approximate weight per foot," "breaking strength," etc., are also provided.

The recommendation covers only wire ropes that comprise the vast majority of tonnage, and which are produced for stock purposes, and does not attempt to deal with the numerous and particular end uses to which wire rope is put. Those special-purpose ropes will be furnished by the manufacturers only when their need has been demonstrated in the light of the war program.

The breaking strength of each item in the schedule is based on a mathematical formula. In consequence, any inaccuracies or inconsistencies respecting breaking strengths which may have existed in the past have been corrected.

General adherence to the recommendation will result in a net reduction in variety from 973 items to 643, or 33.9 per cent. The major production and use of wire rope is covered by four different rope constructions, where the reduction in variety is from 352 items to 182, or 48 per cent.

Until the printed issue is available, mimeographed copies of this recommendation, which became effective on February 15, 1943, may be obtained without charge from the Division of Simplified Practice, National Bureau of Standards, Washington, D. C

THE FRANKLIN INSTITUTE.

MEDAL DAY MEETING.

WEDNESDAY, APRIL 21, 1943.

At 5:30 on the afternoon of Wednesday, April 21, The Franklin Institute began its program of exercises which ended in the award of certificates and medals to several distinguished guests. This was a distinct departure from other years, when the awards were made in the afternoon and a dinner in honor of recipients was held at night. In an effort to conserve time in these busy days, all activity was conducted in the evening, the affair was informal, and the program was ended by 9:45 P.M. Several members of the Institute who were unable to attend the dinner arrived for the presentation of awards which began at approximately 8 P.M.

A list of events, together with awards presented, is given herewith.

Immediately after the dinner the president, Mr. Charles S. Redding, called the meeting to order and stated that, inasmuch as it was a regular monthly meeting of The Franklin Institute, he wished to announce that the minutes of the previous meeting had been printed in full in the JOURNAL for April and that they would stand approved as printed, unless objection were raised. No challenge was offered and the minutes were declared approved.

PROGRAMME.

Reception to Medalists	THE HOSTESS COMMITTEE
Unveiling of Portrait of Past President P. C. Staples	NATHAN HAYWARD
Dinner	MEDALISTS, OFFICIALS AND GUESTS
National Anthem	EDITH E. BRAUN Lecturer on Music, The Franklin Institute
Toast to Benjamin Franklin	W. M. VERMILYE Chairman, National Franklin Committee
Greetings	CHARLES S. REDDING President, The Franklin Institute
Introduction of Medalists of Other Years	THE PRESIDENT
"How We Serve"	HENRY BUTLER ALLEN Secretary and Director, The Franklin Institute
Presentation of Awards	THE PRESIDENT
"Songs of Insects"	GEORGE WASHINGTON PIERCE Franklin Medalist
"The First Ten Years of Heavy Hydrogen"	HAROLD CLAYTON UREY Franklin Medalist
"America"	EDITH E. BRAUN

RECIPIENTS OF AWARDS.

Sponsors

Presentation of Certificate of Merit
Carl S. Hornberger .... M. M. Price
Central Scientific Company
Chicago, Illinois.

Presentation of Longstreth Medals
Jointly to
Robert Griffin De La Mater
and
William Schwemlein } .... Charles D. Galloway
The Parkersburg Rig and Reel Company
Parkersburg, West Virginia.

Presentation of Wetherill Medal
Robert Howland Leach, Vice-President .... William B. Coleman
Handy and Harman
Bridgeport, Connecticut.

Presentation of Brown Medal
(Posthumously)
Albert Kahn .... C. M. Gay
Albert Kahn Associated Architects and Engineers, Inc.
Detroit, Michigan
Received by Mrs. Harry L. Winston.

Presentation of Henderson Medal
Harry Miller Pflager, Senior Vice-President .... R. Eksergian
General Steel Castings Corporation
Granite City, Illinois.

Presentation of Levy Medal
Anders Henrik Bull, Assistant Engineer .... C. B. Bazzoni
Board of Transportation of the City of New York
New York, New York.

Presentation of Potts Medals
Francisco Ballén, Director .... Lionel F. Levy
National Guano Administration
Lima, Peru.

Paul Renno Heyl .... Winthrop R. Wright
National Bureau of Standards
Washington, D. C.

Presentation of Cresson Medal
Charles Metcalf Allen .... Joel D. Justin
Professor of Hydraulic Engineering
Worcester Polytechnic Institute
Worcester, Massachusetts.

Presentation of the Franklin Medal and Certificate of
Honorary Membership
GEORGE WASHINGTON PIERCE .... Stuart Ballantine
Rumford Professor of Physics, Emeritus
Gordon McKay Professor of Communication Engineering, Emeritus
Harvard University
Cambridge, Massachusetts.

Presentation of the Franklin Medal and Certificate of
Honorary Membership
HAROLD CLAYTON UREY .... Frederic Palmer
Professor of Chemistry and Executive Officer
Department of Chemistry
Columbia University
New York, New York.

(A detailed statement of these exercises, together with papers presented by the Franklin Medalists, will appear in an early issue of the JOURNAL.)

COMMITTEE ON SCIENCE AND THE ARTS.

(*Abstract of Proceedings of Stated Meeting held Wednesday, April 14, 1943.*)

HALL OF THE COMMITTEE,
PHILADELPHIA, APRIL 14, 1943.

DR. JOSEPH S. HEPBURN *in the Chair*.

The following report was presented for final action:

No. 3114: Work of Roger Adams.

This report recommended the award of an Elliott Cresson Medal to Roger Adams, of Urbana, Illinois, "In consideration of his signal contributions in the field of Organic Chemistry, which have resulted in important extensions of its frontiers."

JOHN FRAZER,
Secretary to Committee.

LIBRARY NOTES.

The Committee on Library desires to add to the collections any technical works that members would wish to contribute. Contributions will be gratefully acknowledged and placed in the library. Duplicates received will be transferred to other libraries as gifts of the donor.

Photostat prints of any material in the collections can be supplied on request. The average cost for a print 9 × 14 inches is thirty-five cents.

The library and reading room are open on Mondays, Tuesdays, Fridays and Saturdays from nine o'clock A.M. until five o'clock P.M., Wednesdays and Thursdays from two until ten o'clock P.M.

RECENT ADDITIONS.

ASTRONOMY.

COLLINS, A. FREDERICK. The Greatest Eye in the World. 1942.

BIBLIOGRAPHY.

HAUGHTON, J. L. Bibliography of the Literature Relating to Constitutional Diagrams of Alloys. 1942.

BIOGRAPHY.

CLAPESATTLE, HELEN. The Doctors Mayo. 1941.
MIZWA, STEPHEN P. Nicholas Copernicus. 1943.

CHEMISTRY.

HENDERSON, YANDELL, AND HOWARD W. HAGGARD. Noxious Gases. Second and Revised Edition. 1943.
MOELWYN-HUGHES, E. A. The Kinetics of Reactions in Solution. 1933.

ELECTRIC ENGINEERING.

LORENZEN, R. A-C Calculation Charts. 1942.
Massachusetts Institute of Technology. Members of the Staff of the Department of Electrical Engineering. Applied Electronics. 1943.
STEINBERG, MAX J., AND THEODORE H. SMITH. Economy Loading of Power Plants and Electric Systems. 1943.

ENGINEERING.

COX, GLEN N. Engineering Mechanics. 1943.
DEYARMOND, ALBERT, AND ALBERT ARSLAN. Fundamentals of Stress Analysis. Volume 1. 1942.
GEORGE, S. G., AND E. W. RETTGER. Mechanics of Materials. Revised by E. V. Howell. Second Edition. 1943.

GEOLOGY.

SCHUCHERT, CHARLES. Stratigraphy of the Eastern and Central United States. 1943.

GRAPHIC ARTS.

MCMURTRIE, DOUGLAS C. The Book. 1943.

MANUFACTURES.

DOOLEY, WILLIAM H. Textiles. New Revised Edition with Experiments. 1943.
GRANT, JULIUS. A Laboratory Handbook of Pulp and Paper Manufacture. 1942.
GRODZINSKI, PAUL. Diamond and Gem Stone Industrial Production. 1942.

MARINE ENGINEERING.

JACOBS, ROBERT H., AND E. L. CADY. Marine Engine and Fire Room Guide. 1943.
United States Naval Institute. Naval Machinery. 1941.

MATHEMATICS.

STRATTON, J. A., AND OTHERS. Elliptic Cylinder and Spheroidal Wave Functions. 1941.
U. S. Work Projects Administration for the City of New York. Tables of Probability Functions. Volume 2. 1942.

MECHANICAL ENGINEERING.

BOSTON, ORLAN WILLIAM. Metal Processing. 1941.
HYLAND, P. H., AND J. B. KOMMERS. Machine Design. Third Edition. 1943.
WRANGHAM, D. A. The Theory and Practice of Heat Engines. 1942.

METEOROLOGY.

SPILHAUS, ATHELSTAN F., AND JAMES E. MILLER. Workbook in Meteorology. First Edition. 1942.

MILITARY SCIENCE.

WINTRINGHAM, TOM. The Story of Weapons and Tactics. 1943.

NAVAL ARCHITECTURE.

COPE, HARLEY. Serpent of the Seas. 1942.

POLITICAL SCIENCE.

HOOVER, HERBERT, AND HUGH GIBSON. The Problems of Lasting Peace. 1943.

PHYSICS.

BERNHARD, R. K. Mechanical Vibrations. 1943.
GAYDON, A. G. Spectroscopy and Combustion Theory. 1942.
HIRST, H. X-Rays in Research and Industry. 1943.
JEANS, Sir JAMES. Physics & Philosophy. 1943.
MANLEY, R. G. Fundamentals of Vibration Study. 1942.
TAYLOR, LLOYD W., WILLIAM W. WATSON, AND CARL E. HOWE. General Physics for the Laboratory. Revised Edition. 1942.
University of Pennsylvania. Bicentennial Conference. Nuclear Physics. 1941.
WOODWARD, SHERMAN M., AND CHESLEY J. POSEY. Hydraulics of Steady Flow in Open Channels. 1941.

SCIENCE.

ALLEN, JOHN STUART, AND OTHERS. Atoms, Rocks and Galaxies. Revised Edition. 1942.
BAWDEN, ARTHUR TALBOT. Man's Physical Universe. Revised Edition. 1943.

NOTES FROM THE BIOCHEMICAL RESEARCH FOUNDATION.

The Growth of Pasteurella pestis on a Casein Digest Medium.—LOUIS DESPAIN SMITH AND R. LLOYD PHILLIPS. Little work has been done on the problem of devising media suitable for the growth of *Pasteurella pestis*, especially with regard to the use of broth cultures for vaccine production. At the Haffkine Institute in Bombay, a broth medium has been used for this purpose, but the choice of ingredients has been limited by certain religious principles of the people who are the recipients of the vaccine (Taylor, J., *The Indian Medical Research Memoirs*, No. 27, 1933). Since the cow is sacred to the Hindus and the pig is abhorrent to the Mohammedans no commercial peptone could be used, and it was necessary to grow *Past. pestis* on a medium made from hydrolyzed goat meat. Indeed, at one time it was necessary to use broth made from hydrolyzed wheat flour to meet the objections of some vegetarian sects.

The only other investigations into broth media especially suited for *Past. pestis* appear to be those of Drennan and Teague (*Journal of Medical Research*, **36**: 519, 1923) and Meyer and Batchelder (*Journal of Infectious Diseases*, **39**: 370, 1926). The latter workers described a medium for the isolation of *Past. pestis* from infected rodents. They used Huntoon's hormone broth containing sodium sulfite and gentian violet. This medium served to inhibit the growth of many species other than *Past. pestis*, while allowing luxuriant growth of this organism.

Within the past few years, it has been demonstrated that many pathogenic bacteria can be grown on media of relatively simple composition. Indeed, Bernheimer and Pappenheimer (*Journal of Bacteriology*, **43**: 481, 1942) have obtained excellent growth of even such a fastidious organism as group A hemolytic streptococcus on a medium containing hydrolyzed casein as the main source of nutrient material. It seemed to us that a similar simple medium might be devised for *Past. pestis*. Since a medium was desired which would not only be useful

V.2
194

for vaccine production but which also would be suitable for investigation of the antigenic structure of this organism, such a medium should have the following characteristics: 1. It must be well suited to this organism, so that the antigenicity may be maintained unimpaired. 2. It must contain no protein moiety larger than di- or tri-peptides and must be dialyzable through cellulose tubing. 3. It must contain no material of any type which might cause hypersensitivity or allergy on the part of the recipients. 4. It should be inexpensive and easily prepared.

It was found that these requirements were satisfied by a mixture of hydrolyzed casein, inorganic salts, and glucose. The addition of accessory growth factors was not necessary, nor was growth improved when they were added.

METHODS.

The strains of *Pasteurella pestis* used in this study were the virulent strains Yreka, F 8376, and F 8251, obtained through the courtesy of Dr. K. F. Meyer of the Hooper Foundation, San Francisco, and the avirulent strains, Bombay, Java, Soemedang, and Tjiwidej, obtained through the courtesy of Dr. Harry Schütze of the Lister Institute. They were kept in serum agar stabs and on blood agar slants at 0–5° C., with no more subculturing than was necessary to keep the strains available. This procedure was followed to counteract any tendency toward dissociation (Otten, *Mededeelingen van den dienst der volksgezondheid in Nederlandsch-Indie*, **30**: 61, 1941 and Sokhey, *Indian Journal of Medical Research*, **27**: 363, 1939).

The casein digest was prepared by boiling 200 grams of technical casein with 170 ml. HCl and 110 ml. water under a reflux condenser for 24 hours. At the end of this period, the mixture was cooled, shaken with 20 grams of Norit A and clarified by centrifuging. The sediment was discarded and the supernatant fluid was neutralized to pH 7.0–7.2 with 5N NaOH. It was again treated with Norit A. If the supernatant fluid after centrifuging was darker in color than a light yellow, the treatment with Norit was repeated. For the sulfuric acid hydrolysis, 200 grams of technical casein were hydrolyzed with 1000 ml. of 5N H_2SO_4 for 24 hours. The mixture was cooled and neutralized to pH 5.0–5.3 with powdered barium hydroxide. After centrifuging, the supernatant fluid was removed and treated with Norit. The pH was adjusted to 7.0–7.2 with 5N NaOH after the Norit had been removed

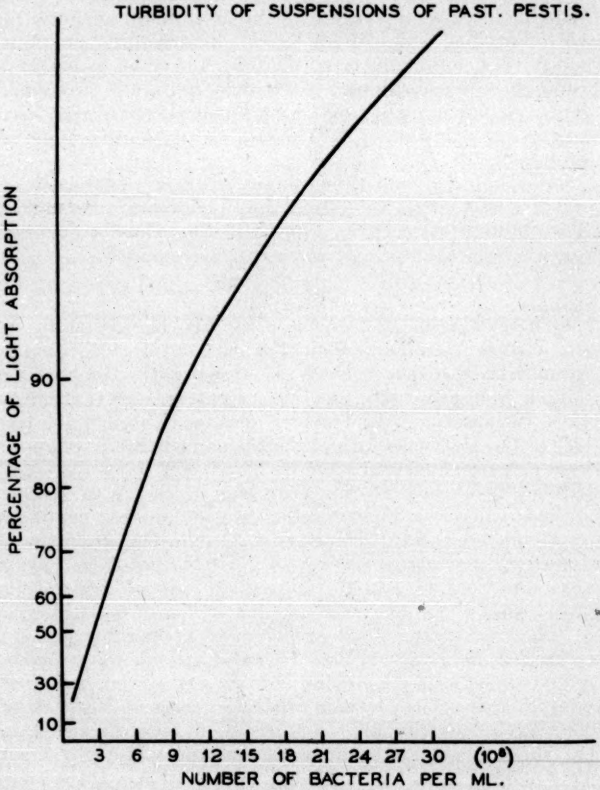

FIG. 1.

by centrifuging. Such stock solutions of hydrolyzed casein were stored with 5 ml. of chloroform as preservative.

Commercially prepared casein hydrolysate was obtained from the Digestive Ferments Co., who prepare a dehydrated casein hydrolysate marketed under the name of "Casamino Acids."

A turbidimetric method, using a photoelectric colorimeter, was employed to estimate the amount of growth in various cultures, the turbidity of the suspensions being correlated with the number of organisms per unit volume. Figure 1 shows the relation between the turbidity of suspensions of *Past. pestis* Soemedang and the number of organisms per ml. as determined with a Petroff-Hausser bacterial counting chamber. These suspensions were obtained by centrifuging a 48 hour culture grown in casein digest broth, washing the organisms with distilled water, and diluting this suspension. Aerosol IB was added (0.1 per cent.) to this suspension to counteract the tendency of the bacteria to clump. From time to time, during the course of this study, counts were made on suspensions whose turbidity was then determined. In no case did the results vary by more than 5 per cent. from those indicated by the curve in Fig. 1. These suspensions were at a stage of growth comparable to that of the culture which was used for determining the standard curve. Cultures older than 48 hours tend to be less turbid, particularly if the culture is neutral or slightly alkaline. One per cent. formalin was added to cultures as a killing agent before turbidity determinations were made. This germicide did not affect the turbidity of the suspensions, as did phenol, cresol, and sodium phenyl phenate.

EXPERIMENTAL.

All three casein digests (hydrolyzed with HCl, hydrolyzed with H_2SO_4, and Casamino acids, Difco) supported growth of *Past. pestis*. Forty-eight hour cultures of Soemedang at 27° C. in 2 per cent. solutions of hydrolyzed casein gave turbidity readings of 30, 30, and 60, respectively.

The influence of glucose, with and without buffering salts is demonstrated by the results shown in Table I. The stimulating effect of glucose is apparent, as is also the effect of the neutralization of the acid formed from the glucose by sodium

TABLE I.

Influence of Glucose and Buffering Salts on Growth of Pasteurella pestis.

Medium	Relative Turbidity (48 hrs. incubation at 27° C.)
H_2SO_4 casein digest − 2%	29
H_2SO_4 casein digest + 0.5% KH_2PO_4	29
H_2SO_4 casein digest + 0.5% Na_2HPO_4	31
H_2SO_4 casein digest + 0.5% KH_2PO_4 + 0.5% Na_2HPO_4	29
H_2SO_4 casein digest + 1% glucose	69
H_2SO_4 casein digest + glucose + 0.5% KH_2PO_4	83
H_2SO_4 casein digest + glucose + 0.5% Na_2HPO_4	83
H_2SO_4 casein digest + glucose + KH_2PO_4 + Na_2HPO_4	79
Casamino acid − 2%	60
Casamino acid + 0.5% KH_2PO_4	76
Casamino acid + 0.5% Na_2HPO_4	72
Casamino acid + 0.5% KH_2PO_4 + 0.5% Na_2HPO_4	68
Casamino acid + KH_2PO_4 + Na_2HPO_4	54
Casamino acid + KH_2PO_4 + Na_2HPO_4 + glucose	73
Casamino acid + KH_2PO_4 + Na_2HPO_4 + glucose + $NaHCO_3$	89

bicarbonate or sodium and potassium phosphate. The glucose was sterilized separately as a 50 per cent. solution, and added to the sterile broth immediately before use.

The accessory growth factors used by Bernheimer and Pappenheimer were tested separately and together. These included biotin, nicotinamide, pyridoxine, calcium pantothenate, thiamine, and riboflavine. Folic acid, diphosphopyridine nucleotide, hematin, and para amino benzoic acid were also tested. None of these gave any stimulation of growth when Casamino acids were used as the source of hydrolyzed casein. Rao (*Indian Journal of Medical Research*, **27**: 833, 1940) reported that diphosphopyridine nucleotide and hematin stimulated the growth of *Past. pestis* in a synthetic medium, although these two factors were not necessary for growth. However, Berkman (*Journal of Infectious Diseases*, **71**: 201, 1942) found no increase in the amount of growth of *Past. pestis* when diphosphopyridine nucleotide and other accessory growth factors were added to a medium composed of amino acids.

The addition of tryptophane, uracil, adenine, and glutamine did not improve growth with any of the casein digests.

V.2
194

The medium for routine use was prepared as follows:

Casamino acids	20 grams
KH_2PO_4	4
KCl	4
Na_2PO_4	2
Water	1000 ml.
Adjusted to pH 6.5–6.7, autoclaved.	
Sterile saturated $NaHCO_3$ solution added	50 ml.
Sterile 50 per cent. glucose solution added	10 ml.

When cultures more than 1 day old were desired, 0.5 per cent. sterile glucose and 0.5 per cent. sterile $NaHCO_3$ were added daily. Three-day cultures on this medium yielded between 600 and 800 mgm. of bacterial protein per liter.

In an attempt to see whether a casein digest medium would support the growth of small inocula, a 72 hour culture of *Past. pestis* was serially diluted in casein digest (HCl hydrolyzed) broth. Measured samples of each dilution were then transferred to 10 ml. tubes of casein broth and heart infusion (Difco) broth. The results after six days' incubation, shown in Table II, indicate that the casein digest medium is not as good as is heart infusion broth in supporting growth from small inocula.

TABLE II.

Growth of Pasteurella pestis from Small Inocula in Heart-Infusion Broth and in Casein Digest Broth.

Dilution of Broth Culture	10^{-1}	10^{-2}	10^{-3}	10^{-4}	10^{-5}	10^{-6}	10^{-7}	10^{-8}	10^{-9}
Heart infusion broth	+	+	+	+	+	+	+	+	+
Casein digest	+	+	+	+	+	+	−	−	−

Note: + indicates growth.
− indicates absence of growth.

Although this medium did not support growth from small inocula as well as might be desired, it did suffice for continued growth for ten successive transfers, at which time the experiment was stopped and the last culture was plated on blood agar. There was no reason to believe that this serial pasage could not have been continued indefinitely. The culture recovered from the blood agar plates had not changed in morphology, colony structure, nor in the degree of encapsulation, to judge from India ink smears.

Since Meyer and Batchelder reported that the addition of sodium sulfite improved the growth of *Past. pestis* in Huntoon's hormone broth, this substance was tested in the casein digest medium. The results are shown in Table III. There

TABLE III.

Effect of Na_2SO_4 *on Growth of Pasteurella pestis.*

			24 Hours Incubation.		
Concentration of Na_2SO_4		0.1%	0.05%	0.025%	0.0125%
Turbidity	77	62	78	82	80
			120 Hours Incubation.		
Concentration of Na_2SO_4		0.1%	0.05%	0.025%	0.0125%
Turbidity	65	62	64	66	65

was a definite though small stimulation of growth in the flask containing 0.025 per cent., which is the same concentration as that recommended by these authors.

Sokhey (*Indian Journal of Medical Research*, **27**: 331, 1939) in studying the growth of *Past. pestis* in relation to the surface-volume ratio, concluded "It is shown that a 48-hour growth of the plague bacillus in a liquid medium bears no relation to the total quantity as such of the medium nor to its surface area, but is directly proportional to the circumference of its surface area." Since it appeared that the comparatively heavy growth in the glucose-containing medium rendered it unlikely that growth was proportional to the surface area, or to the circumference of this area, several series of Pyrex tubes of uniform diameter but containing increasing amounts of casein digest broth were inoculated with *Past. pestis* Soemedang. The results indicated that the growth in the medium without glucose was roughly proportional to the surface area, or perhaps to the periphery of the surface area, but that when glucose was present, this relationship did not hold. The results of one series—all of them were similar—are shown in Table IV.

This tendency for *Past. pestis* to grow at the surface of a fluid medium is somewhat paradoxical in view of the findings of certain workers (Schütze and Hassanein, *The British Journal of Experimental Pathology*, **10**: 204, 1929; Wright, *Journal*

TABLE IV.

Influence of Depth of Medium on Amount of Growth of Pasteurella pestis
(24 hrs. Incubation).

Depth of medium (in mm.)	10	17	23	30	42	57	71
	With Glucose.						
Organisms per ml. ($\times 10^8$)	13.2	11.1	10.5	10.5	9.0	8.1	8.1
	Without Glucose.						
	6.6	4.2	3.3	2.1	1.4	1.3	1.2

of Pathology and Bacteriology, **39**: 381, 1934; and Sokhey, *Indian Journal of Medical Research*, **27**: 321, 1939) that this organism is sensitive to oxygen, and that growth as isolated colonies on agar plates is possible only by either adding reducing substances such as blood, sodium sulfite, serum or copper sulfate to the agar, or by incubating under anaerobic conditions.

The four avirulent strains of *Past. pestis* were grown in casein digest medium and in casein digest medium with glucose, to determine the optimal temperature. These cultures were grown in Pyrex tubes which were immersed in a water bath. The results, shown in Table V, indicate that, in the presence of glucose, the optimal temperature lies between 27° C. and 32° C. In the absence of glucose, however, the

TABLE V.

Growth of Pasteurella pestis at Different Temperatures in the Presence and Absence of Glucose
(24 hrs. Incubation).

Strain	With Glucose.			
	22°	27°	32°	37°
Bombay	87	89	92	78
Java	88	90	91	74
Soemedang	88	90	92	69
Tjiwidej	83	86	91	83
	Without Glucose.			
Bombay	49	51	48	48.5
Java	48	45	32	19
Soemedang	56	49	48	38
Tjiwidej	49	46	48	44

optimal temperature is lower than 32° C., although no sharp optimum exists.

It was noted that generally growth was better in the glucose cultures which had been incubated in the water bath than in similar cultures which had been incubated in an incubator. This appeared to be due to a combination of two factors; a more rapid attainment of temperature by the medium with a consequent decrease in the lag period, and a small but constant vibration imparted by the stirrer in the water bath. Direct agitation of the flasks also resulted in increased growth.

No such effect was shown in the absence of glucose, however. In this case, growth was better when the flasks were allowed to remain undisturbed. Four strains were grown at 27° C. and at 32° C., samples being taken and the flasks being shaken daily for the first three days. They were then allowed to remain undisturbed for three additional days, at the end of which time samples were taken again. The effect of shaking is shown by the drop in turbidity between the second and third days. On being allowed to stand undisturbed, the rate of growth increased, as is indicated by the increase in turbidity between the third and sixth days. The results are shown in Table VI.

The sensitizing properties of Casamino acids were tested by injecting 1.0 mgm. into each of 6 guinea pigs, and 10 mgm.

TABLE VI.

The Effect of Daily Shaking on the Growth of Pasteurella pestis in the Absence of Glucose.

Strain	27° C.			
	24 hours	48 hours	72 hours	144 hours
Bombay	47	83	68	88
Java	48	78	80	90
Soemedang	49	86	78	83
Tjiwidej	49	77	72	88
	32° C.			
Bombay	52	81	72	92
Java	44	80	69	81
Soemedang	50	84	64	86
Tjiwidej	48	87	70	83

V.2
194

into each of 6 guinea pigs, subcutaneously. After 21 days, 10 mgm. were injected into three animals in each group, 100 mgm. being injected into the remaining animals, by the intraperitoneal route. No evidence of sensitivity was shown. These animals were then kept for 25 days, at which time 10 mgm. were injected intravenously into each animal. Again, no evidence of sensitivity was found.

After a 10 per cent. solution of Casamino acids had been dialyzed in cellophane tubing for 7 days against distilled water, the water being changed twice daily, the solution within the tubing gave negative results with biuret, xanthoproteic and Millon tests. Evidently, this casein hydrolysate contained not more than a trace of protein, a finding that agreed with the negative results of the attempt to sensitize guinea pigs to this material.

SUMMARY.

Acid-hydrolyzed casein serves as an excellent nitrogen source for *Pasteurella pestis*. Growth was found to be enhanced by glucose, especially when the medium contained buffering salts.

Although this medium did not support growth with inocula smaller than 100 organisms per ml. serial passage was carried out for 10 subcultures without causing change in morphology, colony structure, or amount of encapsulation.

In the presence of glucose, the total amount of growth was nearly proportional to the amount of medium; in its absence growth was more nearly proportional to the surface area.

No sharp temperature-optimum for growth was found. Growth was generally best between 27° C. and 32° C.

No evidence of sensitivity was found in guinea pigs which had received injections of commercially prepared hydrolyzed casein. All the soluble nitrogen-containing constituents of this medium were found to be dialyzable through cellulose tubing.

BOOK REVIEWS.

Nicholas Copernicus, by Stephen P. Mizwa, A.M., LL.D. 88 pages, illustrations, with 4-color cover portrait of Copernicus by Arthur Szyk. 18 × 25 cms. New York, The Kosciuszko Foundation. 1943. Price $.75.

The 400th anniversary of the death of Copernicus and the publication of his great work, "De Revolutionibus Orbium Coelestium," are being commemorated this year with impressive programs. The Franklin Institute celebration will be centered in the splendid facilities of the Fels Planetarium, in May. Our library possesses copies of both the first (1543) and second (1566) editions of "De Revolutionibus," and they will be displayed.

As a source book for the programs of the occasion, there has recently appeared a very attractive book by the Secretary and Executive Director of the Kosciuszko Foundation. In it, the life-story of Copernicus, his Polish antecedents, and much background material concerning Polish culture have been compressed in very fine form. The many fine illustrations contribute their share in making this book a necessity for anyone at all interested in astronomy, the history of science, or Poland.

A special numbered edition, bound in boards, is also available at a somewhat higher price.

Roy K. Marshall.

The Theory and Practice of Heat Engines, by D. A. Wrangham. 756 pages, charts and diagrams, 17 × 25 cms. New York, The Macmillan Company, 1942. Price $10.50.

The older of the practicing engineers of today will recall the textbooks of this title from their college days. Not many of the younger engineers will recognize it as the title of a book although it is still used considerably as a subject heading. Perhaps the lack of use of the term as a book title recently is due to the inclusion within the limits of its meaning of more knowledge of the old principles as well as an enlargement of the importance of certain types of heat engines, facts which may have acted to break up the subject as an entirety. The appearance of this book with a title of heat engines is therefore taken with interest.

The book was printed in Great Britain and its author is an Englishman. In this connection, the English viewpoint is worthy of note. When referring to energy derived from coal, the author relates that first the fuel must be converted into mechanical energy or heat which is a chemical action; then the heat must be transmitted to a working fluid; and finally a mechanism is required to deliver the energy in the desired form. The design of the engine mechanism requires a comprehensive knowledge without which, combined with experience in the field, man cannot really be called an engineer.

After a brief introduction, the work opens with the study of the kinetic theory of gases, in preparation for the more advanced studies on partial pressures, gas mixtures, expansion of gases and ideal cycles. The use of air in compressors and motors is next taken up, which subject may be said to conclude a preliminary division of the book. The next division starts with vapors and proceeds through the subjects of entropy, mixtures of air and steam, and the reciprocating steam engine. On the basic assumption that heat may be described as a condition of molecular activity, the process of refrigeration is explained and following this is a division covering the flow of fluids, the flow of heat, steam condensers and steam turbines. Considerable space is devoted to a clear conception of combustion at this point, and contrary to the thought that this subject might better have been placed in the early part of the book, it is well projected here. Internal combustion engines is the next topic which is divided into three parts—the gas engine, the "petrol" engine and the oil engine. The latter part of the book is devoted to steam boilers and power plant economy, other subjects which seem somewhat removed from logical progression.

The book is well illustrated, many of the drawings being of different colors. The mathematical examples bear the mark of careful application to the subject matter under discussion. The subject index facilitates reference. The book gives a good and thorough coverage for students of college grade.

R. H. OPPERMANN.

NOXIOUS GASES AND THE PRINCIPLES OF RESPIRATION INFLUENCING THEIR ACTION, by Yandell Henderson and Howard W. Haggard. 294 pages, charts and diagrams, 15 × 23 cms. New York, Reinhold Publishing Corp., 1943. Price $3.50.

In view of the use of gases in warfare and the precautions taken recently in national defense, this subject is a pertinent one today. Yet aside from this, not much attention is generally given to a hardly less important danger of noxious gases in peacetime daily life on the street, in the home, or in industry. The gas hazards, particularly in modern peaceful industry, are very real. In fact, this is almost the only field in the whole range of modern sanitation in which the number of fatalities throughout the civilized world has increased year by year. Noxious gases in war or in peace are due to receive very careful study. Immensely valuable measures of protection against industrial gases have resulted from the study of war gas defense. This book deals only with gases which occur in industry but references are made to recent works dealing with chemical warfare.

After a brief survey of the field, the elements of respiration are taken up, followed by the respiratory functions of the blood and their laws. This not only lays a foundation for the study of the effects of noxious gases but it impresses the reader as to the practicality of the subject. Built up from these subjects are the treatments on the laws of gases and vapors where are shown the kind of use to which these fundamental principles are put in the field of respiration; principles determining absorption, distribution and elimination of volatile substances; the significance of standards for physiological response to various concentrations of gases and vapors. All this leads to a study of the gases themselves. These are classified in tables where the names, chemical formulas and physical characteristics of the gases which occur most often in modern industry are set down along with the general nature of their physiological action. As a means of making the tables of greater practical use the gases are listed in their chemical sequence and reference is indicated to the section of the book describing the physiological action.

Discussion on specific gases is made according to groups of gases. Group I covers irritant gases, Group II asphyxiants, Group III chemical asphyxiants, Group IV inorganic and organometallic gases. General descriptions of the various types of physiological action are given with lists of substances producing these effects. A few gases are treated separately where their physiological characteristics differentiate them from others. In the discussions, the appropriate treatments are, in most cases, more or less fully described. A chapter in the latter part of the book brings out the differences and contrasts the prime features in these treatments. The last chapter is devoted to the prevention of poisoning by noxious gases. There is a subject index in the back.

This is the second and revised edition of this American Chemical Society Monograph. It is the result of expert knowledge of the subject and a painstaking review of the literature up to date. The book has practical value to chemists, engineers and others engaged in industry.

R. H. Oppermann.

Constitution of Alloys Bibliography, by J. L. Haughton, D.Sc. 162 pages, 14 × 22 cms. Suffolk, England, Richard Clay and Company, Ltd., 1942.

This bibliography contains over 5000 references to papers dealing with the constitution of binary, ternary and higher alloy systems, both ferrous and nonferrous. References have been included not only to papers of a purely constitutional character but also to many X-ray and physical-property studies of alloys, which have some bearing on the constitution. To furnish some guide among the references (which in a few systems exceed 100), asterisks have been placed against those in the originals of which a new equilibrium diagram, or portion of one, is to be found. The bibliography is intended to be used in conjunction with the abstracts that the Institute of Metals has published since its foundation, first in the Journal and then in Metallurgical Abstracts (Series II); for convenience, therefore, references have been included to these abstracts, whenever such exist.

The bibliography is up to date and should prove valuable to research workers in metallurgy, metallurgists, and others interested in the subject.

R. H. Oppermann.

Engineering Mechanics, by Glen N. Cox, Ph.D. 301 pages, charts and diagrams, 16 × 23 cms. New York, D. Van Nostrand Company, Inc., 1943. Price $3.00.

The solution of many different kinds of engineering problems depends on a knowledge of engineering mechanics. The subject is essentially a practical one embodying such studies as physics, the motion of planets, the motion of fluids and gases, and the strength of materials. A good understanding of the principles of mechanics is necessary for success in the engineering field. Therefore a text on the subject must be chosen with care. This text is an attempt to coördinate the desires of the engineering teachers of this country to the extent that these desires have been expressed in the various surveys which were conducted under the auspices of the Society for the Promotion of Engineering Education.

With the thought that the principles of mechanics can only be fixed in one's mind by the solution of a large number of problems, the author presents here a

V.2
194

treatment that loses little time and space to anything but the immediate subject. After a review of fundamental conceptions, various force systems are taken up, such as coplanar and non-coplanar, concurrent and non-concurrent. This is followed by a somewhat unusual treatment on friction, where agreement with experimental facts is featured. A rather thorough coverage is given and references are made to the results of various workers on the changes in frictional values with the use of lubricants. Certain loose threads of earlier chapters are consolidated in Chapter VIII on centroids where an adequate exposition is made. The following chapter, entitled "Moment of Inertia of Plane Areas," may confuse some as to the meaning of the title. It actually means that the moment of inertia of an area is an expression of the sum of the products of the various differential areas and the square of their distances from some references. It is known as $\int x^2dA$. The subject of kinematics of particles and rigid bodies precedes the kinetics of rigid bodies. A separate chapter is given over to giving a clear conception of work and energy, and an interesting treatment is accorded to problems involving the action of forces for a given length of time utilizing in their solution the impulse-momentum type of equation. An interesting appendix is devoted to flexible cables when there are covered cables used for supporting a load distributed uniformly along a horizontal direction, as in the suspension bridge; for supporting their own weight, as in an electric transmission line; and for the transportation of loads over rough terrain.

The author makes free use of diagrams in his explanations and also uses, quite freely, worked-out illustrative problems. A very helpful feature is that the answers are attached to the problems given for exercise. This makes for accuracy, encouragement to solve the problems, and impressionable technique in solution and a confidence that the problems were designed for a special purpose and that their solutions have been checked. The book contains a subject index in the back adding to its value as a reference. It is a reliable text.

R. H. OPPERMANN.

TRANSIENTS IN LINEAR SYSTEMS, Volume I, by Murray F. Gardner and John L. Barnes. 389 pages, charts and diagrams, 16 × 23 cms. New York, John Wiley and Sons, Inc., 1942. Price $5.00.

Many dynamical systems need to be studied in the transient state—some for the purpose of minimizing unwanted transient effects, others for the purpose of controlling and employing desirable effects. But in whichever aspect transients may occur, desirable or undesirable, their treatment is a problem of engineering importance and their calculation often a matter of difficulty. In fact, it is not always possible to handle simply and completely by mathematics any type of dynamical system in the transient state. It is this fact which the authors of this book recognized when they chose the linear type system first as capable of being handled most simply. It is a very important type in engineering and physics.

This book is the first of a two volume set. Restricted entirely to systems having lumped parameters, it leads to ordinary integrodifferential or difference equations. Distributed parameter systems which bring in partial integrodifferential equations are to be treated in Volume II it is planned. Volume I, however, is complete in itself. It opens with a brief reference to certain basic ideas regarding the nature of transients and reasons for the choice of the Laplace-transformation method for the mathematical treatment of linear physical systems in the transient state. Proceeding on the foundation of the subject, there are shown convenient choices of variables, and systematic ways of setting up differential equations and expressing the initial conditions for electric and mechanical systems. The basis of analysis is pointed out. Attention is directed to the formulation of one-dimensional integrodifferential equations of the type whose solution is simplified by the L-transformation method and later the L-transformation is brought out so that it, together with its inverse, may be applied intelligently in solving equations. The transformation and its application to simple functions is treated as are applications to integrodifferential equations in one independent variable as well as rational algebraic fractions.

What should be of interest in many branches of science and engineering is the solution of a general linear second-order differential equation with constant coefficients. This is well carried out preliminary to taking up examples of the complete solution by the L-transformation method of one-dimensional problems in specific electric and mechanical systems. The latter part of the book is devoted to additional properties of the L-transformation and the solution of Linear difference equations with constant coefficients. The latter may be taken as a transition chapter between one dimensional problems and multi-dimensional problems which is to be the subject of Volume II. Appendixes included in the book are a summary of theorems and transform pairs, a comparison of the Laplace and the Fourier-Integral transformation methods, and some historical notes on the mathematical theory. There is also a bibliography and a subject index.

This mathematical presentation is outstanding for its completeness and logical progression. It is a distinct contribution toward a better understanding of the subject.

R. H. OPPERMANN.

PUBLICATIONS RECEIVED.

The Chemistry of Natural Coloring Matters, The Constitutions, Properties, and Biological Relations of the Important Pigments, by Fritz Mayer, Ph.D. 354 pages, diagrams, 15 × 23 cms. New York, Reinhold Publishing Corp., 1943. Price $10.00.

The Chemical Technology of Petroleum, by William A. Gruse and Donald R. Stevens. 733 pages, charts and diagrams, 16 × 23 cms. New York, McGraw-Hill Book Co., Inc., 1942. Price $7.50.

Empirical Equations and Nomography, by Dale S. Davis. 20 pages, illustrations, 16 × 24 cms. New York, McGraw-Hill Book Co., Inc., 1943. Price $2.50.

The Elements of Aerofoil and Airscrew Theory, by H. Glauert. 228 pages, illustrations, 14 × 22 cms. New York, The Macmillan Co., 1943. Price $3.50.

An Introduction to Fluid Mechanics, by Alex. H. Jameson, M.Sc., M.Inst., F.K.C. 245 pages, illustrations, 14 × 22 cms. New York, Longmans, Green & Co., 1942. Price $3.40.

The First Century of Flight in America, by Jeremiah Milbank, Jr. 248 pages, pictures, 15 × 22 cms. New Jersey, Princeton University Press, 1943. Price $2.75.

The Amazing Petroleum Industry, by V. A. Kalichevsky. 234 pages, diagrams, 13 × 19 cms. New York, Reinhold Publishing Corp., 1943. Price $2.25.

CURRENT TOPICS.

Automotive Machine Tools, Once Discarded, Are Rebuilt for Important War Assignments.—(*Automotive War Production*, Vol. 1, No. 8.) By ordinary standards, the equipment was obsolete. It was a machine tool known as a vertical boring mill, once used to make rims for automobile wheels. When the size and type of the wheel changed a few years ago, most firms got rid of their vertical boring mills of this type. But the value of machine tools is relative. Due to changed circumstances, the equipment which once was deemed suited for the scrap heap is now badly needed. There are only a few tools left in one automotive city to make the type of circular cut made by vertical boring mills. And the demand is so great for such equipment in war work that the various firms now exchange jobs in order to utilize the existing boring mills to their fullest capacity. There have been numerous cases where machines, designed specifically for some automobile manufacturing operation, have virtually been rebuilt in order that they might be used in the automotive war job. A serious bottleneck in the production of Army 4 × 4 trucks was eliminated by adapting to war production several gear cutting machines which had been lying around "in the grease," unused since the advent of hypoid gears in late model cars. An ingenious gear cutting specialist of an automotive company thought of the old machines that had been lying around idle. Experimenting with ways to adapt them to the job, he designed a special cam arrangement which generated the machines in such a way as to cut the four separate faces of a ball-race to specifications. Still another automotive company recently rescued an old punch press from the scrap pile and, adapting it to its gun job, effected an important short cut in production time. Formerly obdurator rings were inserted into the breach of the gun barrel by hand. By retooling the old punch press and through the use of a special fixture the rings whose insertion formerly required about 15 minutes each, are now squeezed into place in less than a minute each.

R. H. O.

Boring Chuck for Thin Walled Cylinder.—(*The Iron Age*, Vol. 150, No. 23.) One of the problems in boring a thin-walled metal cylinder is to prevent distortion in the machining operation. On a cylinder 6 in. o.d. and 6 in. long which is to be bored to 5.000 ± 0.001 in. after turning, for example, the pressure required to grip and drive the work in a conventional three-jaw chuck may distort the piece as much as 5 or 6 thousandths, resulting in scrapped work. At the Lima, Ohio, plant of Westinghouse Electric & Mfg. Co., a special chuck has been developed for such work which eliminates out-of-round distortion on such cylinders. The workpiece is gripped by a spring steel band which is held by clamping lugs which act as a driving dog. The band floats circumferentially in a pot-type holder. This holder has three supports which fit the outside of the piece snugly and control the concentricity of the bore with the o.d. One support has a movable face that can be withdrawn slightly for loading. The supports are slotted on the faces to allow the spring band to pass through freely. The cylinder is placed in the chuck. The band is clamped tightly around it and provides sufficient friction to drive the cut without distortion in the piece after the clamp and workpiece are rotated until the lugs stop against one of the supports which serves as a driver. The release screws on the movable face are then tightened with pressure sufficient to hold the cylinder radially but not enough to distort it.

R. H. O.

V.2
194

Moisture in the Menu.—Which of the common vegetables is most watery? Active research into dehydration of vegetables as a part of the war effort by the U. S. Department of Agriculture has developed information to guide commercial dryers in their work. In planning drying equipment, one fact the dryer must know, says the Agricultural Research Administration, is the quantity of water he will have to remove from the material while it is being processed. W. B. Van Arsdel of the Bureau of Agricultural Chemistry and Engineering has prepared a table giving the moisture content of nearly a score of vegetables as they are when ready for dehydration. This is substantially the same as the fresh vegetables prepared for home cooking. The relative rank in "wateriness" may upset some of the casual impressions of housewives. Sweetpotatoes are the driest of the common vegetables with from 2 to $3\frac{1}{2}$ pounds of water for each pound of bone-dry material. Sweet corn ranks next with 3 to 4 pounds, followed by peas and potatoes with from $3\frac{1}{2}$ to $4\frac{1}{2}$ pounds of water to a pound of dry matter. Kale has 6 to $7\frac{1}{2}$ pounds; table beets 6 to 9, and beet greens 9 to 10; with rutabagas 7 to 10 and carrots $7\frac{1}{2}$ to 10. Snap beans have 8 to 10 pounds of water, onions 8 to 11, spinach 8 to 13, chard 9 to 12, mustard greens 9 to 13. The vegetables with the most water to remove are cabbage with from 10 to 15 pounds of water to each pound of dry matter and celery with 12 to 20.

R. H. O.